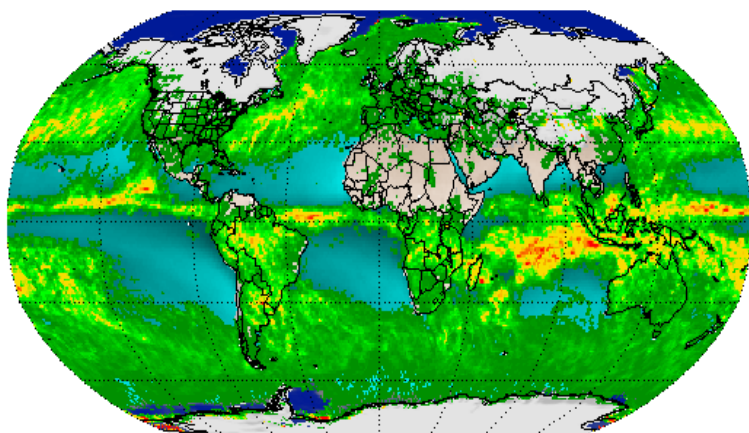




Microwave Integrated Retrieval System (MiRS)

User Manual (MiRS version 11.6)

July 2020



Prepared for:

U.S. Department of Commerce
National Oceanic and Atmospheric Administration (NOAA)
National Environmental Satellite, Data, and Information Service (NESDIS)
Center for Satellite Applications and Research (STAR)

Prepared by:

Quanhua Liu, NOAA/NESDIS/STAR,
Christopher Grassotti, U. Maryland/ESSIC/CICS,
Kevin Garrett, NOAA/NESDIS/STAR,
Shuyan Liu, Colorado State University/CIRA,
Sid Boukabara, NOAA/NESDIS/STAR

NOAA/NESDIS/STAR
MIRS-UM-01

July 31, 2020

Microwave Integrated Retrieval System (MIRS)

User Manual (UM)

July 2020

Prepared for:

U.S. Department of Commerce
National Oceanic and Atmospheric Administration (NOAA)
National Environmental Satellite, Data, and Information Service (NESDIS)

Approval Page

Document Numbers: 1 NOAA/NESDIS/STAR MIRS-UM-01	Approved: July 2020
---	---------------------

Document Title Block:

Microwave Integrated Retrieval System (MIRS)

User Manual (UM)

PROGRAM: MIRS	DOCUMENT RELEASE DATE: July 31, 2020	
APPROVALS		
GROUP: NOAA/NESDIS/STAR	Date	GROUP: NOAA/NESDIS/STAR
NAME: Quanhua Liu, Science Lead		NAME: Sid Boukabara, Oversight Panel Chair
GROUP: NOAA/NESDIS/OSPO	Date	GROUP: NOAA/NESDIS/STAR
NAME: Limin Zhao, Oversight Panel member		NAME: Ralph Ferraro, Oversight Panel member
CM RELEASE APPROVAL:	Date	
NAME: Quanhua Liu, Configuration Manager		

Version Description Record

DOCUMENT CHANGE HISTORY			
DCN No.	Revision	Date	Description of Change
	1.0	January 31 st , 2007	Initial Release of MIRS User's Manual
	1.1	April 27 th , 2007	Kleespies Initial Review
	1.2	June 15 th , 2007	Second Release of MIRS User's Manual
	1.3	December 15 th , 2007	Third Release of MIRS User's Manual
	1.4	June 15 th , 2008	Fourth Release of MIRS User's Manual
	1.5	December 15 th , 2008	Fifth Release of the MIRS User's Manual
	1.6	June 15 th , 2009	Sixth Release of the MIRS User's Manual
	1.7	June 15 th , 2010	Seventh Release of the MIRS User's Manual
	1.8	November 9th, 2012	Eighth Release of the MIRS User's Manual
	1.9	January 8 th , 2013	Ninth Release of the MIRS User's Manual
	1.10	March 31, 2014	Tenth Release of the MiRS User's Manual
	1.11	September, 2014	Eleventh Release of the MiRS User Manual
	1.12	June, 2015	Twelfth Release of the MiRS User Manual
	1.13	August, 2016	Thirteenth Release of the MiRS User Manual
	1.14	March, 2019	Fourteenth Release of the MiRS User Manual

DOCUMENT TITLE: <i>Microwave Integrated Retrieval System (MIRS) User Manual (UM)</i>			
DOCUMENT CHANGE HISTORY			
DCN No.	Revision	Date	Description of Change
	1.15	April, 2020	Fifteenth Release of the MiRS User Manual
	1.16	July, 2020	Sixteenth Release of the MiRS User Manual

Preface

This document comprises the National Oceanic and Atmospheric Administration (NOAA) National Environmental Satellite, Data, and Information Service (NESDIS) publication of the Microwave Integrated Retrieval System (MIRS) *User Manual (UM)*.

This User Manual provides important information for MIRS users. It gives an overview of the MIRS system including software and hardware requirements, directory structure, levels of user interaction and operation and product generation procedures. It also provides succinct treatments of MIRS algorithm theoretical basis, component processes and applications and inputs and outputs, and detailed treatment of MIRS product validation and accuracy. Also included is useful information on MIRS product dissemination, quality assurance monitoring and software implementation procedures.

The document is controlled under the configuration management tool in NOAA/NESDIS/STAR and will be updated as required.

Table of Contents

Section 1.0	How to Use this Manual	11
1.1	Inside Each Section	11
1.2	Additional Documentation	11
1.3	How to Get Help.....	12
Section 2.0	Introduction	13
2.1	Hardware Requirements	13
2.2	Software Architecture.....	13
2.2.1	Requirements.....	13
2.2.2	Directory Structure	14
2.2.3	Interfaces	15
2.2.4	User's Interaction	16
2.2.4.1	High-Level Interaction.....	16
2.2.4.2	Mid-Level Interaction	17
2.2.4.3	Low-Level Interaction	18
2.3	Procedures for Normal Operations	19
2.4	Required Training.....	20
2.5	System Limitations.....	21
Section 3.0	Algorithm Description	22
3.1	Theoretical Basis	22
3.2	MIRS Applications and Products	23
3.3	MIRS Components	24
3.3.1	Radiance Processing.....	25
3.3.1.1	Antenna Pattern Correction.....	26
3.3.1.2	Footprint Matching	26
3.3.1.3	Bias Removal	27
3.3.2	Inversion Processing.....	27
3.3.2.1	Heritage Algorithms.....	28
3.3.2.2	Advanced Algorithm (<i>IDVAR</i>).....	29
3.3.2.3	Vertical Integration and Post-Processing.....	30
3.3.3	Conversion to User-Driven Formats	31
3.3.4	Area-Of-Interest (AOI) Segmentation.....	31
3.3.5	Level-III Compositing	32
3.4	Microwave Systems Supported by MIRS	32
Section 4.0	MIRS Input Files	37
4.1	Set-Up Files.....	37
4.2	External Files.....	37
4.2.1	Sensor Data Files (<i>level 1b</i>).....	38
4.2.2	Gridded NWP Analysis Files	38
4.2.3	Gridded NWP Forecast Files.....	38
4.2.4	Gridded NWP SFR Forecast Files.....	38
4.3	Static Data Files.....	38

4.3.1	Forward Operator Look-Up Tables (<i>CRTM files</i>)	38
4.3.2	Nominal Instrumental Error Covariance Matrices (<i>NEDT files</i>).....	39
4.3.3	Geophysical Mean and Covariance Matrices	39
4.3.4	Snow Water Equivalent Climatology Files	39
4.3.5	Topography Files.....	39
4.3.6	Tuning Files.....	39
4.3.7	Emissivity Catalog Data Files	40
4.3.8	Regression Coefficient Files	40
Section 5.0	MIRS Output Files	41
5.1	MIRS Retrieval Files.....	41
5.1.1	Main Product Swath Binary Files (<i>level II-a, EDR</i>)	41
5.1.2	Derived Product Swath Binary Files (<i>level II-a, DEP</i>)	41
5.1.3	Image Files	41
5.2	netCDF Swath Files (<i>level II-a, EDR</i>).....	42
5.3	Product Monitoring Figures	42
5.4	Product Quality Assurance / Quality Control.....	42
5.4.1	Interpretation and Usage of the Convergence Metrics	42
5.4.2	Interpretation and Usage of Quality Control.....	43
5.4.3	Interpretation and Usage of the Uncertainty Matrix	43
5.4.4	Interpretation and Usage of the Contribution Function.....	43
5.4.5	Interpretation and Usage of the Average Kernel.....	44
Section 6.0	Products Validation and Accuracy	45
6.1	Validation Methodology.....	45
6.2	Validation Results	45
6.2.1	Vertical Temperature Profile.....	46
6.2.2	Vertical Humidity Profile	47
6.2.3	Surface Emissivity.....	49
6.2.4	Surface Temperature	52
6.2.4.1	Over Land	52
6.3	Validation of MIRS Derived Products	53
6.3.1	Total Precipitable Water.....	53
6.3.1.1	Total Precipitable Water Over Ocean	53
6.3.1.2	Total Precipitable Water Over Non-Ocean Surfaces	55
6.3.2	Non-Precipitating Cloud Liquid Water (CLW).....	57
6.3.3	Rain Rate	58
6.3.4	Rain Water Path.....	63
6.3.5	Ice Water Path	65
6.3.6	Snow Water Equivalent (SWE).....	67
6.3.7	Snow Grain Size (SGS)	68
6.3.8	Sea Ice Concentration (SIC).....	69
6.3.9	Sea Ice Age (SIFY, SIMY)	71
6.3.10	Snowfall Rate (SFR)	72
Section 7.0	MIRS Products Dissemination	73

7.1	Retrieved Products Dissemination	73
7.2	Product Maps Dissemination.....	73
7.3	Quality Assurance Monitoring	75
Section 8.0	MIRS Software Implementation Procedure	76
8.1	Obtaining the MIRS Software	76
8.1.1	Accessing the Delivery Algorithm Package (<i>DAP</i>)	76
8.2	Description of the MIRS Package	76
8.3	How to Install, Compile and Run	76
8.3.1	Preliminary Steps	76
8.3.2	How to Run MIRS.....	77
8.3.2.1	Testbed Run	77
8.3.2.2	Direct Application Run (<i>IDVAR</i>)	78
8.4	Directory Tree Structure.....	78
8.5	Benchmark Testing.....	80
8.6	Licensing	81
8.7	Referencing MIRS.....	81

Appendices

Appendix A. Acronyms and Abbreviations	82
Appendix B. Bibliography	84

List of Figures

Figure 1. MIRS top level directory structure. The source code, scripts for running MIRS, the set-up files, executables, documentation, graphical user interface, data and logs files are kept under separate directories.....	15
Figure 2. MIRS source code directory structure. Note the library directories in Fortran-95 (lib), IDL (lib_idl),and Java (lib_java) which include code for performing generic functions. The “testbed” directory includes code for MIRS real-time applications, e.g. footprint matching, bias-correction, figure generation, etc.	15
Figure 3. Description of the three (nested) levels of user interaction. The innermost small blocks represent the low-level interaction consisting of individual applications and the control files as input (indicated by red arrows) to their executables. The mid-level interaction is represented by the (outer) panels with the PCFs and SCSs for a particular satellite that control the sequencing of the individual applications. The outermost panel represents the highest level of interaction through the GUI-based MCP.....	16
Figure 4. Snapshot of the MIRS Control Panel (MCP) showing some of the options available in the main window.....	17
Figure 5. Sample of the Paths & Configuration File (PCF) generated automatically by the MIRS Control Panel (MCP).	18
Figure 6. Overall conceptual diagram of the Microwave Integrated Retrieval System (MIRS) concept. Shown are the major components, the radiance and the inversion processing blocks... ..	25
Figure 7. Conceptual diagram of the radiance processing block, detailing the component processes involved.....	26
Figure 8. High-level diagram of the Inversion process block showing the MIRS concept of merging heritage, advanced and derived products.	28
Figure 9. Heritage algorithms within MIRS. These algorithms depend on specific sensors. For NOAA-18 and METOP-A AMSU-MHS, the heritage algorithms are represented by MSPPS... ..	29
Figure 10. General description of the 1DVAR retrieval iterative system. The Initial state vector (or first guess) starts the iterations, the update of the solution takes place at each iteration depending on the local derivatives, simulated brightness temperatures, etc (see text). The solution is reached when the final simulations are fitting the measurements within the noise level. CRTM is used to generate the simulated measurements.....	29
Figure 11. Schematic diagram of the MIRS main and derived products.....	30
Figure 12. Schematic representation of emissivity spectrum post-processing	31
Figure 13. Representation of the quality control structure.	43
Figure 14. Overall MIRS system including the routine and non-routine monitoring. The routine monitoring is performed daily by comparing retrieved outputs (EDRs) with assimilation NWP model outputs (GDAS), both radiometric and geophysical.....	45
Figure 15. Standard deviation (left) and mean bias (right) of the atmospheric temperature profile retrieved from MIRS (red) and the MIRS first-guess (teal) as well as other sources with respect to radiosonde measurements	46
Figure 16. Comparison of horizontal fields of temperature at 500 millibars on June 6 2008 retrieved from the MIRS NOAA-18 AMSU-MHS (left panel) and from collocated GDAS assimilation field (right panel)	47

Figure 17. Comparison of horizontal fields of temperature at 500 millibars on June 5 2008 retrieved from the MIRS METOP-A AMSU-MHS (left panel) and from collocated GDAS assimilation field (right panel) Similar comparisons are made with respect to ECMWF assimilation fields.....	47
Figure 18. Standard deviation (left) and mean bias (right) of the atmospheric water vapor profiles retrieved from MIRS (red) and the MIRS first-guess (teal) as well as other sources with respect to radiosondes	48
Figure 19. Comparison of fields of water vapor mixing ratio at 500 millibars over ocean, retrieved from the MIRS for NOAA-18 AMSU-MHS (right panel) and from the collocated GDAS assimilation system (left panel) on June 6, 2008	48
Figure 20. Comparison of fields of water vapor mixing ratio at 500 millibars, retrieved from the MIRS for METOP-A AMSU-MHS (right panel) and from the collocated GDAS assimilation system (left panel) on June 5, 2008	49
Figure 21. Qualitative validation of the surface emissivity retrieved by the MIRS algorithm (left), channel 31.4 GHz. The ocean emissivity is lower than that of land. As expected, river surfaces lower the surface emissivity. Scan-dependent variation of the emissivity over ocean can also be seen. The right panel represents the convergence metric showing that the system is able to fit the measurements within noise levels.....	50
Figure 22. Global distribution of emissivity at 50 GHz AMSU-MHS channel routinely retrieved from MIRS (left panel) and analytically computed from GDAS data (right panel).....	50
Figure 23. Global distribution of emissivity over ocean at the 50 GHz AMSU-MHS channel routinely retrieved from MIRS (left panel) and analytically computed from ECMWF data (right panel). Shown is the clear contrast of emissivities over water and sea ice surfaces.....	51
Figure 24. Global distribution of the 50 GHz emissivity differences retrieved from MIRS and analytically computed from collocated NWP ECMWF analysis geophysical inputs (left panel) and statistical assessment results (right panel)	51
Figure 25. Routine statistical comparisons between MIRS retrieved emissivity at AMSU-MHS 50 GHz and the analytically derived emissivities using collocated radiosonde geophysical data as inputs. Shown is the bias and standard deviation computed for all AMSU-MHS channels. Results indicate good retrievals for most AMSU-MHS channels. Accuracy degrades for channels 16-20.	52
Figure 26. Example of MIRS Metop-B retrieved LST (top left) with ECMWF analysis of LST (top right) valid July 27, 2014, along with scatter plot (bottom left).....	53
Figure 27. Performance assessment results of MIRS-retrieved TPW over ocean for NOAA-18 AMSU-MHS versus GDAS (left panel) and ECMWF (right panel).....	54
Figure 28. Performance assessment results of MIRS-retrieved TPW over ocean versus TPW derived from radiosonde measurements	54
Figure 29. Comparison between MIRS-retrieved and MSPPS-retrieved TPW over ocean for NOAA-18 AMSU-MHS	55
Figure 30. Performance assessment results computed from routine monitoring for MIRS retrieved global TPW with respect to GDAS (left panel) and ECMWF (right panel).....	56
Figure 31. Performance assessment results computed from routine monitoring for MIRS retrieved global TPW with respect to TWP derived from radiosonde measurements	56
Figure 32. Example of routine comparison of global distribution of TPW retrieved from MIRS for NOAA-18 AMSU-MHS (left panel) and from collocated ECMWF (right panel).....	57
Figure 33. Integrated Cloud Liquid Water (CLW) retrieved from MIRS (upper left) and from ECMWF analysis (upper right). Included are a scatter and density histogram to show the	

correlation of MIRS NOAA-18 AMSU-MHS retrieved CLW to ECMWF, as well as the distribution of each.....	58
Figure 34. Performance assessment results of MIRS NOAA-18 AMSU-MHS and CloudSat CLW. Scatter plot (left) and density histogram (right). The correlation between MIRS and CloudSat CLW is 0.64.....	58
Figure 35. MIRS derived Rain Rate (left) compared to Operational MSPPS Rain Rate (right) for Metop-A on August 1, 2014.....	59
Figure 36. Scatter plots of MIRS rain rates vs. MSPPS for NOAA-18 for September 9, 2008 over land (left) and ocean (right). The correlations are 0.85 and 0.71 respectively.....	59
Figure 37. IPWG assessment of MIRS rainfall rate (mm/day) compared to rain gauge and radar observations over the continental U.S. from 13Z May 20, 2009 to 12Z May 21, 2009.....	61
Figure 38. Timeseries of MIRS rainfall rate (mm/day) correlation (left) and false alarm ratio (right) compared to rain gauge observations over the continental U.S. The black line represents MIRS, while the red line represents radar versus rain gauge.....	62
Figure 39. MIRS daily rainfall rate (upper left) and CPC rain gauge analysis (upper right) from May 15, 2009 12Z to May 16, 2009 12Z. Timeseries of MIRS daily rainfall rate correlation (bottom left) and detection failure ratio (bottom right) compared to CPC, stratified by sensor...	63
Figure 40. MIRS rain water path retrieval for NOAA-18 valid on July 27, 2014.....	64
Figure 41. Comparison of MIRS rain water path for NOAA-18 with TRMM 2A12 product over ocean.....	64
Figure 42. Comparison of MIRS rain water path path for NOAA-18 with TRMM 2A12 product over land.....	65
Figure 43. MIRS ice water path retrieval for Metop-B valid on July 27, 2014.....	66
Figure 44. Comparison of MIRS ice water path path retrieval histograms for Metop-B with MM5 simulated histograms. For MiRS, both v9.2 (previous version of MiRS) and the current v11 algorithms are shown indicating improved agreement with MM5 distribution in the current v11 algorithm.....	66
Figure 45. Comparison of MIRS ice water path path for NOAA-18 with TRMM 2A12 product over land.....	67
Figure 46. Scatter plots and performance statistics of MIRS (top) and MSPPS (bottom) SWE versus measured SWE.....	67
Figure 47. Comparison of MIRS N-18 AMSU/MHS snow water equivalent product (top left) with that from AMSR2 JAXA algorithm (top right) for January 30, 2013, along with corresponding scatterplot (bottom left).....	68
Figure 48: Comparison of N18 (top left), and F18 (top right) SGS retrievals (radius, mm) on January 30, 2013 with the GlobSnow analysis (bottom left). GlobSnow grain size is not an operational product. Courtesy of FMI/ESA.....	69
Figure 49. Scatter plots and performance statistics of MIRS Metop-B (left) SIC retrievals when compared with F17/SSMIS NASA Team (center) SIC on January 27, 2014, and August 1, 2014. Scatter plots are shown for Northern Hemisphere (top) and Southern Hemisphere (bottom).....	70
Figure 50: Comparison of MiRS F18 SSMIS first year sea ice concentration (SIFY) and multiyear concentration (SIMY) with dominant ice type analysis from the OSI-SAF operational system on January 2, 2013. OSI-SAF data available courtesy of NMI/EUMETSAT.....	72
Figure 51: Comparison of MiRS MetopB SFR (left) on February 26, 2015 with MSPPS SFR from OSPO website (right).....	73
Figure 52. Snapshot of the MIRS Menu Options	74

Figure 53. Snapshot of the MIRS Online Monitoring Tool (MOMT).....	75
Figure 54. MIRS source code directory structure	79
Figure 55. MIRS data directory structure	80

List of Tables

Table 1. Hardware requirements for MIRS package for NOAA-18 configuration (AMSU and MHS), for one-day processing. The platform type is not sensor-dependent.	13
Table 2. MIRS software requirements	13
Table 3.The heritage, MIRS 1DVAR and MIRS derived products. *Note that the SFR is an optional product based on MSPPS heritage algorithms currently requiring availability of ancillary NWP data from the GFS model (see text for further details). **Sea ice age and snow grain size are preliminary products.	24
Table 4. AMSU-A channels and passband characteristics	33
Table 5. MHS channels and passband characteristics	33
Table 6. SSMIS channels and passband characteristics.....	34
Table 7. SSM/I channels and passband characteristics.....	34
Table 8. ATMS channels and passband characteristics.....	35
Table 9. AMSR-E channels and passband characteristics.....	35
Table 10. TRMM TMI channels and passband characteristics.....	35
Table 11. Megha-Tropiques MADRAS channels and passband characteristics	35
Table 12. Megha-Tropiques SAPHIR channels and passband characteristics	36
Table 13. GPM GMI channels and passband characteristics.....	36
Table 14. Performance statistics of MIRS and MSPPS SIC versus SIC computed from collocated IMS data over the Northern hemisphere during 2006.	71

Section 1.0 How to Use this Manual

1.1 Inside Each Section

Section 1 gives instructions of how to get information not contained in this manual or request further assistance.

Section 2 provides a general description of the MIRS system application. It includes details on hardware and software requirements, levels of user interaction, normal operations, required training and system limitations.

Section 3 provides theoretical algorithm description, followed by descriptions of MIRS component processes.

Section 4 provides a brief description of the input files.

Section 5 provides a brief description of the output files.

Section 6 provides validation examples of the MIRS retrieved parameters.

Section 7 describes the procedures for the operational dissemination of the MIRS products. The web links to MIRS online product monitoring are also provided in this section.

Section 8 provides useful information on MIRS software implementation including access to the MIRS package, compilation, running and modes of implementation.

1.2 Additional Documentation

This document is intended for using MIRS. It briefly describes all components of the system, overall performance, software and data structures, and running procedures. The following documents provide further details for the interested reader:

- MIRS Algorithm Theoretical Basis Document (ATBD) contains detailed description of MIRS science algorithms
- MIRS Interface Control Document (ICD) contains detailed description of MIRS data files
- MIRS System Description Document (SDD) contains specific information on system functionality and software and hardware requirements
- MIRS Maintenance Manual (MM) contains detailed information on the software, operating environment and maintenance procedures as well as installation and compilation, product processing controls.

- MIRS Operations Manual (OM) contains specific information on system runs, setup procedures, run schedules and controls, error procedures, system security, product distribution and back-up/recovery procedures.

1.3 How to Get Help

To get help on topics not covered in the referenced documents above, send an email to the following persons:

- For software, validation & products quality assurance, please send your e-mail to: *Quanhua (Mark) Liu, Ph.D., Science Lead, quanhua.liu@noaa.gov*
- For operational availability and access to operationally generated files, please send your e-mail to: *Limin Zhao, Ph.D., MIRS Operational Team Lead, Limin.Zhao@noaa.gov*
- For management, please send your e-mail to: *Ralph Ferraro (Ralph.R.Ferraro@noaa.gov)*
- For web site related requests, please send your e-mail to: *Lori Brown, STAR Webmaster, Lori.Brown@noaa.gov.*

Section 2.0 Introduction

This section gives an overview of MIRS applications. First, it provides the user with useful information on hardware and software requirements. Next, the levels of interaction for running part of or the entire system are described in detail, followed by description of procedures for normal operations, required training and system limitations.

2.1 Hardware Requirements

Currently, 1 CPU, 1GB memory, and 5 GB available hard drive space is the minimum required hardware configuration needed to run MIRS (Table 1). These hardware requirements (CPU, RAM, and Hard Disk space) are for the NOAA-18 AMSU-MHS sensor configuration for one day of operations. This is roughly the requirement for the daily processing of MIRS at the NOAA/NESDIS Center for Satellite Applications and Research (STAR). The disk space available is currently over 1 TB and the CPU speed is between 2.5 and 3.3 GHz.

MIRS Requirements	Minimum# of CPUs	Minimum RAM	Min. Hard Disk Space	Platform Type
	1	1 GB	5 GB	LINUX/UNIX

Table 1. Hardware requirements for MIRS package for NOAA-18 configuration (AMSU and MHS), for one-day processing. The platform type is not sensor-dependent.

2.2 Software Architecture

2.2.1 Requirements

Most of the MIRS applications and processes have been implemented in a standard Fortran-95. Process control and configuration, e.g., for testbed applications, is implemented in BASH scripts. Visualization and performance monitoring are implemented using IDL. The Graphical User Interface (GUI) is implemented using Java software. A small amount of code is written in C and C++, mainly related to reading Level 1b raw data records (RDRs) and for optionally writing MiRS output products to netCDF files. The system is designed using dynamic memory allocation, allowing it to be sensor- and parameter-independent. It is highly modular, so its maintenance and updates are easy to implement. Table 2 summarizes the MIRS software requirements.

MIRS Requirements	Operating System	F95 Compiler	C/C++ Compiler	Commercial Software(s)	Freeware(s)
	LINUX/UNIX	Standard	Standard	IDL v5 and up	BASH, JAVA v1.6. & up

Table 2. MIRS software requirements

2.2.2 Directory Structure

The directory structure of MIRS has been designed to be streamlined and compatible with operational needs and requirements. Figure 1 depicts the top level and source level directories, which is briefly described below:

- The “/src” directory contains all source code files in Fortran-95, C/C++, IDL, BASH and JAVA.
- The “/bin” directory contains all executable files. Sensor-specific processes and applications are distinguished by prefix. For example, the “fm_n18_amsua_mhs” executable runs the process of foot-print (fm) matching for NOAA 18 AMSU-MHS.
- The “/scripts” directory contains all the scripts used for system control and configuration.
- The “/setup” directory contains the setup control files used for setting up paths to data, processes and applications.
- The “/gui” directory contains the GUI-based MIRS Control Panel (MCP) used for user-friendly interaction with and control of processes and applications.
- The “/doc” directory contains all the documents including User Manual, Interface Control Document, System Description Document, and the Directory Structure.
- The “/data” directory contains all the data files organized into sub-directories by functionality, e.g., raw sensor and analysis data are categorized as external data, the set-up files are categorized as static data, and footprint-matched sensor data as dynamic data.
- The “/logs” directory contains all log files generated by MIRS.

The main highlights of this structure are:

- Consolidation of all executables into the “/bin” directory
- Consolidation of all source code files (F95, C/C++, IDL, BASH and JAVA) into the “/src” directory, decoupled from the control and input files. This makes it easy to remove all source files from the package, e.g., when transitioning to operations.
- MIRS scripts are written to be *data-location-independent* (file and path names moved into setup files). Data directory structure can be modified through the setup file with the control scripts.

Figure 2 depicts the organization of the source code sub-directory structure, which is briefly described as follows:

- The “/1dvar” directory contains 1DVAR code for generating EDRs from radiance data.
- The “/fwd” directory contains the forward operator code for reproducing radiances from EDRs.
- The “/crtm” directory contains the Community Radiative Transfer Model (CRTM) code.
- The “/lib” directory contains the library modules written in Fortran-95 for data typing, input/output reading and writing and the inverse processing.

- The “/lib_idl” directory contains the IDL libraries for data typing, input/output reading and writing, data collocation, background covariance computations, etc.
- The “/lib_java” directory contains Java code general utility functions.
- The “/lib_cpp” directory contains C++ code general utility functions.
- The “/qcDelivery” directory contains the IDL code for comparing MIRS-generated EDRs with benchmark files.
- The “/testbed” directory contains codes for MIRS applications, e.g. footprint matching, bias correction and monitoring, figure generation, etc.

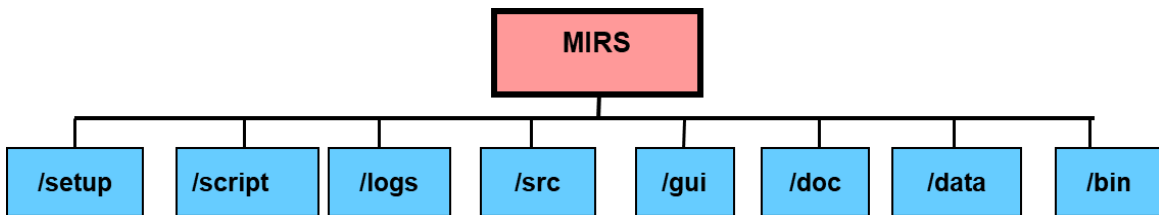


Figure 1. MIRS top level directory structure. The source code, scripts for running MIRS, the set-up files, executables, documentation, graphical user interface, data and logs files are kept under separate directories.

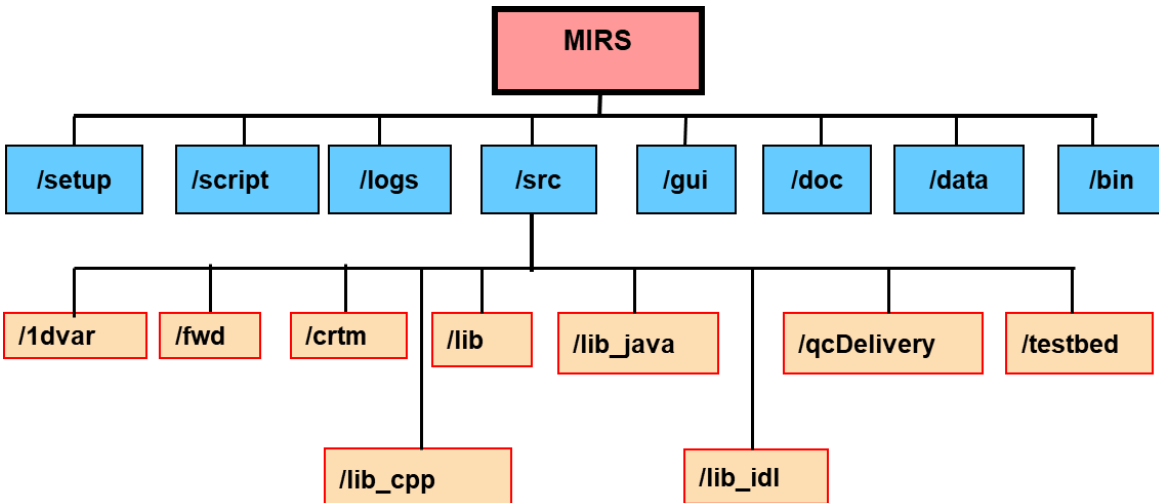


Figure 2. MIRS source code directory structure. Note the library directories in Fortran-95 (lib), IDL (lib_idl), and Java (lib_java) which include code for performing generic functions. The “testbed” directory includes code for MIRS real-time applications, e.g. footprint matching, bias-correction, figure generation, etc. .

2.2.3 Interfaces

MIRS interfaces with the external input files and the post-inversion processes that utilize MIRS output files. External input interfaces involve level 1b sensor data files and the Numerical Weather Prediction (NWP) analysis files. The NWP files are only used for calibration and performance monitoring, and are not required for 1DVAR retrievals. Internal input interfaces include the static

data files, described below in section 4. For more detailed description of these files the reader is referred to the Interface Control Document (ICD). Care must be taken to ensure that the external input files have formats that are consistent with MIRS. The external data files are put under the “/data/ExternalData” sub-directory. Reading of these data files requires sensor-specific code. The NWP data files are also read using NWP-specific readers. These readers are found under the “/src/lib/io” sub-directory which contains all Fortran-95 input/output modules. Similarly, the output of MIRS can be read via existing modules under “/src/lib/io” for Fortran-95 readers and “/src/lib_idl” for IDL readers.

2.2.4 User's Interaction

MIRS can accommodate three levels of interaction, each depending mainly on the need and level of expertise of the user. Figure 3 presents a diagram that shows the top-to-bottom interactions that the user could have with MIRS with increasing level of expertise.

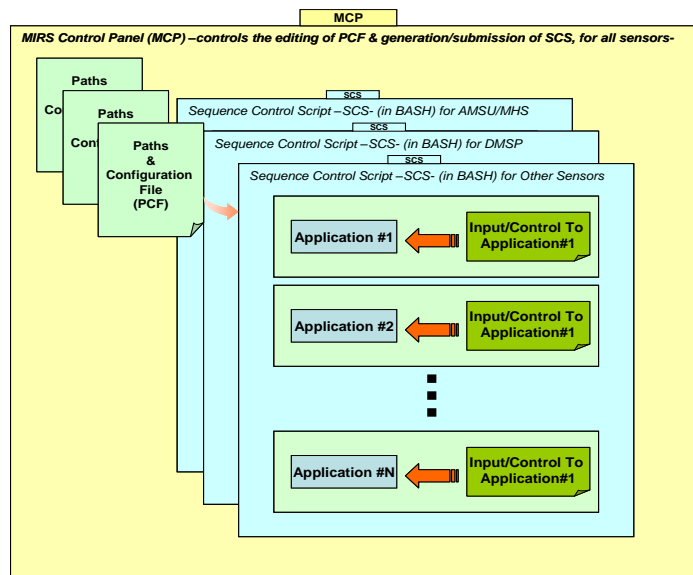


Figure 3. Description of the three (nested) levels of user interaction. The innermost small blocks represent the low-level interaction consisting of individual applications and the control files as input (indicated by red arrows) to their executables. The mid-level interaction is represented by the (outer) panels with the PCFs and SCSS for a particular satellite that control the sequencing of the individual applications. The outermost panel represents the highest level of interaction through the GUI-based MCP.

The highest level would only require working with a GUI-based tool called the MIRS Control Panel (MCP). At the mid-level interaction, the user would directly edit the Sequence Control Scripts (SCS) for an individual sensor, and the associated Paths & Configuration File (PCF) to control which process to run, what options to turn ON/OFF, etc. At the lowest level of interaction, the user would directly execute the individual application, e.g. 1dvar, footprint matching, and edit the associated control/input file (a namelist file for F95 applications and a similar controlling-parameters list file for IDL applications). Further details are given below

2.2.4.1 High-Level Interaction

At the highest level, the user would make use of the MIRS Control Panel (MCP) to run and control MIRS processes and applications. The MCP is a Graphical User Interface (GUI) Java- based tool aimed at making the use of MIRS as user-friendly as possible. It also makes the maintenance of the MIRS system as seamless as possible, since all tasks are centralized in one place. The MCP allows the user to interactively adapt the data directory structure to the user's particular needs, modify compilation and running using different scientific options, run each or a collection of MIRS processes, dynamically generate BASH scripts in order to later submit them through cronjobs and/or other schedulers, switch between the daily and orbital mode processing and select parameters to be retrieved in 1DVAR. A snapshot of the MCP display is presented in Figure 4.

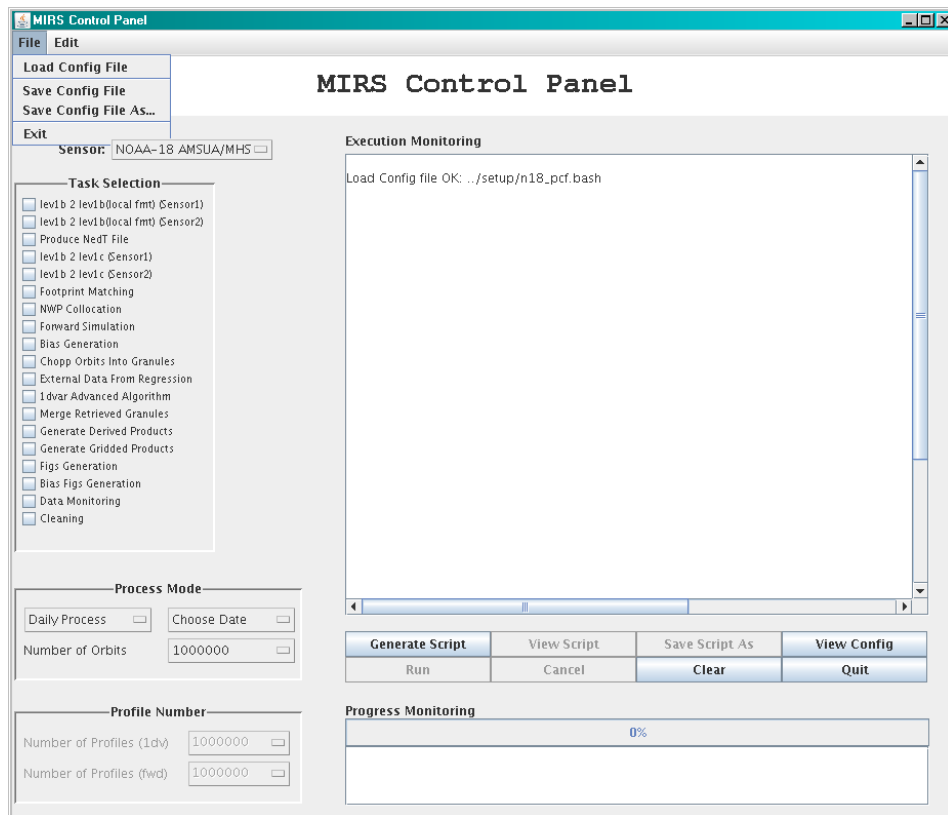


Figure 4. Snapshot of the MIRS Control Panel (MCP) showing some of the options available in the main window.

To activate the MCP, the following command lines are executed in the “gui” top level directory:
make - for compiling and,
make run - for running the MCP. The MCP panel will pop up.

2.2.4.2 Mid-Level Interaction

As part of the MIRS package, a number of Sequence Control Scripts (SCS) written in BASH are distributed as benchmark files. Corresponding to these scripts are the Paths and Configuration Files (PCFs) from which the SCS extracts the information on configuration and paths. The PCFs and SCSs can be interactively modified and generated via the MCP. The user can also manually generate his own SCSs and PCFs by changing the content of the provided SCSs or the PCFs. An example of the PCF content is given in Figure 5.

```
#-----
# SECTION OF DATA AND PATHS
#-----
#   Satellite, sensor and default date used in GUI
#-----
satId=n18
sensor1=amsua
sensor2=mhs
date=2006-02-01
#-----
# Major root paths
#-----
rootPath=/net/orbit006l/home/sidb/mirs'
dataPath=${rootPath}/data'
binpath=${rootPath}/bin'
#-----
#   External data & Paths
#-----
externalDataPath=${dataPath}/ExternalData
rdrSensor1Path=${externalDataPath}/rdr/n18_amsua_mhs
rdrSensor2Path=${externalDataPath}/rdr/n18_amsua_mhs
rdrOrbitPath=${externalDataPath}/rdr/OrbitalMode
nwpGdasGridPath=/net/orbit138l/disk2/pub/wchen/gdas
nwpEcmwfGridPath=/net/orbit138l/disk2/pub/wchen/ecmwf
#-----
#   Static data & Paths
#-----
staticDataPath=${dataPath}/StaticData'
instrumentPath=${staticDataPath}/InstrConfigInfotopographyFile=${staticDataPath}/Topogr
aphy/topography.bin_sgi
#-----
# SECTION OF SWITCHES (WHICH APPLICATION TO RUN)
#-----
step_rdr2tdrSensor1=1 #RDR->TDR (Sensor1)
step_rdr2tdrSensor2=1 #RDR->TDR (Sensor2)
step_mergeNedt=1      #MERGE NEDTs (Sensor1 and Sensor2)
#-----
# SECTION OF CONTROLLING FLAGS
#-----
processMode=1 #0:Orbit processing 1:Daily processing
sensorId=1   #Sensor:1:N18,2:MetopA,3:F16, 4:Windsat
nAttempts=1   #Number of retrieval attempts in case of non-convergence
```

Figure 5. Sample of the Paths & Configuration File (PCF) generated automatically by the MIRS Control Panel (MCP).

2.2.4.3 Low-Level Interaction

Low-level interaction requires the user to control each individual application, e.g. 1dvar, forward operator, footprint matching, by manually editing the control file (namelist) and modifying the inputs required for the particular application. The control files are located in the “/data/ControlData” sub-directory and are distinguished by process and sensor represented

by prefix in their names. The input files named in the control file are located in the “/data/InputsData” sub-directory. The executables for all applications are consolidated in the “/bin” top level directory. An example of manually running an application through this low-level interaction is the following command line which executes the footprint matching process for NOAA-18 satellite:

```
~user/mirs/bin/fm < ~user/mirs/data/ControlData/n18_fm_YYYY-mm-dd.in
```

2.3 Procedures for Normal Operations

The normal operation procedure of MIRS can be accomplished via each level of interaction, i.e., GUI-based, manually based by controlling execution of MIRS processes with the SCSs and PCFs, or manually based by executing each individual application. The normal modes of execution on an operational machine are provided below.

➤ *The daily processing mode:* This mode is used for processing a set of sensor data files all at once. This could be the set of orbit files for a full day or a subset of a day’s orbits, or a number of files corresponding to a full week. In this mode, the sensor data files are placed under a single directory. To run MIRS in this mode, execute the sensor-specific Sequence Control Script (SCS) located in the “/scripts” top level directory with or without an argument. There are three forms that the argument to the SCS can take:

- **Conventional date (yyyy-mm-dd):**

n18_scs.bash

n18_scs.bash 2014-09-12

The examples above are for running NOAA-18 configuration, distinguished by the “n18” prefix. The first command directs MIRS to look for level 1b inputs from a directory with the name YYYY-MM-DD corresponding to the previous day’s date, appended to the “externalDataPath” variable in the PCF (located in the “/setup” top level directory). This directory would exist under, for instance, the “/data/ExternalData/rdr” sub-directory whose full path is defined in the PCF.

The second command specifically forces MIRS to search for a local directory named after the requested date e.g. 2014-09-12 under the “/data/ExternalData/rdr” sub-directory. This is the current operating mode daily at STAR. A cronjob is scheduled every night to execute the command “n18_scs.bash”

- **Full input directory path:**

n18_scs.bash </Full/path/to/rdr/directory>

In this example the user can specify the full directory path to the location of the level 1b (RDR) data. For example, if the location of the RDR files (normally representing an entire day) was

- ```
/data/data006/pub/user/mirs_working/data/ExternalData/rdr/n18_amsua_m
hs/benchmarkData
```
- then this would be entered directly as the argument to the SCS
- **Partial input directory path:**  
*n18\_scs. bash <relative/path/to/rdr/directory>*

In this example the user can also specify a partial or relative path to the location of the RDR files. In order to use this option, the user must make sure that the path to the external data (externalDataPath) is properly specified in the PCF. For example, if the PCF contains the definition:

```
externalDataPath=/data/data006/pub/user/mirs_working/data/ExternalData
a
```

and the user enters:

```
n18_scs. bash benchmarkData2
```

then the full directory path that will be used as the location of the RDR data would be:

```
/data/data006/pub/user/mirs_working/data/ExternalData
rdr/n18_amsua_mhs/benchmarkData2
```

- *The orbital processing mode:* This mode is specifically designed to run MIRS for one orbit at a time. In this case, one argument is required and it must correspond to the name of an orbital data file (like the AMSU or MHS level 1b orbit files). Note that the name cannot have a path. The path that MIRS will use to search for these orbit filenames is defined in the PCF. An example for running MIRS under this mode is execution of the following command line in the “/scripts” top level directory for an AMSU orbit on September 12, 2014:

```
n18_scs. bash NSS.AMAX.NN.D14255.S0051.E0246.B4798283.GC
```

In this mode and in an operational setting, the operational user would normally have a script which runs frequently to detect the presence of a new orbit that arrived and in which case it will trigger the call to MIRS with the filename of the newly arrived orbit using the command above.

Note that every sensor has its own SCS, e.g., n18\_scs.bash for NOAA-18 AMSU-MHS, n19\_scs.bash for NOAA-19 AMSU-MHS, metopA\_scs.bash for METOP-A, metopB\_scs.bash for METOP-B, f16\_scs.bash for F-16 SSMIS, f18\_scs.bash for F-18 SSMIS, etc. The log files (also identifiable by the sensor-specific prefix) are found under the “data/logs” sub-directory.

## 2.4 Required Training

There is no particular training required to be able to run MIRS other than the instructions given in this Manual. The MIRS user is encouraged to read the User Manual in its entirety. For a deeper understanding of the MIRS system it is suggested that the algorithm theoretical basis document be read as well. The Interface Control Document (ICD) presents the details of the input and output files (contents, format, etc.).

## 2.5 System Limitations

There are known limitations that limit the applications of MIRS. Most of these limitations are of a scientific nature. Other limitations are more directly related to the system or to its external components.

- MIRS inversion algorithm is based on the assumption that the forward modeling is quasi-linear. This might not be the case in cloudy and precipitating conditions. As a result, the solution reached by the retrieval algorithm may not be optimal, or it may be the case that no solution is reached at all (no convergence).
- MIRS is also based on the assumption that the geophysical state vector follows a normal probability density distribution. This is the case for some geophysical parameters but not for all of them. Most notably, the water vapor parameter does not follow a normal distribution. This also could cause the solution to be non-optimal. The cloud and precipitation parameters do not follow a normal distribution. A work-around to this limitation was implemented in MIRS by performing the retrieval in logarithmic space. This method obviously does not resolve non-optimality or non-convergence entirely. However, it improves it considerably.
- MIRS covariance matrices were developed based on a limited set of radiosonde measurements. These matrices are clearly not representative of all natural variations, especially for the upper atmosphere humidity. Note that for processing of Megha-Tropiques/SAPHIR data, a different set of covariance matrices are used which are derived from ECMWF analyses in the tropics.
- The MIRS package runs well on Linux platforms. It was also tested successfully on AIX but with the version 8.1 of the xlf compiler, a patch to a compiler bug was implemented. The other versions of the IBM xlf compiler had a bug but no patch to them. The IBM fix patch for these later versions has been released, but no internal test has been performed to test its effect.

---

## Section 3.0 Algorithm Description

### 3.1 Theoretical Basis

MIRS is based on the one dimensional variational retrieval (1DVAR) approach. The inversion is an iterative physical algorithm that optimally extracts the information content present in the measurements. It performs the retrieval in a consistent fashion, with the end result being a set of geophysical parameters or Environmental Data Records (EDRs) that are computed simultaneously and, when used as inputs to the forward model, would nominally fit the measured radiances to within the noise level. The retrieval is performed in a reduced space by using Empirically Orthogonal Function (EOF) decomposition to allow a more stable inversion, a faster retrieval and to avoid the null space. MIRS is coupled with the Joint Center for Satellite Data Assimilation (JCSDA) Community Radiative Transfer Model (CRTM) which is valid in both microwave and infrared spectral regions, in clear, cloudy and precipitating conditions and over all surface types.

The mathematical basis for the inversion problem is to find a vector  $X$ , in this case, a set of geophysical parameters, given a vector of measurements  $Y^m$ , in this case a vector of radiometric data (radiances or brightness temperatures). Several techniques are available, the suitability of which mainly depends on the nature of the inversion problem. These techniques have different names but generally result in the same mathematical expressions. Among the names found in the literature are: maximum probability solution (MPS), one-dimensional variational retrieval (1D-VAR), Bayesian algorithm, Optimal Estimation Theory, etc. Two important assumptions are made, namely, the local-linearity of the forward problem and the Gaussian nature of both the geophysical state vector and the simulated radiometric vector around the measured vector. With these assumptions, the mathematical problem can be formulated as a minimization of the following cost function:

$$J(X) = \left[ \frac{1}{2} (X - X_0)^T \times B^{-1} \times (X - X_0) \right] + \left[ \frac{1}{2} (Y^m - Y(X))^T \times E^{-1} \times (Y^m - Y(X)) \right]$$

where  $X_0$  and  $B$  are the mean vector and covariance matrix of the vector  $X$  respectively.  $E$  is the measurement and/or modeling error covariance matrix.  $Y$  is a forward operator capable of simulating a measurements-like vector. The left term represents the penalty in departing from the background value (a-priori information) and the right term represents the penalty in departing from the measurements. The solution that minimizes this two-termed cost function is sometimes referred to as a constrained solution. The minimization of this cost function is also the basis for the variational analysis retrieval. The solution that minimizes this cost function is easily found by solving for:

$$\frac{\partial J(X)}{\partial X} = J'(X) = 0$$

which has the following iterative solution:

$$\Delta X_{n+1} = \left\{ BK_n^T (K_n B K_n^T + E)^{-1} \right\} \left[ (Y^m - Y(X_n)) + K_n \Delta X_n \right]$$

where  $n$  is the iteration index,  $K$  is the matrix of partial derivatives of  $Y$  with respect to the state vector  $X$  (Jacobian) and  $\Delta X$  is the departure from the background value. At each iteration  $n$ , a new optimal departure from the background is computed given the current geophysical and radiometric departures. The derivatives and the covariance matrices (error/modeling covariance and the geophysical covariance) are also computed. This is an iterative-based numerical solution that accommodates slightly non-linear problems or parameters with slightly non-Gaussian distributions. MIRS performs the retrieval in one loop. The whole geophysical vector is retrieved as one entity, ensuring a consistent solution that fits the radiances. The constraints are in the form of the measurements as well as the assumed a-priori information. In the retrieval scheme used by MIRS, the departure from the measured radiances is normalized by the noise level (NEDT) impacting the measurements and the uncertainty in the forward modeling, making it possible to sometimes use the signal of a particular channel when the geophysical signature (through the derivative) is stronger than the noise (leading to a useful signal-to-noise level), and some other times dismiss the same channel when the signal in question is within the uncertainty/noise level. The departure from the background is also scaled by the uncertainty placed on the background. This makes it harder for the retrieval to depart from the background information if it is deemed accurate. The source of these backgrounds can vary from simple climatology (loose background errors) to NWP forecast fields (tight errors in the temperature background).

The MIRS system was designed to be a flexible retrieval tool and is therefore suited for applications in the microwave as well as the infrared, although it has been applied only to microwave frequencies instruments thus far.

## 3.2 MIRS Applications and Products

MIRS is the retrieval platform for current and future microwave systems such as the NOAA, METOP, DMSP, NPP/JPSS sensors (AMSU, MHS, SSMI/S, ATMS) and could be an exploratory algorithm for IR sensors onboard JPSS and GOES-R. It is used operationally at NOAA to produce a number of products for several users.

The list of products generated by MIRS is given in Table 3. Also included is the list of heritage products, e.g., generated by MSPPS. “Standard” products are labeled those that have been routinely retrieved and for which extensive validation and testing has been done. “Experimental” products are routinely retrieved, but have not been and extensively tested or validated. “Preliminary” products are those which are routinely produced, and have passed beyond “experimental” phase to a higher level of maturity based on validation and testing. They are considered the last step prior to full standard operational status. Listed are the MIRS 1DVAR and derived products. MIRS 1DVAR products include the parameters that are part of the retrieval state vector. MIRS derived products are those generated using MIRS 1DVAR parameters as inputs and a post-processing procedure, e.g., a simple vertical integration of retrieved water vapor profile for computing Total Precipitable Water (TPW), a new algorithm, e.g., for the estimation of Snow Water Equivalent (SWE) from the retrieved surface emissivities, or an integration of a heritage algorithm from MSPPS such as Snowfall Rate (SFR). Note in the Table MIRS profiling capability,

which is lacking in MSPPS. Note also the list of MIRS experimental products (1DVAR and derived) which would require new validation efforts.

| MIRS Heritage Products                | MIRS 1DVAR Products                    | MIRS derived products                |
|---------------------------------------|----------------------------------------|--------------------------------------|
| <i>Standard Products</i>              |                                        |                                      |
| Total Precipitable Water (TPW)        | Atmospheric temperature profile (T)    | Q-based TPW                          |
| Cloud Liquid Water (CLW)              | Atmospheric humidity profile (Q)       | Non-precipitating-based CLW          |
| Land Surface Temperature (LST)        | Land Surface Temperature (LST)         | IGP-based IWP                        |
| Emissivity at certain window channels | Emissivity vector (Em)                 | RP-based Rain Water Path (RWP)       |
| Rain Rate (RR)                        |                                        | Em-based SIC                         |
|                                       |                                        | Em-based First-Year SIC**            |
|                                       |                                        | Em-based Multi-Year SIC**            |
| Ice Water Path (IWP)                  |                                        | Em-based SCE                         |
| Snow Water Equivalent (SWE)           |                                        | Em-Based Surface Type                |
| Sea Ice Concentration (SIC)           |                                        | CLW,RWP&IWP-based RR                 |
| Snow Cover Extent (SCE)               |                                        | Em-based SWE                         |
|                                       |                                        | Em-based Snow Effective Grain Size** |
|                                       |                                        | SFR*                                 |
| <i>Experimental Products</i>          |                                        |                                      |
|                                       | Ice Surface Temperature (IST)          |                                      |
|                                       | Snow Surface Temperature (SST)         |                                      |
|                                       | Non-precipitating Cloud Profile (NPCP) |                                      |
|                                       | Rain Profile (RP)                      |                                      |
|                                       | Ice/Graupel Profile (IGP)              |                                      |

Table 3. The heritage, MIRS 1DVAR and MIRS derived products. \*Note that the SFR is an optional product based on MSPPS heritage algorithms currently requiring availability of ancillary NWP data from the GFS model (see text for further details). \*\*Sea ice age and snow grain size are preliminary products.

An expected benefit of using MIRS would be self-consistency of the retrieved EDRs. Because the same physical approach is used consistently across the platforms (different channels spectra, polar and geostationary orbits), the time series of these retrievals would thus be self consistent, making the resulting climate data records free of jumps due to changes in sensor-dependent algorithms. The sensor characteristics to which MIRS has been or will be applied are summarized in subsection 3.4.

### 3.3 MIRS Components

This section provides a description of MIRS components. *Top-to-bottom* descriptions are provided: first, the high-level blocks are described, followed by individual and more detailed descriptions of each block. Figure 6 presents the basic conceptual diagram of the high-level MIRS blocks. The radiance processing is the interface with the inputs to MIRS, e.g., sensor data files and with the inversion processing (1DVAR). It generates bias-free, ready-to-invert radiances or

brightness temperatures that are used as main inputs to the inversion process. The inversion process generates retrieved EDRs from these bias-free radiances.

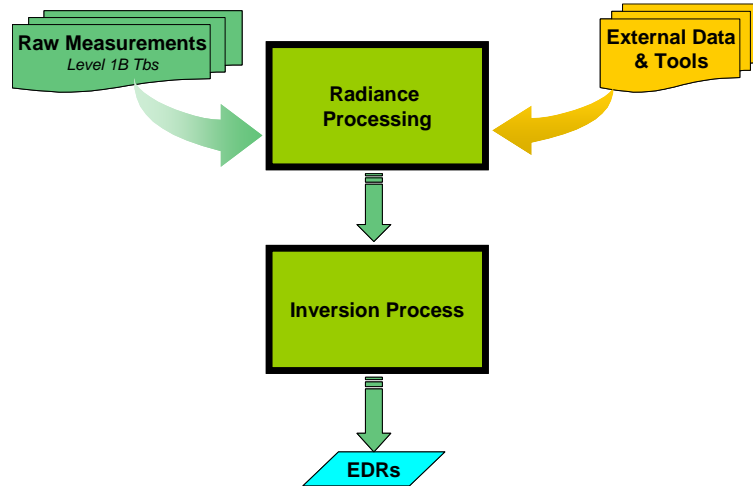
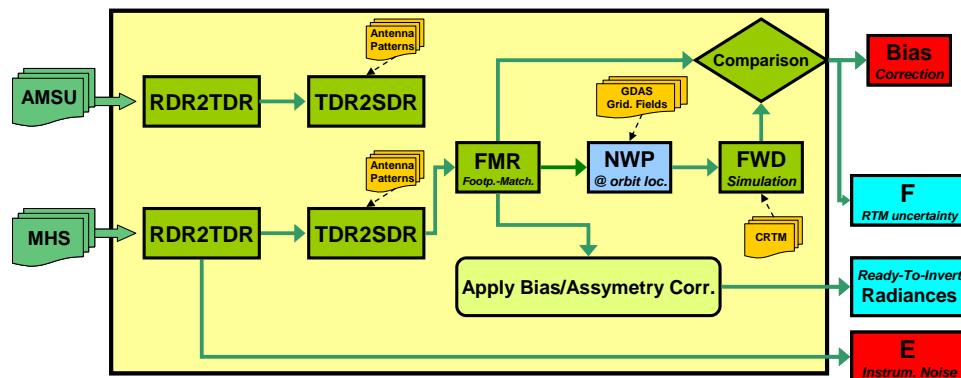


*Figure 6. Overall conceptual diagram of the Microwave Integrated Retrieval System (MIRS) concept. Shown are the major components, the radiance and the inversion processing blocks.*

### 3.3.1 Radiance Processing

The radiance processing is described in detail in Figure 7. The figure shows the chain of applications for converting raw sensor data, e.g. AMSU and MHS from the decoded raw sensor data to ready-to invert radiances. First, raw sensor data are converted into MIRS internal format (rdr2tdr). Next, MIRS internal format sensor data are antenna-pattern corrected (tdr2sdr), footprint-matched ( $f_m$ ) and bias-corrected. This block also generates the noise files (NEDT) used for computing instrument noise matrix  $E$  (only for AMSU-MHS). The noise values are assessed as part of the performance monitoring. This block collocates gridded NWP fields with satellite measurements. These collocated NWP data files are used as inputs to the forward model to simulate brightness temperatures and compare them with measurements for assessment of instrumental bias. This assessed bias is channel and scan position dependent. Along with the bias file, the radiative transfer model (RTM) uncertainty is also assessed based on the standard deviation between the measured and simulated radiances.



---

*Figure 7. Conceptual diagram of the radiance processing block, detailing the component processes involved.*

### **3.3.1.1 Antenna Pattern Correction**

Currently, this application is a simple placeholder. No antenna pattern is applied at this time. There is therefore no difference between the TDR and the SDR files in MIRS. The first order effect of not accounting for the antenna pattern is a bias in the obtained field of view measurements. This first order effect is removed through the bias removal procedure described below. A second order effect is due to the scene interaction with the antenna pattern which increases the standard deviation of the difference between the true brightness temperature and the actual one impacted by the side lobes of the antenna. This effect is currently not removed in MIRS.

### **3.3.1.2 Footprint Matching**

Footprint matching is the procedure that ensures that all channels for the retrieval view the same location on the Earth. The footprint matching is a sensor-specific application because every sensor has its own characteristics and viewing geometry. For example, the default nominal footprint matching implemented in MIRS between the AMSU and the MHS (for NOAA-18, NOAA-19 and MetopA, and MetopB systems) is high-resolution mode, in which the AMSU measurements are assumed valid across the 3x3 MHS footprints, resulting in a 20-channel measurement at the MHS resolution. Alternatively, the footprint matching may be done using a simple 3x3 averaging technique of MHS microwave measurements to produce a set of 20 channels (AMSU and MHS together) having the same (AMSU) footprint. This option may be selected in the PCF.

For ATMS, the footprint averaging/resampling algorithm from the EUMETSAT ATOVS and AVHRR Preprocessing Package (AAPP) is used. As currently implemented, the lower frequency channels 1 and 2 (23 and 31 GHz) which have an original measurement beam width of 5.2 degrees are resampled to an equivalent beam width of 3.3 degrees. Channels 3 through 16 (50 through 88 GHz) which have a beam width of 2.2 degrees, and channels 17 through 22 (165 through 183 GHz) which have a beam width of 1.1 degrees, are not averaged or resampled. Because the AAPP algorithm is used for ATMS measurements, the handling of input TDR files (granules) is slightly different than for other sensors. In order to apply the algorithm (96 footprints/scan line) the footprint matching algorithm normally requires several scan lines immediately before and after the current scan line currently being processed. Since ATMS granule files are small (12 scan lines per granule), the normal procedure is to automatically read in the granules immediately preceding and following the current granule file being processed. The exceptions to this would be (1) one or more missing granule files due to some technical problem, or (2) the first and last granules of the day being processed. In either of these cases, the AAPP footprint matching will simply “mirror” the first several and/or last several scan lines of the granule (as is normally done for the footprints at the edge of each scan line) to create a buffer of footprint values required for the successful execution of the algorithm.

For the DMSP SSMIS sensor measurements (e.g. F17, F18), footprint matching resolution may also be selected by the user. The current nominal matching is performed at high-resolution. This means that both the temperature sounding channels (LAS) 1-7, the surface window channels

(ENV) 12-16, and the water vapor and high-frequency window channels (IMG) 8-11, 17-18 are all averaged and subsampled to produce collocated measurements with an effective spatial resolution of 20-40 km and a horizontal spacing along scan of 25 km (90 footprints per scan line). Alternative footprint matching options (course and low resolution) will produce 30 and 60 footprints per scan line, respectively.

For Megha-Tropiques/SAPHIR, the footprint matching step can be run at three different resolutions and two different sampling modes. The spatial resolutions for SAPHIR footprint matching are high resolution, low resolution, and coarse resolution, referred to as HR, LR, and CR, respectively. At HR or full resolution, no modification of the original resolution is done and the data are processed at a resolution of 10 km (nadir) using all measurements along a scan line (130 per scan). In LR, only half the number of measurements are used (65 per scan), and in CR, one quarter of the measurements are used (23 per scan). The footprint matching sampling modes are either thinning, or averaging. For LR and CR in thinning mode (the default), the measurements are sub-sampled along the scan to obtain the reduced number of samples, and the original spatial resolution of each measurement is retained. In averaging mode, the individual FOVs are averaged along the scan to obtain the reduced number of samples, thereby reducing the effective spatial resolution of each measurement. Note that in HR footprint matching, the sampling mode has no effect since all the data are used at the full resolution.

### 3.3.1.3 Bias Removal

The bias removal is a procedure that applies a pre-computed bias offset (generated in the radiance processing) to the sensor measurements to produce ready-to-invert radiances. Bias removal is a generic term to define the removal of systematic differences between the forward operator and the actual measurements. Several bias removal techniques are incorporated into MIRS.

- Offset bias removal. A mean value of the differences between the simulations and the measurements is computed for each scan position for every channel and stored. The application of the bias is also simple. It is done by applying an additive term to the measurements.
- Slope/Intercept Correction. Instead of computing the mean bias, the slope and intercept are computed from linear regression of the measurements against the simulations. These slope/intercept pairs are then applied to the brightness temperatures.
- Histogram Adjustment: This methodology removes bias by adjusting the histogram of the brightness temperature difference between simulated and actual measurements to make it centered around zero. This process reduces the sensitivity of measurements to clouds, precipitation and coastal contamination.

The bias removal method used by default in MIRS is histogram adjustment.

### 3.3.2 Inversion Processing

Figure 8 describes the conceptual organization of the inversion process. As shown, ready-to-invert measurements generated from the radiance processing are used as inputs to the heritage algorithms and MIRS 1DVAR, the latter referred to in the figure as “advanced”. The heritage algorithm products can optionally be used as first guess in the advanced retrievals. Note that this does not violate the mathematical requirement that the background errors and the instrumental/RTM errors be uncorrelated. This required condition is not violated because the heritage algorithms are used as first guesses, not as background constraints.

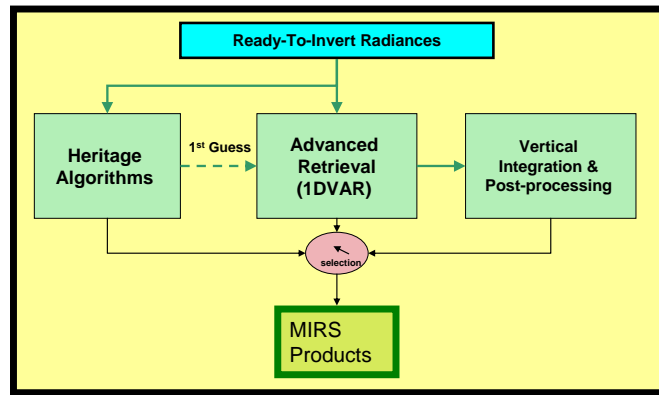


Figure 8. High-level diagram of the Inversion process block showing the MIRS concept of merging heritage, advanced and derived products.

The vertical integration and post-processing generates derived products from 1DVAR EDRs. A selection mechanism is implemented for final MIRS product generation (see Figure 8). This selection is based mainly on the degree of confidence and the extent of the validation performed.

### 3.3.2.1 Heritage Algorithms

The heritage algorithms (Figure 9) include the existing regression- and physically-based non-iterative algorithms such as MSPPS algorithms based on AMSU-MHS, or other sensor-specific algorithms such as those based on DMSP SSMIS and WINDSAT. Main purpose of these algorithms is their application in the MIRS 1DVAR processing as first guesses. Additionally, new regression algorithms, referred to as “locally developed algorithms”, are developed for the retrieval of a wider range of EDRs that can be integrated more efficiently and utilized in the 1DVAR processing as first guesses. These local algorithms have been developed off-line from brightness temperature data collocated with geophysical parameters. The geophysical parameters may be obtained from a variety of data sources. The current release of the MIRS uses ECMWF analysis. Current regression algorithms are available to retrieve temperature, moisture, skin temperature, emissivity, TPW, and CLW for use as a first guess to the 1DVAR.

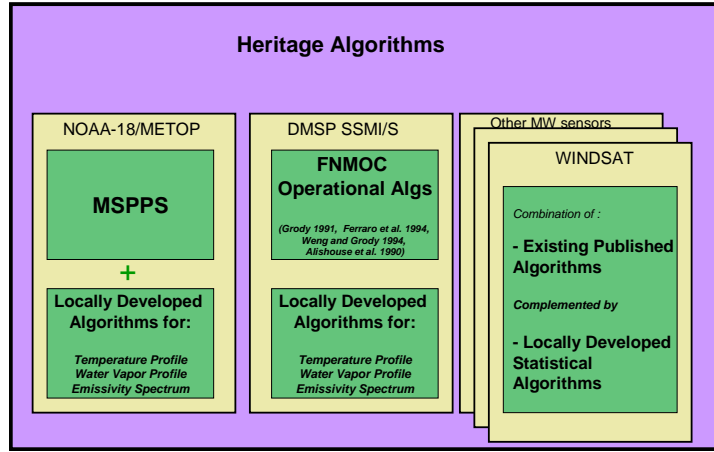


Figure 9. Heritage algorithms within MIRS. These algorithms depend on specific sensors. For NOAA-18 and METOP-A AMSU-MHS, the heritage algorithms are represented by MSPPS.

### 3.3.2.2 Advanced Algorithm (1DVAR)

The 1DVAR approach to retrievals is referred to as “advanced” since it is more optimal compared to heritage algorithms and it incorporates a sophisticated forward operator (missing in heritage algorithms) that fully assimilates sensor radiance measurements. It is schematically represented in Figure 10. The forward operator is based on the Community Radiative Transfer Model (CRTM) developed by the Joint Center for Satellite Data Assimilation (JCSDA). The CRTM produces the simulated radiances  $Y$  as well as the Jacobians  $K$ . The iterative loop is ended when convergence is reached. The unconstrained cost function is used as a metric for deciding if convergence has been reached.

$$\chi^2 = [Y^m - Y(X)]^T E^{-1} [Y^m - Y(X)]$$

Convergence is reached when  $\chi^2 \leq 1.0$ . The iterative loop is also ended if the convergence criterion is not met within seven iterations.

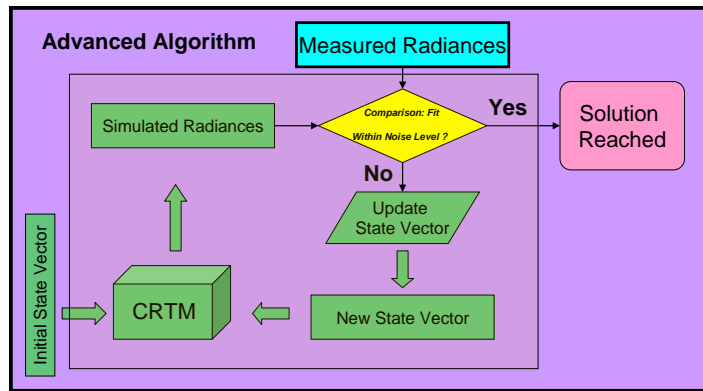


Figure 10. General description of the 1DVAR retrieval iterative system. The Initial state vector (or first guess) starts the iterations, the update of the solution takes place at each iteration depending on the local derivatives, simulated brightness temperatures, etc (see text). The solution is reached when the final simulations are fitting the measurements within the noise level. CRTM is used to generate the simulated measurements.

### 3.3.2.3 Vertical Integration and Post-Processing

The products generated by 1DVAR are utilized in a post processing stage to generate derived products, as shown in Figure 11. This post-processing can take the form of a simple vertical integration e.g. to derive TPW by vertically integrating the water vapor profile Q, or an algorithm, e.g., to derive the surface properties of snow cover and sea ice based on the 1DVAR retrieved parameters of surface emissivities and skin temperature.

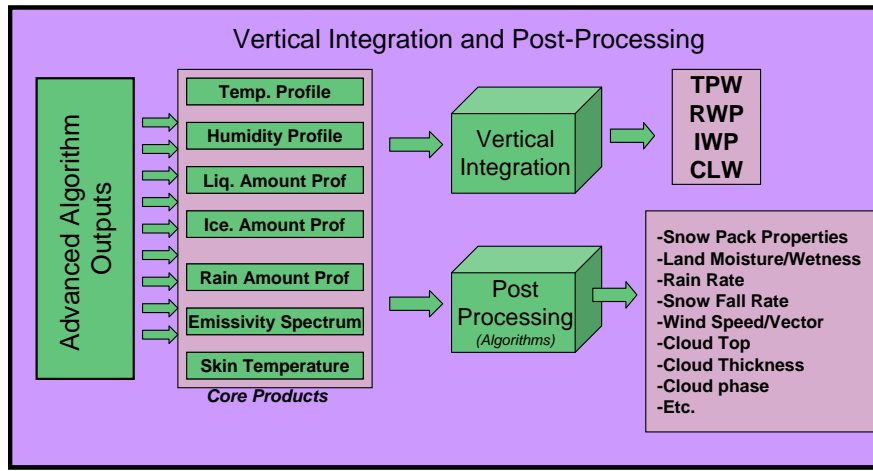


Figure 11. Schematic diagram of the MIRS main and derived products

To summarize, the derived products generated by vertically integrating the corresponding MIRS core retrieved products are: total precipitable water (TPW, from the retrieved water vapor mixing ratio profile), rain water path (RWP, from the retrieved rain water profile), ice water path (IWP, from the retrieved ice water profile), and cloud liquid water (CLW, from the retrieved cloud water profile).

Also related to the hydrometeor retrievals described above is the retrieval of surface rainfall rate (RR) which is derived from a post-processing algorithm which operates on the vertically integrated products CLW, RWP, and IWP. The algorithm to derive rain rate takes advantage of the physical relationship found between atmospheric hydrometeor amounts and surface rain rate. As shown in the equations below, the MIRS rain rate algorithm uses a regression approach that requires integrated CLW, IWP, and RWP (in mm), and a set of regression coefficients corresponding to each hydrometeor in order to retrieve the instantaneous rain rate in mm/hr over ocean and land.

$$RR_{ocean} = a_1 CLW^{b1} + a_2 (RWP + IWP)^{b2}$$

$$RR_{land} = a_3 IWP^{b3}$$

Where RR is the estimated surface rain rate, given in mm/hr, and  $a_1$ ,  $a_2$ ,  $a_3$ ,  $b_1$ ,  $b_2$ ,  $b_3$  are the regression coefficients. The regression coefficients are static components in the algorithm that

have been determined based on an off-line training using collocated sets of rainfall rate and hydrometeor products from both the Penn State University and the National Center for Atmospheric Research Mesoscale Model (MM5) data.

Post-processing of the retrieved emissivity spectrum relies on the development of an offline-computed catalog of emissivity spectra (indicated schematically in Figure 12 below), for a multitude of values of the parameters to be derived. The post-processing stage is then a simple look-up-table procedure that searches for the catalog pre-computed value that corresponds to a spectrum that matches closely with the retrieved one.

The MIRS derived products generated by post-processing the core retrieved emissivity spectrum and skin temperature are: snow water equivalent (SWE), effective snow grain size (SGS), total sea ice concentration (SIC), first year sea ice concentration (SIFY), and multiyear sea ice concentration (SIMY). The SWE product uses the retrieved surface emissivities as inputs and a catalog of surface emissivities and snow pack properties derived off-line from a one-layer Dense Media Radiative Transfer snow emissivity model. The retrieved MIRS emissivity spectra are compared with those from the catalog to find the closest match. The SIC, SIFY, and SIMY products use MIRS retrieved surface emissivities and skin temperature as inputs and a catalog of surface emissivities and ice fractions derived off-line from emissivity spectra of pure water and ice surface types. The retrieved MIRS emissivity spectra are compared with those from the catalog to find the closest match and compute SIC, SIFY, and SIMY.

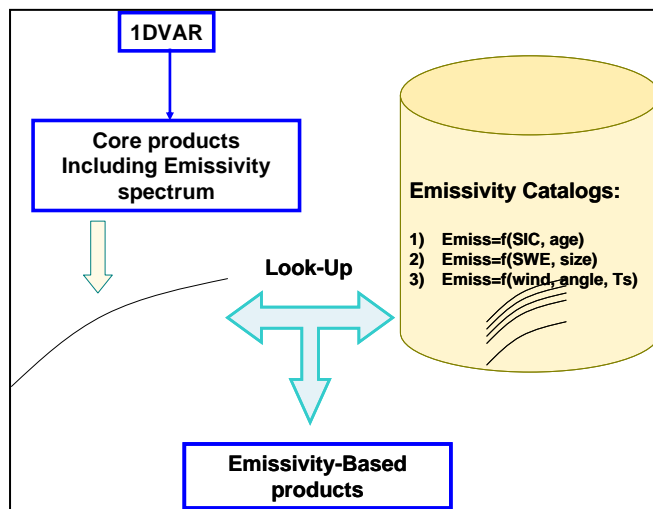


Figure 12. Schematic representation of emissivity spectrum post-processing

### 3.3.3 Conversion to User-Driven Formats

Work in progress

### 3.3.4 Area-Of-Interest (AOI) Segmentation

MIRS provides capability for Area-Of-Interest (AOI) segmentation, where processing is restricted to a user-defined geographic region. This is done by specifying the minimum and maximum latitude and longitude for the desired AOI, as well as setting the “geoLimit” flag to 1 in the MIRS Paths and Configuration File which was described in Section 2.2.4.2. MIRS radiance processing will proceed normally until the footprint matching step. The outputs from the footprint matching step are then only the Field-of-Views (FOVs) for the specified AOI. The option is available regardless of the selected sensor resolution (e.g. low resolution or high resolution).

### 3.3.5 Level-III Compositing

Work in progress

## 3.4 Microwave Systems Supported by MIRS

The following are current and future microwave sensors utilized by MIRS:

- NOAA Polar-orbiting Operational Environmental Satellites (POES) AMSU/MHS pair
- US Department of Defense (DoD) polar-orbiting satellites DMSP SSMI and SSMI/S
- European Meteorological Operational Satellite (METOP) AMSU/MHS pair
- National Polar-orbiting Operational Environmental Satellite System (NPOESS) Preparatory Project (NPP) and Joint Polar Satellite System (JPSS) ATMS
- National Aeronautics and Space Administration (NASA) Earth Observing System (EOS) AMSR-E
- National Aeronautics and Space Administration (NASA) Global Change Observation Mission (GCOM-W1) AMSR2
- China National Space Agency (CNSA) FY-3
- NASA Tropical Rainfall Measuring Mission (TRMM) Microwave Imager TMI
- NASA Global Precipitation Mission (GPM) Microwave Imager GMI
- Indian/French Megha-Tropiques Satellite SAPHIR (the MADRAS instrument failed in early 2013)

Main sensor characteristics are given in Tables 4-12.

| Channel Number | Center Frequency (MHz) | No of bands | Bandwidth (MHz) | Beam width (deg) | CF Stability (MHz) | Sensitivity (NEDT) (K) | Accuracy (K) | Polarization at Nadir |
|----------------|------------------------|-------------|-----------------|------------------|--------------------|------------------------|--------------|-----------------------|
| 1              | 23000                  | 1           | 270             | 3.3              | 10                 | 0.3                    | 2.0          | V                     |
| 2              | 31400                  | 1           | 180             | 3.3              | 10                 | 0.3                    | 2.0          | V                     |
| 3              | 50300                  | 2           | 180             | 3.3              | 10                 | 0.4                    | 1.5          | V                     |
| 4              | 52800                  | 1           | 400             | 3.3              | 5                  | 0.25                   | 1.5          | V                     |
| 5              | 53596 ±115             | 1           | 170             | 3.3              | 5                  | 0.25                   | 1.5          | H                     |
| 6              | 54400                  | 1           | 400             | 3.3              | 5                  | 0.25                   | 1.5          | H                     |
| 7              | 54940                  | 1           | 400             | 3.3              | 5                  | 0.25                   | 1.5          | V                     |

|    |                                       |   |        |     |     |      |     |   |
|----|---------------------------------------|---|--------|-----|-----|------|-----|---|
| 8  | 55500                                 | 1 | 330    | 3.3 | 10  | 0.25 | 1.5 | H |
| 9  | 57290.344                             | 1 | 330    | 3.3 | 0.5 | 0.25 | 1.5 | H |
| 10 | 57290.344<br>$\pm 217$                | 2 | 78     | 3.3 | 0.5 | 0.4  | 1.5 | H |
| 11 | 57290.344<br>$\pm 322.2$<br>$\pm 48$  | 4 | 36     | 3.3 | 1.2 | 0.4  | 1.5 | H |
| 12 | 57290.344<br>$\pm 322.2$<br>$\pm 22$  | 4 | 16     | 3.3 | 1.2 | 0.6  | 1.5 | H |
| 13 | 57290.344<br>$\pm 322.2$<br>$\pm 10$  | 4 | 8      | 3.3 | 0.5 | 0.8  | 1.5 | H |
| 14 | 57290.344<br>$\pm 322.2$<br>$\pm 4.5$ | 4 | 3      | 3.3 | 0.5 | 1.2  | 1.5 | H |
| 15 | 89000                                 | 1 | < 6000 | 3.3 | 50  | 0.5  | 2.0 | V |

Table 4. AMSU-A channels and passband characteristics

| Channel Number<br>(see Note 1) | Center Frequency<br>(GHz) | No of pass bands | CF band width<br>(see Note 2) | Sensitivity<br>(NEDT)<br>(K)<br>(see Note 3) | Polarization at Nadir<br>(see Note 4) |
|--------------------------------|---------------------------|------------------|-------------------------------|----------------------------------------------|---------------------------------------|
| H1                             | 89                        | 1                | 2800                          | 0.22                                         | V                                     |
| H2                             | 157                       | 1                | 2800                          | 0.34                                         | V                                     |
| H3                             | 183.311 $\pm$ 1.0         | 2                | 2 x 500                       | 0.51                                         | H                                     |
| H4                             | 183.311 $\pm$ 3.0         | 2                | 2 x 1000                      | 0.40                                         | H                                     |
| H5                             | 190.311                   | 1                | 2200                          | 0.46                                         | V                                     |

Table 5. MHS channels and passband characteristics

Notes:

1. The five MHS channels provide data continuity with AMSU-B channels 16 to 20, with some minor changes in frequency allocation and polarization, and improved performance.
2. The quoted values for the maximum bandwidths are double-sideband values and represent the maximum permissible bandwidths at the 3 dB points.
3. Ground measured values for the first flight model (NOAA-N).
4. The V and H polarizations correspond respectively to electrical fields normal or parallel to the ground track at nadir, both rotating by an angle equal to the scan angle for off-nadir directions.

| Channel | Center Frequency<br>(GHz) | Pass bands<br>(MHz) | Frequency stability<br>(MHz) | Polarization | NEDT<br>(Max)<br>(K) | Sampling Interval<br>(km) | IFOV<br>(km) |
|---------|---------------------------|---------------------|------------------------------|--------------|----------------------|---------------------------|--------------|
| 1       | 50.3                      | 400                 | 10                           | H            | 0.4                  | 37.5                      | 38 x 39      |
| 2       | 52.8                      | 400                 | 10                           | H            | 0.4                  | 37.5                      | 38 x 39      |
| 3       | 53.596                    | 400                 | 10                           | H            | 0.4                  | 37.5                      | 38 x 39      |
| 4       | 54.4                      | 400                 | 10                           | H            | 0.4                  | 37.5                      | 38 x 39      |
| 5       | 55.5                      | 400                 | 10                           | H            | 0.4                  | 37.5                      | 38 x 39      |
| 6       | 57.29                     | 350                 | 10                           | RCP          | 0.5                  | 37.5                      | 38 x 39      |
| 7       | 59.4                      | 250                 | 10                           | RCP          | 0.6                  | 37.5                      | 38 x 39      |

|    |                                     |       |      |     |      |      |         |
|----|-------------------------------------|-------|------|-----|------|------|---------|
| 8  | 150                                 | 1500  | 200  | H   | 0.88 | 37.5 | 13 x 15 |
| 9  | 183.31±6.6                          | 1500  | 200  | H   | 1.2  | 37.5 | 13 x 15 |
| 10 | 183.31±3                            | 1000  | 200  | H   | 1    | 37.5 | 13 x 15 |
| 11 | 183.31±1                            | 400   | 200  | H   | 1.25 | 37.5 | 13 x 15 |
| 12 | 19.35                               | 400   | 75   | H   | 0.7  | 25   | 47 x 74 |
| 13 | 19.35                               | 400   | 75   | V   | 0.7  | 25   | 47 x 74 |
| 14 | 22.235                              | 500   | 75   | V   | 0.7  | 25   | 47 x 74 |
| 15 | 37                                  | 1500  | 75   | H   | 0.5  | 25   | 45 x 31 |
| 16 | 37                                  | 1500  | 75   | V   | 0.5  | 25   | 45 x 31 |
| 17 | 91.655                              | 1500  | 100  | V   | 0.9  | 12.5 | 13 x 15 |
| 18 | 91.655                              | 1500  | 100  | H   | 0.9  | 12.5 | 13 x 15 |
| 19 | 63.283248<br>± 0.285271             | 3.0   | 0.08 | RCP | 2.4  | 75   | 75 x 75 |
| 20 | 60.792668<br>± 0.357892             | 3.0   | 0.08 | RCP | 2.4  | 75   | 75 x 75 |
| 21 | 60.792668<br>± 0.357892<br>± 0.002  | 6.0   | 0.08 | RCP | 1.8  | 75   | 75 x 75 |
| 22 | 60.792668<br>± 0.357892<br>± 0.0055 | 12.0  | 0.12 | RCP | 1.0  | 75   | 75 x 75 |
| 23 | 60.792668<br>± 0.357892<br>± 0.016  | 32.0  | 0.34 | RCP | 0.6  | 75   | 75 x 75 |
| 24 | 60.792668<br>± 0.357892<br>± 0.050  | 120.0 | 0.84 | RCP | 0.7  | 37.5 | 38 x 39 |

Table 6. SSMIS channels and passband characteristics

Notes:

1. Channels 1-5 are vertically polarized on F16.

| Center Frequency (GHz) | Band Width (MHz) | EFOV (km x km) | Polarization |
|------------------------|------------------|----------------|--------------|
| 19.35                  | 10-250           | 69 x 43        | V            |
| 19.35                  | 10-250           | 69 x 43        | H            |
| 22.235                 | 10-250           | 60 x 40        | V            |
| 37.0                   | 100-1000         | 37 x 28        | V            |
| 37.0                   | 100-1000         | 37 x 28        | H            |
| 85.5                   | 100-1500         | 15 x 13        | V            |
| 85.5                   | 100-1500         | 15 x 13        | H            |

Table 7. SSM/I channels and passband characteristics

| Channel Number | Center Frequency (GHz) | Band width (MHz) | Sensitivity (NEDT) (K) | Accuracy (K) | Static beam width (MHz) |
|----------------|------------------------|------------------|------------------------|--------------|-------------------------|
| 1              | 23.8                   | 0.27             | 0.9                    | 2.0          | 5.2                     |
| 2              | 31.4                   | 0.18             | 0.9                    | 2.0          | 5.2                     |
| 3              | 50.3                   | 0.18             | 1.2                    | 1.5          | 2.2                     |
| 4              | 51.76                  | 0.4              | 0.75                   | 1.5          | 2.2                     |
| 5              | 52.8                   | 0.4              | 0.75                   | 1.5          | 2.2                     |
| 6              | 53.596±0.115           | 0.17             | 0.75                   | 1.5          | 2.2                     |
| 7              | 54.4                   | 0.4              | 0.75                   | 1.5          | 2.2                     |
| 8              | 54.94                  | 0.4              | 0.75                   | 1.5          | 2.2                     |
| 9              | 55.5                   | 0.33             | 0.75                   | 1.5          | 2.2                     |
| 10             | 57.2903                | 0.33             | 0.75                   | 1.5          | 2.2                     |
| 11             | 57.2903±0.115          | 0.078            | 1.2                    | 1.5          | 2.2                     |
| 12             | 57.2903                | 0.036            | 1.2                    | 1.5          | 2.2                     |
| 13             | 57.2903±0.322          | 0.016            | 1.5                    | 1.5          | 2.2                     |

|    |                         |       |     |     |     |
|----|-------------------------|-------|-----|-----|-----|
| 14 | 57.2903±0.322<br>±0.010 | 0.008 | 2.4 | 1.5 | 2.2 |
| 15 | 57.2903±0.322<br>±0.004 | 0.003 | 3.6 | 1.5 | 2.2 |
| 16 | 87-91(88.20)            | 2.0   | 0.5 | 2.0 | 2.2 |
| 17 | 164-167                 | 3.0   | 0.6 | 2.0 | 1.1 |
| 18 | 183.31±7                | 2.0   | 0.8 | 2.0 | 1.1 |
| 19 | 183.31±4.5              | 2.0   | 0.8 | 2.0 | 1.1 |
| 20 | 183.31±3                | 1.0   | 0.8 | 2.0 | 1.1 |
| 21 | 183.31±1.8              | 1.0   | 0.8 | 2.0 | 1.1 |
| 22 | 183.31±1.0              | 0.5   | 0.9 | 2.0 | 1.1 |

Table 8. ATMS channels and passband characteristics

| Center Frequency (GHz) | Band Width (MHz) | Beam width (deg) | Sensitivity (K) | IFOV (km x km) | Sampling rate (km x km) | Integration time (msec) | Beam efficiency (%) | Polarization |
|------------------------|------------------|------------------|-----------------|----------------|-------------------------|-------------------------|---------------------|--------------|
| 6.925                  | 350              | 2.2              | 0.3             | 43 x 74        | 10 x 10                 | 2.2                     | 95.3                | H + V        |
| 10.65                  | 100              | 1.4              | 0.6             | 30 x 51        | 10 x 10                 | 1.4                     | 95.0                | H + V        |
| 18.7                   | 200              | 0.8              | 0.6             | 16 x 27        | 10 x 10                 | 0.8                     | 96.3                | H + V        |
| 23.8                   | 400              | 0.9              | 0.6             | 18 x 318       | 10 x 10                 | 0.9                     | 96.4                | H + V        |
| 36.5                   | 1000             | 0.14             | 0.6             | 8 x 14         | 10 x 10                 | 0.4                     | 96.3                | H + V        |
| 89                     | 3000             | 0.18             | 1.1             | 4 x 6          | 5 x 5                   | 0.18                    | 96.0                | H + V        |

Table 9. AMSR-E channels and passband characteristics

| Channel Number | Center Frequency (GHz) | Band Width (MHz) | Sensitivity (K) | IFOV (km x km) | Polarization |
|----------------|------------------------|------------------|-----------------|----------------|--------------|
| 1              | 10.65                  | 100              | 0.63            | 36 x 59        | V            |
| 2              | 10.65                  | 100              | 0.54            | 36 x 60        | H            |
| 3              | 19.35                  | 500              | 0.50            | 18 x 31        | V            |
| 4              | 19.35                  | 500              | 0.47            | 18 x 30        | H            |
| 5              | 21.3                   | 200              | 0.71            | 17 x 27        | V            |
| 6              | 37.0                   | 2000             | 0.36            | 10 x 16        | V            |
| 7              | 37.0                   | 2000             | 0.31            | 10 x 16        | H            |
| 8              | 85.5                   | 3000             | 0.52            | 5 x 7          | V            |
| 9              | 85.5                   | 3000             | 0.93            | 5 x 7          | H            |

Table 10. TRMM TMI channels and passband characteristics

| Channel Number | Center Frequency (GHz) | Band Width (MHz) | Sensitivity (K) | IFOV (km x km) | Polarization |
|----------------|------------------------|------------------|-----------------|----------------|--------------|
| 1              | 18.7                   | 100              | 0.7             | 40 x 67        | V            |
| 2              | 18.7                   | 100              | 0.7             | 40 x 67        | H            |
| 3              | 23.8                   | 200              | 0.7             | 40 x 67        | V            |
| 4              | 36.5                   | 500              | 0.7             | 40 x 67        | V            |
| 5              | 36.5                   | 500              | 0.7             | 40 x 67        | H            |
| 6              | 89                     | 1350             | 1.1             | 10 x 17        | V            |
| 7              | 89                     | 1350             | 1.1             | 10 x 17        | H            |
| 8              | 157                    | 1350             | 2.2             | 6 x 10         | V            |
| 9              | 157                    | 1350             | 2.2             | 6 x 10         | H            |

Table 11. Megha-Tropiques MADRAS channels and passband characteristics

| Channel Number | Center Frequency (GHz) | Band Width (MHz) | Sensitivity (K) | IFOV at Nadir (km x km) | Polarization at Nadir |
|----------------|------------------------|------------------|-----------------|-------------------------|-----------------------|
| 1              | 183.31±0.20            | 200              | 2.35            | 10 x 10                 | H                     |
| 2              | 183.31±1.10            | 350              | 1.45            | 10 x 10                 | H                     |
| 3              | 183.31±2.80            | 500              | 1.36            | 10 x 10                 | H                     |
| 4              | 183.31±4.20            | 700              | 1.38            | 10 x 10                 | H                     |
| 5              | 183.31±6.80            | 1200             | 1.03            | 10 x 10                 | H                     |
| 6              | 183.31±11.0            | 200              | 1.10            | 10 x 10                 | H                     |

Table 12. Megha-Tropiques SAPHIR channels and passband characteristics

| Channel Number | Center Frequency (GHz) | Band Width (MHz) | Sensitivity (NEDT) (K) | IFOV (km x km) | Polarization |
|----------------|------------------------|------------------|------------------------|----------------|--------------|
| 1              | 10.65                  | 100              | 0.96                   | 19 x 32        | V            |
| 2              | 10.65                  | 100              | 0.96                   | 19 x 32        | H            |
| 3              | 18.7                   | 200              | 0.84                   | 11 x 18        | V            |
| 4              | 18.7                   | 200              | 0.84                   | 11 x 18        | H            |
| 5              | 23.8                   | 400              | 1.05                   | 9 x 15         | V            |
| 6              | 36.5                   | 1000             | 0.65                   | 9 x 14         | V            |
| 7              | 36.5                   | 1000             | 0.65                   | 9 x 14         | H            |
| 8              | 89.0                   | 6000             | 0.57                   | 4 x 7          | V            |
| 9              | 89.0                   | 6000             | 0.57                   | 4 x 7          | H            |
| 10             | 166.0                  | 3000             | 1.5                    | 4 x 7          | V            |
| 11             | 166.0                  | 3000             | 1.5                    | 4 x 7          | H            |
| 12             | 183.31±3.0             | 3500             | 1.5                    | 4 x 7          | V            |
| 13             | 183.31±7.0             | 4500             | 1.5                    | 4 x 7          | V            |

Table 13. GPM GMI channels and passband characteristics

## Section 4.0 MIRS Input Files

This section provides a brief description of the input data files. Details on data content and format are found in the Interface Control Document (ICD). The input files consist of the *set-up* files, the *external* data files and the *static* data files. The set-up files are scripts that define paths to MIRS data and applications. External data files contain dynamic input data coming from external sources: level 1-b sensor data and the NWP analysis or forecast data. Static data files contain input data that do not or rarely change: CRTM data, the nominal instrumental noise (NEDT) data, the nominal geophysical covariance matrices data, the topography data, tuning data and emissivity catalogs.

### 4.1 Set-Up Files

The purpose of the set-up files, also called the Path and Configuration Files (PCF), is to define the paths to MIRS sub-routines, libraries, applications, processes and data. PCFs can be constructed via the GUI-based MCP or can be constructed manually. Once constructed, they are called by the MIRS Sequence Control Scripts (SCS) that reside in the “/scripts” directory. A major advantage of the PCFs is enhanced modularity which eliminates the need for hand-coding in the MIRS software.

SCSs are the main scripts that control the flow of MIRS processes and applications. Similar to PCFs, the SCSs can also be constructed via the MCP interface or manually. SCSs are sensor-specific scripts denoted as “*sensor*\_scs.bash” where “*sensor*” denotes satellite sensor name, e.g., “n18\_amsua\_mhs”, “n19\_amsua\_mhs”, “metopA\_amsua\_mhs”, “metopB\_amsua\_mhs”, “f16\_ssmis”, “f17\_ssmis”, “f18\_ssmis”, “npp\_atms”, and “mtsa\_saphir” for NOAA-18 AMSU-MHS, NOAA-19 AMSU-MHS, Metop-A AMSU-MHS, Metop-B AMSU-MHS, F16-SSMI/S, F17-SSMI/S, F18-SSMI/S, NPP ATMS, and MT SAPHIR, respectively.

PCFs reside in the “/setup” top level directory. They consist of two general utility files and a sensor-specific file, e.g., for AMSU-MHS, SSMIS, etc. The general utility files are designated as “paths” and “paths\_idl.pro”, and they define paths to MIRS sensor-independent libraries and subdirectories such as CRTM, IDL code libraries and execution subdirectories. The other PCF is a BASH script that defines paths to sensor-specific and sensor-independent processes, data and applications. In the case of AMSU-MHS, this set up file is named “n18\_pcfc.bash” .

### 4.2 External Files

The external datasets are the input data coming from external sources. They consist of raw sensor data files, e.g., AMSU-A and MHS and SSMI/S, and the NWP analysis and/or forecast gridded files. These files reside in the “/data/ExternalData” sub-directory. Note that the NWP files are used only for monitoring radiometric and geophysical performances and are not used in the retrieval. The one exception currently is the optional snowfall rate product (SFR) which requires the availability of GFS forecast data files.

#### **4.2.1 Sensor Data Files (*level 1b*)**

For the case of NOAA-18, these will be level 1b data files. For DMSP sensors, these will be the NRL TDR files. The ICD provides further details as to their content, format, type, etc.

#### **4.2.2 Gridded NWP Analysis Files**

The NWP data files contain atmospheric and surface EDRs. Currently, two sources of NWP data sets are being utilized and processed: the Global Data Assimilation System (GDAS) analysis data, and the European Center for Medium-range Weather Forecasting (ECMWF) analysis data. These are *optional* data files and are used only for calibration in the radiance processing and for product monitoring. They are not used in the inversion process. They might be used however in the 1DVAR as first guesses at user discretion if it is deemed that they help convergence of certain parameters. These files reside in the “/data/ExternalData/gridNWP\_analys” sub-directory.

#### **4.2.3 Gridded NWP Forecast Files**

Similar to NWP analysis files, these forecast files are also *optional* files that serve the same purpose. They can however also be used as first guess to the retrieval. All parameters or just a portion of them can be used, depending on the user’s confidence in each parameter provided by the forecast model. Currently, the Global Forecast System (GFS) data are being utilized and processed.

#### **4.2.4 Gridded NWP SFR Forecast Files**

The heritage SFR algorithm, which has been integrated into MiRS in this version, requires ancillary information coming from Global Forecast System (GFS) files. In order to generate the required files in the correct format, the user must first have access to the operational GRIB format forecast files at 0.5 degree horizontal resolution. The sample scripts located in the *source\_ospo* and *source\_star* subdirectories should be used to unpack the original GRIB files. Users requiring this capability should contact the MiRS team or OSPO directly. Also note that if SFR is not required, then step\_sfr can be turned off either in the PCF or via the GUI.

### **4.3 Static Data Files**

The static data files contain various nominal instruments, system and processes input parameters. These are permanent files, i.e., “as is”. These data files include the CRTM files, nominal instrument noise files (NETDs), geophysical covariance matrices files, topography files and tuning files. These data files reside in the “/data/StaticData” sub-directory. Each of the static data files is briefly described below.

#### **4.3.1 Forward Operator Look-Up Tables (CRTM files)**

These are files containing coefficient parameters as input to the CRTM module. They come as part of the CRTM package and are not generated by MIRS.

#### **4.3.2 Nominal Instrumental Error Covariance Matrices (*NEDT files*)**

These are ASCII files containing instrument antenna temperature error covariance matrices needed as input to 1dvar. These nominal NEDT values are used for those sensors where it is not possible to compute noise values “on the fly”, e.g., SSMI/S. For the AMSU-MHS, the NEDTs are dynamically generated following the methodology as described in Mo (2002).

#### **4.3.3 Geophysical Mean and Covariance Matrices**

These data are ASCII files containing nominal surface and atmospheric parameter covariance matrices needed as input to 1dvar. They also contain the mean background information derived from climatological studies. Currently, two different sets of mean atmospheric background data files are available: (1) a single mean background profile for each of the four main surface types based on a global data set of atmospheric profiles, and (2) a temporally and spatially varying atmospheric background derived from a large number of global analyses from the operational European Centre for Medium Range Weather Forecasting (ECMWF). The choice of one of these options is specified by the user in the paths and configuration file (PCF).

#### **4.3.4 Snow Water Equivalent Climatology Files**

MiRS allows optional use of a static spatially and temporally variable climatology of SWE as an a priori constraint during the SWE estimation algorithm. This climatology (both mean and standard deviation) are based on 20 years of SSMI retrieval data and is stored in two separate ascii files.

#### **4.3.5 Topography Files**

The Topography Tables represent binary gridded file containing surface type and elevation data. The source of these Tables is the United States Geological Survey (USGS).

#### **4.3.6 Tuning Files**

The tuning data files are sensor-specific ASCII files that contain tuning parameters needed to customize retrieval attempts. They contain such parameters as which EDRs to retrieve, channels selected, the maximum number of iterations, etc. Up to two tuning files per sensor are permitted. This means that a retrieval is performed using the parameter set contained in the first tuning file and if the user requires it a second retrieval will be attempted (if the first retrieval did not converge) using the second tuning file. The control of the number of attempts and the names of the tuning files are set in the paths and configuration file (PCF). These files reside in the “Data/StaticData/TuningData” subdirectory” and follow the naming convention “TunParams\_*sensor*.in”, where *sensor* is notation used for a specific sensor, e.g., n18\_amsua\_mhs, n19\_amsua\_mhs, metopA\_amsua\_mhs, metopB\_amsua\_mhs, f16\_ssmis, f17\_ssmis, f18\_ssmis, and npp\_atms for NOAA-18 AMSU-MHS, NOAA-19 AMSU-

MHS, Metop-A AMSU-MHS, Metop-B AMSU-MHS, F16 SSMI/S, F17 SSMI/S, F18 SSMI/S, and NPP ATMS, respectively.

#### **4.3.7 Emissivity Catalog Data Files**

The emissivity catalog files are ASCII files that contain surface emissivity spectra and geophysical parameters computed off-line from physical models. These files are used as input to the MIRS Vertical Integration and Post-Processing (VIPP) module to compute emissivity-based EDRs. There are two emissivity catalog files for each sensor: the sea ice and snow cover catalogue files. For NOAA-18 AMSU-MHS, these files are denoted as “SeaIceEmissCatalog\_n18\_amsua\_mhs.dat” and “SnowEmissCatalog\_n18\_amsua\_mhs.dat”, respectively. The sea ice emissivity catalog is used for computing sea ice parameters and the snow emissivity catalog is used for computing snow cover parameters.

#### **4.3.8 Regression Coefficient Files**

Users may also *optionally* specify whether external data for the retrieval first guess and/or background will come from a multilinear regression estimate based on observed brightness temperatures. This option is available for several sensors, and the elements of the scene that can be specified from the regression are sensor-dependent. The regression coefficient files are located in the “/data/SemiStaticData/regressAlgors” sub-directory.

## Section 5.0 MIRS Output Files

This section provides a brief description of the MIRS output files. For more detailed description the reader is referred to the ICD. The output data files consist of the level II retrieval files in binary swath format, the image files and other output files in HDF-EOS format derived from the retrieval files through format conversion processing.

### 5.1 MIRS Retrieval Files

MIRS retrieval files consist of swath binary and image files and gridded and point-to-point binary files. The swath binary and image files represent primary output products for external access and delivery, whereas the gridded and point-to-point binary files contain specific retrieved or monitoring parameter outputs converted from swath data for map generation and plotting purposes.

The swath (level II) binary files consist of two files: the main product file (*edr*) and the derived product file (*dep*). The *edr* file contains retrieved parameters from 1dvar processing, and the *dep* file contains parameters derived from *edr* parameters as inputs through vertical integration and post-processing algorithms. For instance, the TPW and CLW parameters are stored in the *dep* file since they are derived from the (1DVAR) retrieved *edrs* of profiles of water vapor and liquid water, respectively, through vertical integration. Similarly, the sea ice concentration is stored in the *dep* file since it is derived from retrieved surface emissivities and skin temperature. The image files are PNG files of specific retrieved (*edr* and *dep*) and monitoring parameters.

MIRS *edr* swath files reside in the “/data/TestBedData/Outputs/edr/” subdirectory and the *dep* swath files reside in the “/data/TestBedData/Outputs/dep/” subdirectory. The grid and point-to-point binary data files reside in the “/data/TestBedData/Outputs/grid/” subdirectory and the image files reside in the “/data/TestBedData/Outputs/figs/” subdirectory.

#### 5.1.1 Main Product Swath Binary Files (level II-a, EDR)

The MIRS swath binary product file is generated by MIRS Input/Output modules. Both Fortran-95 and IDL readers are available to manipulate this file. File specifications are given in the ICD. The code for reading/writing swath product data also is provided in Appendix D of the ICD.

#### 5.1.2 Derived Product Swath Binary Files (level II-a, DEP)

The MIRS Derived Product (DEP) swath binary file is generated by MIRS Input/Output modules written in both Fortran-95 and IDL. Both Fortran-95 and IDL readers are available to manipulate this file. File specifications are given in the ICD. The code for reading/writing swath product data is also provided in Appendix D of the ICD.

#### 5.1.3 Image Files

---

The image files are PNG files of specific *edr*, *dep* and monitoring parameters. They are generated using modules written in IDL. The image files are also used for providing the product monitoring figures on-line. These files reside in the “/data/TestbedData/Outputs/figs” sub-directory.

## 5.2 netCDF Swath Files (*level II-a, EDR*)

For operational data distribution and archiving of NPP ATMS products, MIRS output data will be reformatted as netCDF4 files. Each MIRS output EDR and DEP binary data file will be rewritten as two netCDF4 files. One is the profile netCDF4 file (filename beginning with “SND\_”) which contains the retrieved atmospheric profile products for each layer and the other is the image product netCDF4 file (filename beginning with “IMG\_”) which contains the retrieved image products. This is an *optional* step, and the files are saved under the “/data/TestBedData/Outputs/nc” subdirectory.

## 5.3 Product Monitoring Figures

Extensive use of monitoring tools is a hallmark of MIRS. These tools provide significant leverage and opportunities for users to monitor MIRS retrieved parameters qualitatively and quantitatively. Main MIRS monitoring functionalities are provided in the MIRS System Description Document.

## 5.4 Product Quality Assurance / Quality Control

Along with the MIRS products, several quality parameters (QPs) are provided. These parameters are applicable and relevant only to the advanced algorithm products. They are (or will be) part of the binary swath outputs file (*level 2a*):

- Convergence metrics ( $\chi^2$  &  $Y^{fwd}$ )
- Quality Control Flag (QC)
- Uncertainty matrix ( $S$ )
- Contribution functions ( $D$ )
- Average kernel ( $A$ )

### 5.4.1 Interpretation and Usage of the Convergence Metrics

The convergence metric  $\chi^2$  is the root mean square of all residuals between the last-simulated brightness temperatures (using the forward operator) and the measurements. Only those channels selected and effectively utilized in the 1dvar retrieval are used to compute this metric. There is one single value of  $\chi^2$  for every profile. Nominally, the convergence is deemed reached when:

$$\chi^2 \leq 1$$

Users can however relax this criterion to allow the use of profiles that reach a value of 10. Above this value of 10, the retrievals are deemed unreliable. In addition to  $\chi^2$ , the last-simulated brightness temperatures using the forward operator  $Y^{fwd}$  are also part of the output fields. These simulated radiances can be used to examine the individual (channel by channel) residuals between the measurements and the brightness temperatures that were simulated using the retrieved state vector.

### 5.4.2 Interpretation and Usage of Quality Control

In addition to the convergence metric, a detailed quality control structure is implemented and its content is also part of the output file. It contains four words, each one of sixteen bits. Figure 13 shows the structure and contents of the quality control flag. A general description of each word is as follows:

- The first word, QC(1), is defined as the general validity control flag. It ranks the quality of all MIRS products at a specific location as good (value set to 0), use with caution (value set to 1), and bad (value set to 2). This general ranking is made based on the flags contained in the second, third and fourth word of the quality flag structure.
- The second word, QC(2), provides information about the convergence, the presence and the type of precipitation (light, medium or heavy). Also, a set of out-of-band flags are implemented. Those flags are turned on if one of the MIRS products is out of the predefined bound values. If any bits 1-5 are flagged, then QC(1) is set to 1. If any of bit 0 or bits 6-14 are set, then QC(1) is set to 2. It also contains 2 separate bits (16 -17) related to the SFR algorithm.
- The third word, QC(3), provides information about the detection of temperature lapse rate (including super-adiabatic lapse rate), temperature inversion, super saturation, humidity inversion and cloud detection. If any bits in QC(3) 0-5 are flagged, then QC(1) is set to 1. If any QC(3) bits 6-13 are flagged, then QC(1) is set to 2.
- The fourth word, QC(4), provides information about the quality of the measurements. It also provides information on surface type. If any bits in QC(4) 0-10 are set, QC(2) bit 14 is flagged, and QC(1) is set to 2.

|                                        | Bit 0                                        | Bit 1                                               | Bit 2                            | Bit 3                                                   | Bit 4              | Bit 5 | Bit 6              | Bit 7 | Bit 8 | Bit 9 | Bit 10 | Bit 11 | Bit 12   | Bit 13 | Bit 14          | Bit 15               | Bit 16 | Bit 17 | Bit 18 | Bit 19 |
|----------------------------------------|----------------------------------------------|-----------------------------------------------------|----------------------------------|---------------------------------------------------------|--------------------|-------|--------------------|-------|-------|-------|--------|--------|----------|--------|-----------------|----------------------|--------|--------|--------|--------|
| 0 = GOOD, 1= SOME EVENT/PROBLEM, 2=BAD |                                              |                                                     |                                  |                                                         |                    |       |                    |       |       |       |        |        |          |        |                 |                      |        |        |        |        |
|                                        |                                              |                                                     |                                  |                                                         |                    |       |                    |       |       |       |        |        |          |        |                 |                      |        |        |        |        |
| QC (1)                                 | CONVERGENCE I<br>(ChiSq >= 10)               | CONVERGENCE II<br>(5<-ChiSq <10)                    | PRECIPITATION<br>(YES/NO)        | TYPE OF PRECIPITATION                                   |                    |       | OUT-OF-BOUND FLAGS |       |       |       |        |        | MEAS. QC |        | SFR             |                      |        |        |        |        |
| QC (2)                                 | LIGHT                                        | MEDIUM                                              | HEAVY                            | TSKIN                                                   | TEMP               | Q     | EMISS              | TPW   | ICLW  | RWP   | GWP    |        |          |        | RTM CONVERGENCE | SFR LOW/UNDETERMINED |        |        |        |        |
| QC (3)                                 | TEMPERATURE LAPSE RATE                       | TEMPERATURE INVERSION<br>(Range:Psfc-200mb to Psfc) | SUPERSATURATION<br>(RH > 99.9 %) | SUPERSATURATION<br>3 CONTIGUOUS LAYERS<br>(RH > 99.9 %) | HUMIDITY INVERSION | CLOUD | VALIDITY FLAGS     |       |       |       |        |        |          |        |                 |                      |        |        |        |        |
| QC (4)                                 | ALLOCATED FOR EACH ELEMENT OF MEASUREMENT QC |                                                     |                                  |                                                         |                    |       |                    |       |       |       |        |        | OCEAN    | LAND   | Calibration     |                      |        |        |        |        |

Figure 13. Representation of the quality control structure.

Finally, note that both the swath EDR and DEP binary files contain a QC variable, with the same structure described above. The QC variable in the DEP file will largely contain the same information as that from the EDR file, but with several bits possibly changed due to additional information obtained in the post-processing generation of the derived products (e.g. the presence of rainfall or hydrometeors).

### 5.4.3 Interpretation and Usage of the Uncertainty Matrix

Work in progress

### 5.4.4 Interpretation and Usage of the Contribution Function

Work in progress

#### **5.4.5 Interpretation and Usage of the Average Kernel**

Work in progress

## Section 6.0 Products Validation and Accuracy

### 6.1 Validation Methodology

Validation of MIRS products consists of routine daily monitoring and non-routine studies. Daily monitoring is extensive; It involves comparisons with the NPW analysis (GDAS and ECMWF) products, the heritage microwave products (MSPPS for AMSU-MHS), and comparisons with radiosonde measurements and other data sources. The daily monitoring and validation is automated and incorporated into the MIRS processing system as shown in Figure 14. The outputs of these comparisons are displayed online through a web-based monitoring tool.

Non-routine validation studies are conducted off-line with respect to ground truth observations limited in time and geographical extent. The ground truth sources that have been used include the radiosondes from the Integrated Global Radiosonde Archive (IGRA) project, the Hurricane Research Center (HRC) airborne dropsondes collocated with NOAA-18 and DMSP microwave sensors as well as the pre-existing TIROS Operational Vertical Sounder collocation sets.

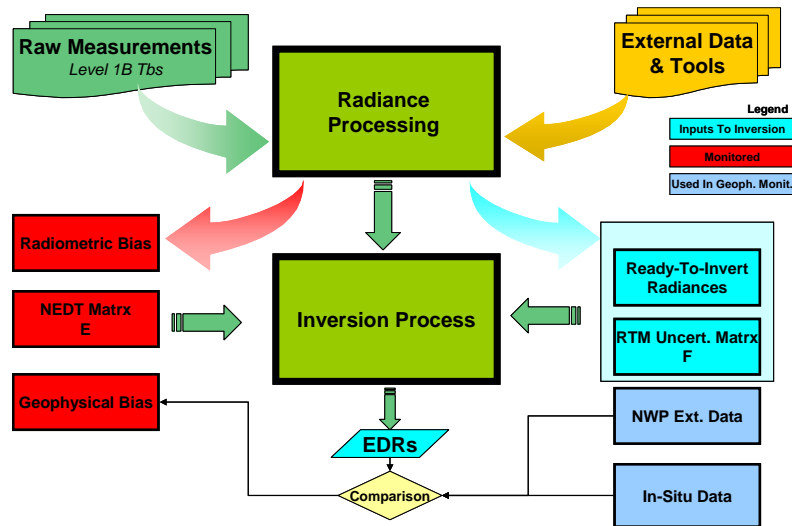


Figure 14. Overall MIRS system including the routine and non-routine monitoring. The routine monitoring is performed daily by comparing retrieved outputs (EDRs) with assimilation NWP model outputs (GDAS), both radiometric and geophysical.

### 6.2 Validation Results

The main retrieval products are the parameters generated from 1DVAR. These parameters are all elements of the geophysical state vector, inverted from the vector of ready-to-invert radiances or the brightness temperatures. They include the temperature profile, the humidity profile, the surface emissivity spectrum, the skin temperature and the cloud and rain parameters (liquid and frozen

states). The derived MIRS products are those parameters that are computed *a-posteriori* from the main products, either using a simple vertical integration or an entirely new algorithm i.e. as represented in Figure 13 above. The total precipitable water (TPW) is an example of a derived product in that it is derived from the vertical integration of the 1DVAR retrieved water vapor profile. The cloud liquid water (CLW) is also a vertical integration of the non-precipitating liquid cloud amount profile. Snow Water Equivalent (SWE) and Sea Ice Concentration (SIC) are examples of derived products from retrieved emissivities using new MIRS post-processing algorithms. Rainfall rate is an example of a product regressed from MIRS retrieved rain water path (RWP) and/or CLW. The following sub-sections present the validation results from routine (on-line) monitoring as well as from off-line validation studies. Note that not all products have been validated. The document will be updated as progress is made.

### 6.2.1 Vertical Temperature Profile

MIRS retrieved temperature profiles are routinely collocated and compared with radiosonde measurements and other data sources. Comparison figures and statistics are displayed on the MIRS online monitoring menus. Figure 15 presents validation results for the NOAA-18 AMSU-MHS sensor on October 25, 2008. Shown are computed standard deviations and mean biases for the retrieved profiles and those obtained from other sources with respect to radiosonde measurements over ocean. Included are the MIRS retrieval performances using the regression-based algorithm output as a first-guess, as well as the first-guess performances. The actual standard deviation between retrieved and measured profiles and the standard deviation thresholds according to the NPOESS-recommended requirements (IORD-II) are also shown for reference. Note that the temperature profiles have been vertically-averaged following the IORD-II recommendations. Representative profiles have been constructed for tropical, polar and mid-latitude profiles.

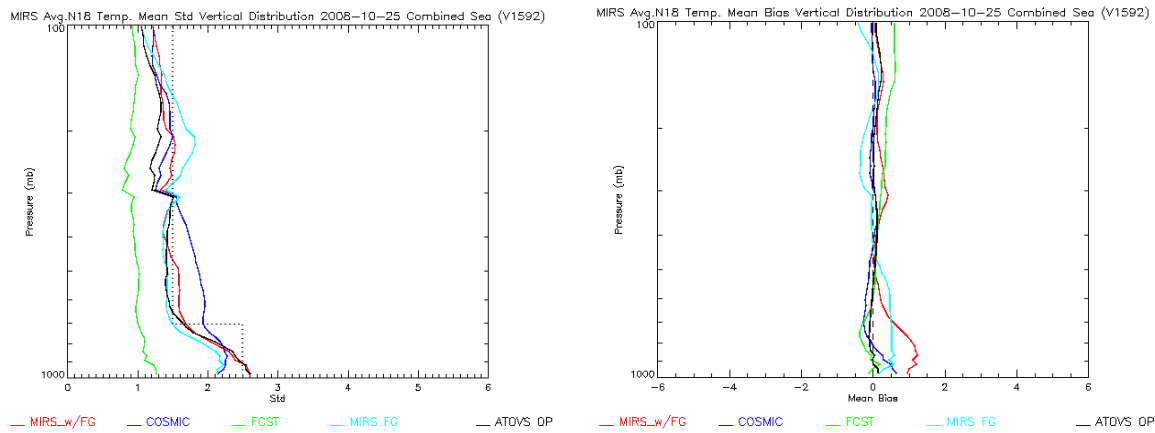
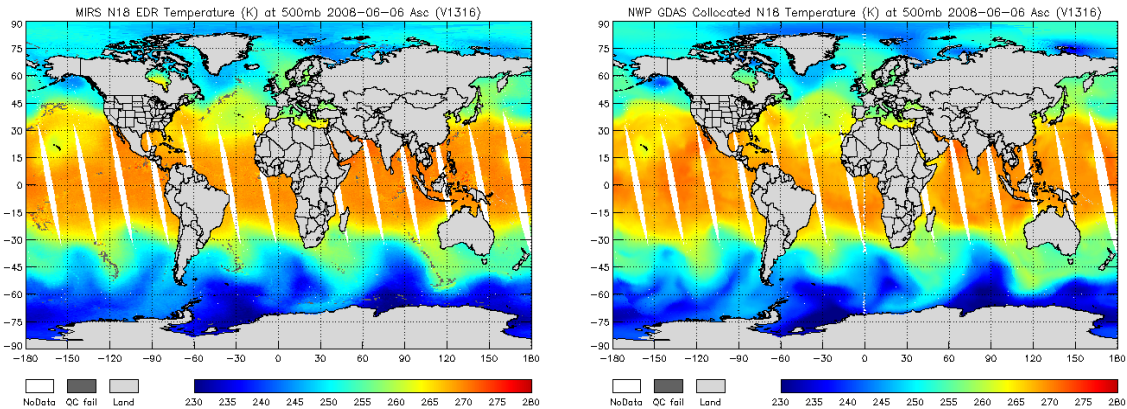
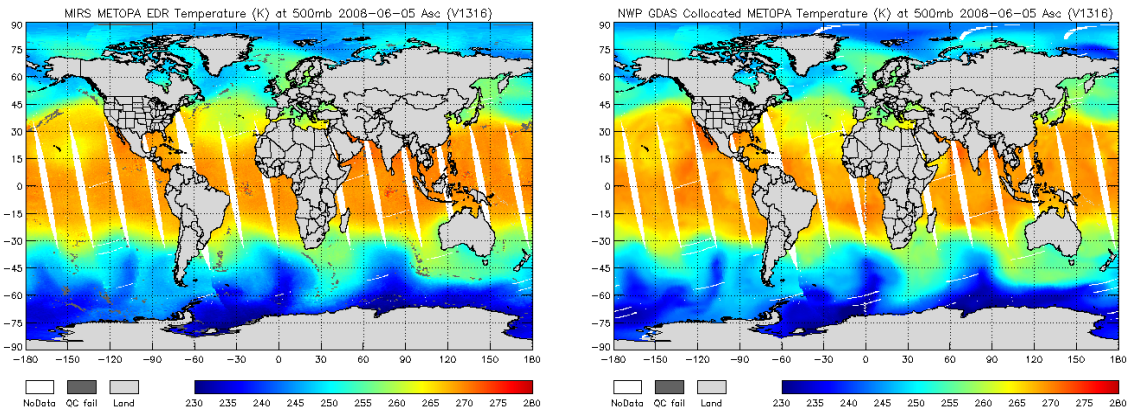


Figure 15. Standard deviation (left) and mean bias (right) of the atmospheric temperature profile retrieved from MIRS (red) and the MIRS first-guess (teal) as well as other sources with respect to radiosonde measurements

Figure 16 and Figure 17 present global maps of horizontal temperature fields over ocean retrieved from MIRS for the NOAA-18 and MetopA AMSU-MHS sensors (left panels) and GDAS (right panels) collocated with each instrument and routinely generated and accessible through the online monitoring tool. As shown, the general features of GDAS are well captured by MIRS.



*Figure 16. Comparison of horizontal fields of temperature at 500 millibars on June 6 2008 retrieved from the MIRS NOAA-18 AMSU-MHS (left panel) and from collocated GDAS assimilation field (right panel)*



*Figure 17. Comparison of horizontal fields of temperature at 500 millibars on June 5 2008 retrieved from the MIRS METOP-A AMSU-MHS (left panel) and from collocated GDAS assimilation field (right panel) Similar comparisons are made with respect to ECMWF assimilation fields.*

### 6.2.2 Vertical Humidity Profile

MIRS retrieved humidity profiles are routinely compared with validation data and displayed online in a similar fashion. Figure 18 presents validation results for the NOAA-18 AMSU-MHS sensor on October 25, 2008. Shown are computed standard deviations and mean biases for the retrieved profiles and those obtained from other sources with respect to radiosonde measurements over ocean. Included are the MIRS retrieval performances using the regression-based algorithm output as a first-guess, as well as the first-guess performances. The actual standard deviation between retrieved and measured profiles and the standard deviation thresholds according to the NPOESS-recommended requirements (IORD-II) are also shown for reference. Note that the temperature profiles have been vertically-averaged following the IORD-II recommendations. Representative profiles have been constructed for tropical, polar and mid-latitude profiles.

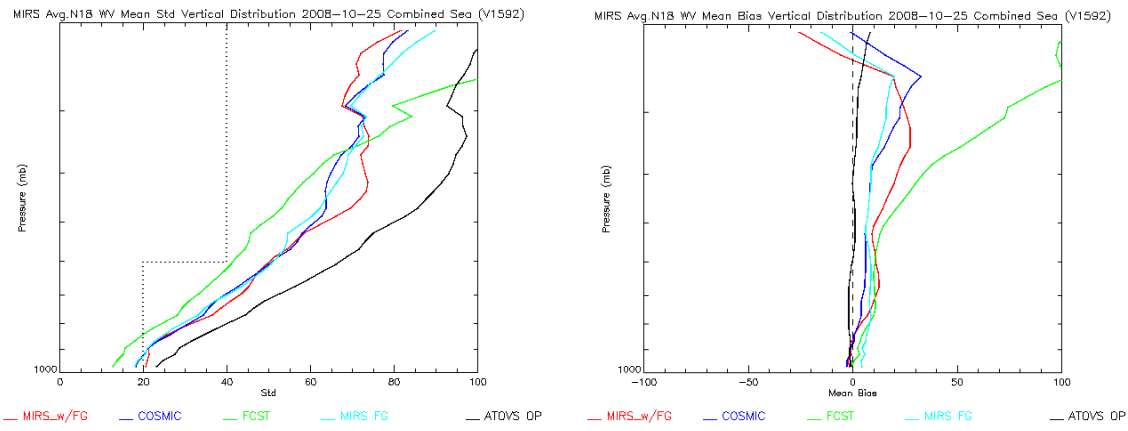


Figure 18. Standard deviation (left) and mean bias (right) of the atmospheric water vapor profiles retrieved from MIRS (red) and the MIRS first-guess (teal) as well as other sources with respect to radiosondes

Figure 19 and Figure 20 show global maps of the horizontal fields of water vapor retrieved from the MIRS for NOAA-18 and Metop-A AMSU-MHS satellites (left panels) and from GDAS (right panels) collocated with each instrument for June 6, 2008. As shown, most features are very well captured by MIRS over ocean and land surfaces.

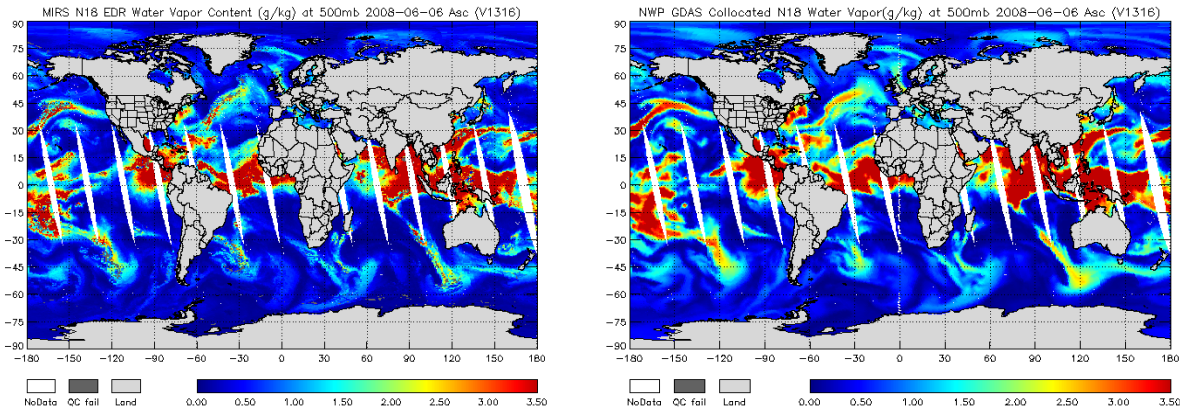


Figure 19. Comparison of fields of water vapor mixing ratio at 500 millibars over ocean, retrieved from the MIRS for NOAA-18 AMSU-MHS (right panel) and from the collocated GDAS assimilation system (left panel) on June 6, 2008

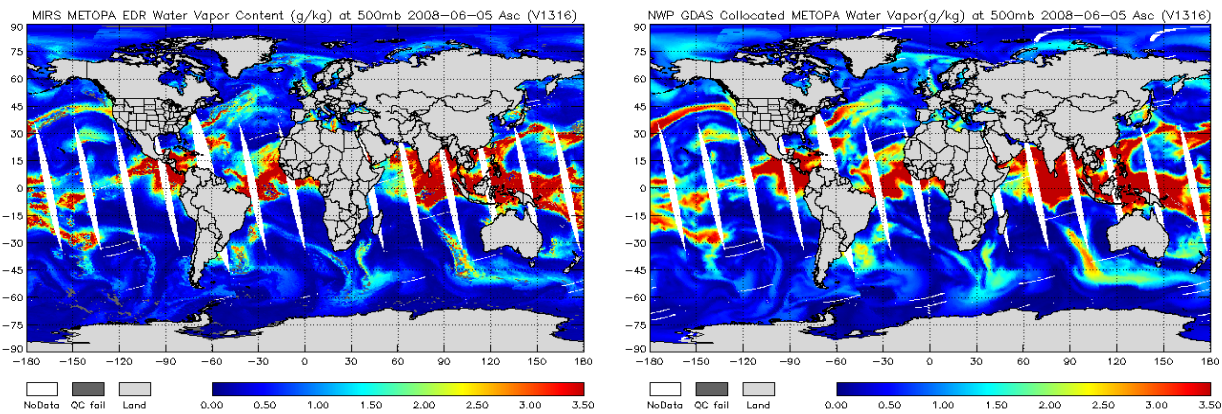
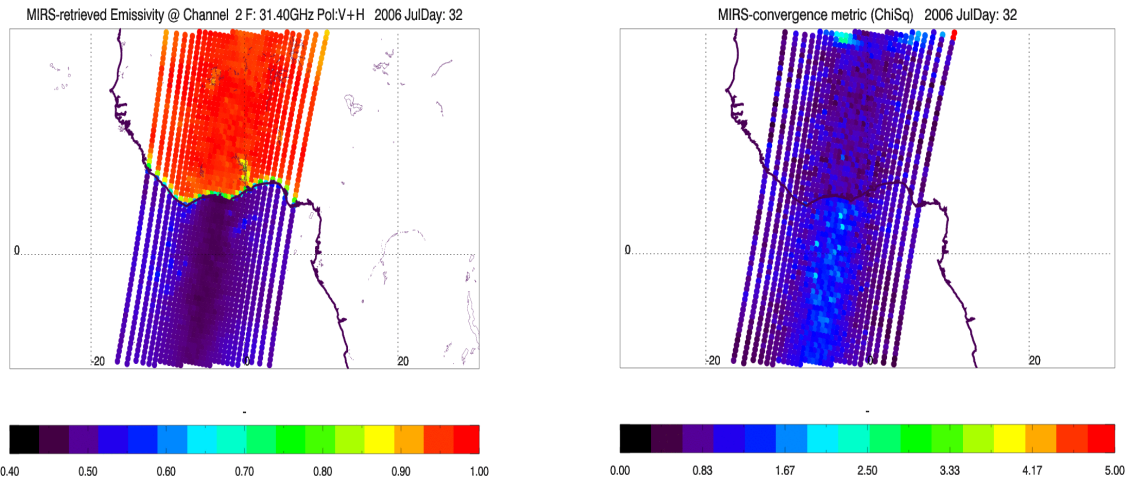


Figure 20. Comparison of fields of water vapor mixing ratio at 500 millibars, retrieved from the MIRS for METOP-A AMSU-MHS (right panel) and from the collocated GDAS assimilation system (left panel) on June 5, 2008

### 6.2.3 Surface Emissivity

Surface emissivity is part of the state vector being retrieved over all surface types. First, surface type is determined by a surface pre-classification algorithm. Depending on the detected surface type, the MIRS switches covariance matrices. The retrieved emissivities represent *effective* values that accounts for local geography, penetration depth, surface heterogeneity and other surface factors. Figure 26 depicts a portion of an orbit of retrieved emissivity at AMSU channel 2 (31.4 GHz). It clearly shows the expected contrast between ocean and land emissivities. It also shows the mixed pixels emissivities (river and coastal points) where the emissivity value is somewhat between the land and ocean values. Also depicted is the convergence metric.

The validation of surface emissivities are routinely conducted by comparing MIRS retrieved emissivities with those analytically computed by using NWP (GDAS and ECMW) and radiosonde measurements and sensor brightness temperature data as inputs. Figure 22 and Figure 23 show global distribution of emissivities at AMSU-MHS 50 GHz retrieved from MIRS and analytically computed from collocated NPW analysis geophysical data and brightness temperatures as inputs. As shown, the major emissivity features are retrieved well. Note the scan dependence of emissivity over ocean as well as the clear contrast in emissivity over ice and ocean surfaces. Figures 29 and Figure 30 show routine comparisons and statistics of MIRS retrieved emissivities with those analytically derived using analysis or radiosonde data as inputs.



**Figure 21.** Qualitative validation of the surface emissivity retrieved by the MIRS algorithm (left), channel 31.4 GHz. The ocean emissivity is lower than that of land. As expected, river surfaces lower the surface emissivity. Scan-dependent variation of the emissivity over ocean can also be seen. The right panel represents the convergence metric showing that the system is able to fit the measurements within noise levels.

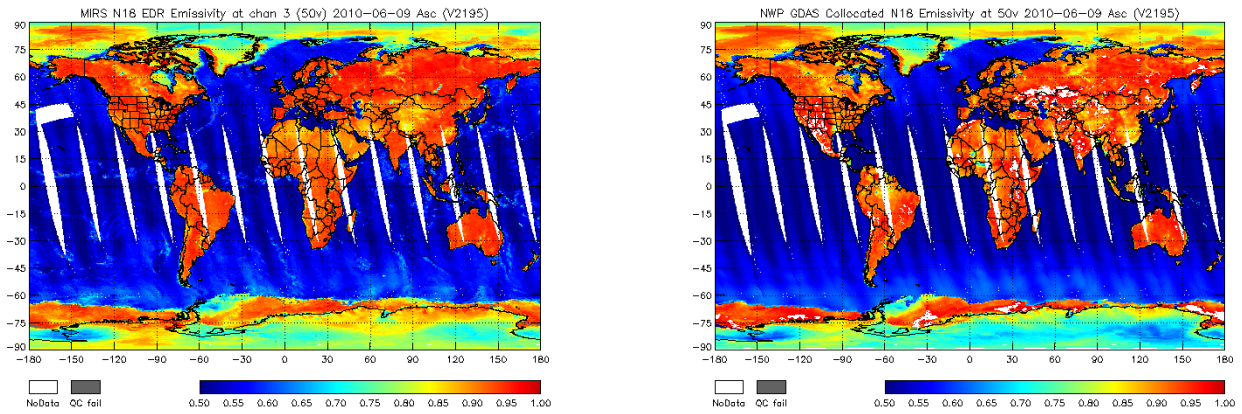


**Figure 22.** Global distribution of emissivity at 50 GHz AMSU-MHS channel routinely retrieved from MIRS (left panel) and analytically computed from GDAS data (right panel)

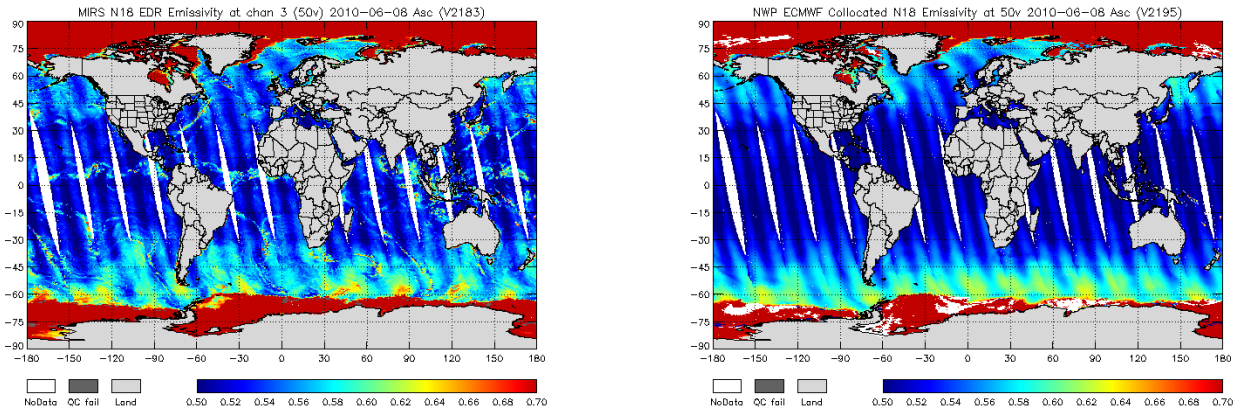


*Figure 23. Global distribution of emissivity over ocean at the 50 GHz AMSU-MHS channel routinely retrieved from MIRS (left panel) and analytically computed from ECMWF data (right panel). Shown is the clear contrast of emissivities over water and sea ice surfaces.*

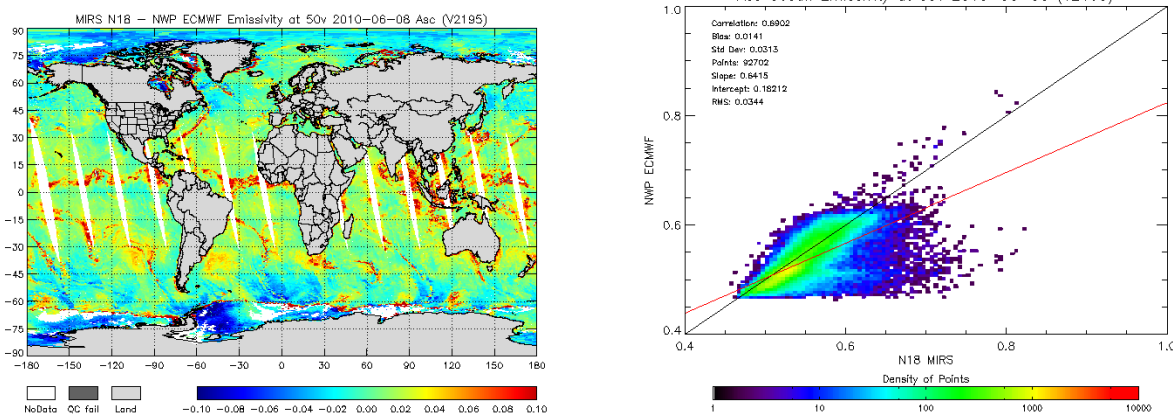


*Figure 24. Global distribution of the 50 GHz emissivity differences retrieved from MIRS and analytically computed from collocated NWP ECMWF analysis geophysical inputs (left panel) and statistical assessment results (right panel)*

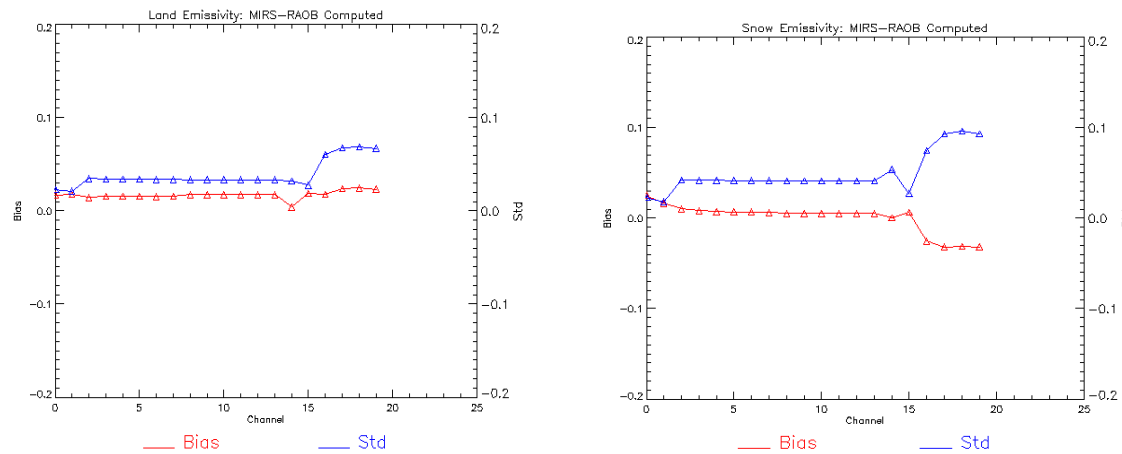
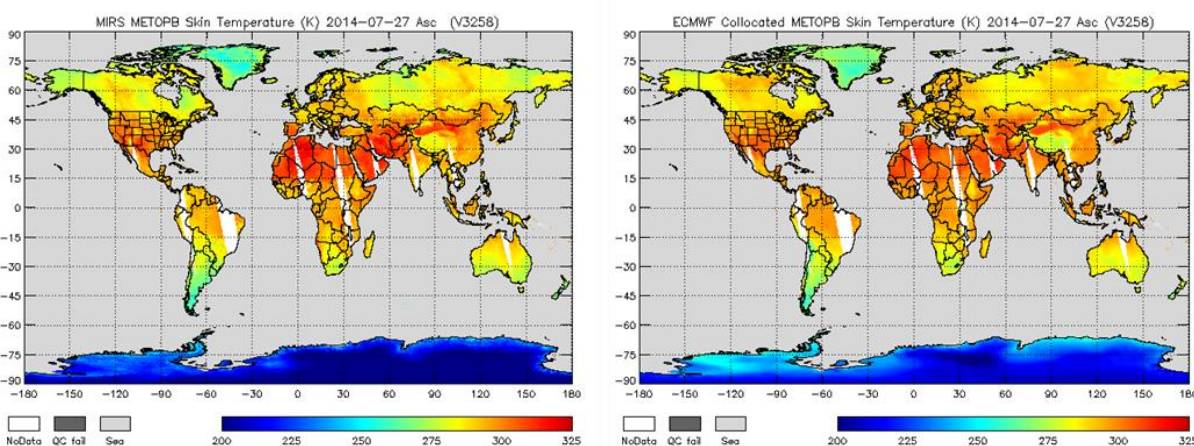


**Figure 25.** Routine statistical comparisons between MIRS retrieved emissivity at AMSU-MHS 50 GHz and the analytically derived emissivities using collocated radiosonde geophysical data as inputs. Shown is the bias and standard deviation computed for all AMSU-MHS channels. Results indicate good retrievals for most AMSU-MHS channels. Accuracy degrades for channels 16-20.

## 6.2.4 Surface Temperature

Surface (skin) temperature is retrieved directly in MIRS as part of the geophysical state vector and is core retrieved product. While surface temperature is retrieved over all surface types, only the land surface temperature (LST) is an official MIRS product.

### 6.2.4.1 Over Land



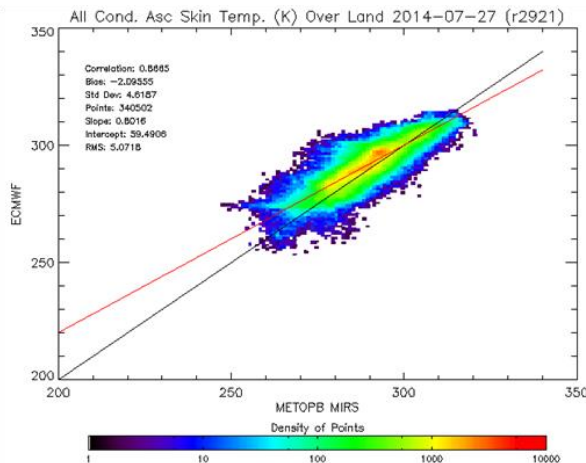


*Figure 26. Example of MIRS Metop-B retrieved LST (top left) with ECMWF analysis of LST (top right) valid July 27, 2014, along with scatter plot (bottom left).*

## 6.3 Validation of MIRS Derived Products

### 6.3.1 Total Precipitable Water

Traditionally, total precipitable water (TPW) has been retrieved only over ocean. Over land, sea ice and snow surfaces, reliable retrievals are more difficult due to diminished contrast with the atmosphere. Validation results show that reliable retrievals are possible to a sufficient degree of accuracy. Note that MIRS extends the MSPPS capability of TPW retrievals to non-ocean surfaces. MIRS retrieved TPW is compared daily against radiosonde measurements as well as GDAS and ECMWF analysis fields over snow cover, snow-free land, sea-ice and ocean surfaces. In addition, off-line validation studies have also been conducted and are summarized below.

#### 6.3.1.1 Total Precipitable Water Over Ocean

Figure 27 and Figure 28 present performance assessment results derived from MIRS daily routine monitoring of MIRS retrieved TPW versus TPW obtained from collocated GDAS and ECMWF analysis fields and versus TPW obtained from collocated radiosonde measurements. Figure 29 presents inter-comparison results of TWP over ocean with that retrieved from MSPPS.

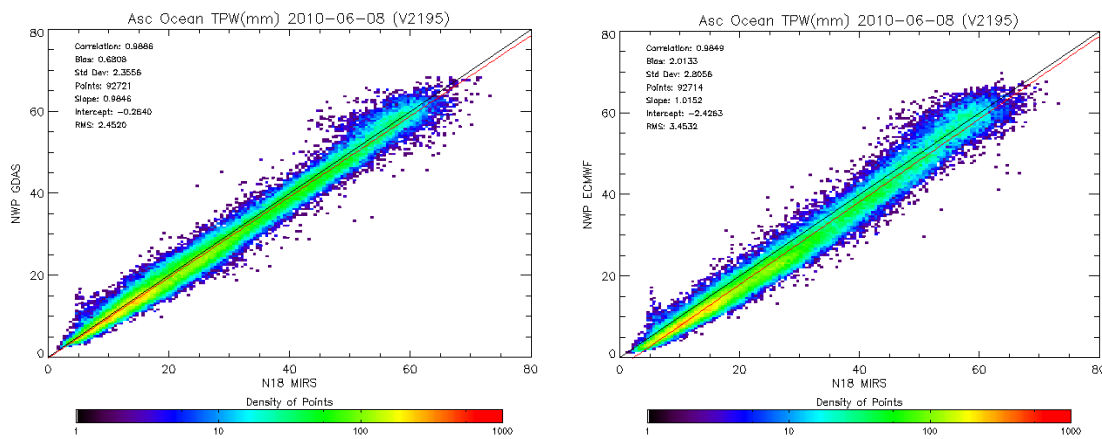


Figure 27. Performance assessment results of MIRS-retrieved TPW over ocean for NOAA-18 AMSU-MHS versus GDAS (left panel) and ECMWF (right panel).

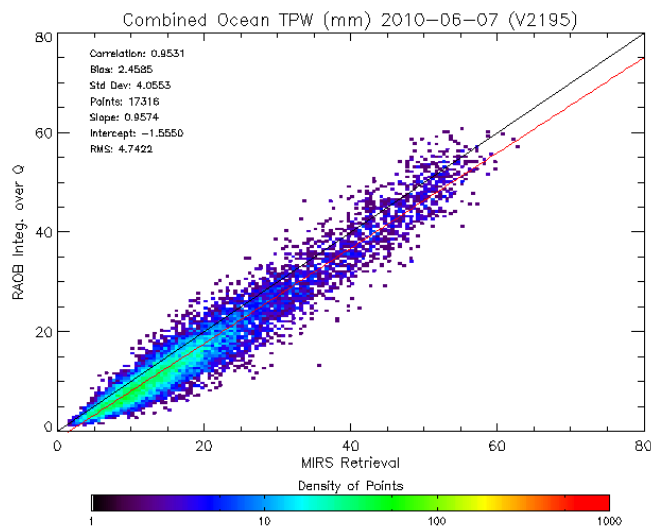


Figure 28. Performance assessment results of MIRS-retrieved TPW over ocean versus TPW derived from radiosonde measurements.

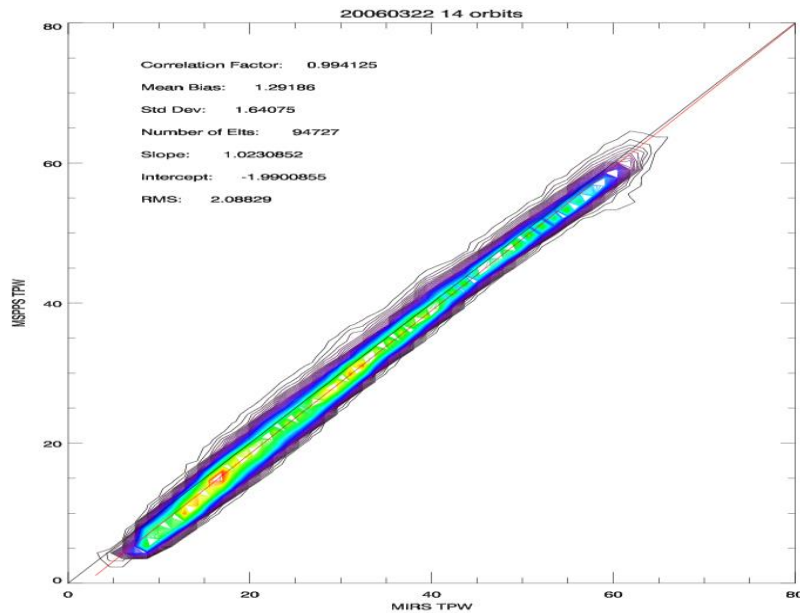


Figure 29. Comparison between MIRS-retrieved and MSPPS-retrieved TPW over ocean for NOAA-18 AMSU-MHS

### 6.3.1.2 Total Precipitable Water Over Non-Ocean Surfaces

From a physical standpoint, retrievals of atmospheric parameters in MIRS are independent of the surface background. The only difference between retrievals over ocean and over land, snow or ice is the spectral constraints put on the emissivity retrievals. Over ocean, these constraints are developed using a surface emissivity model (FASTEM5), while over land, these constraints are built using statistics based on a database of emissivities derived from coincident satellite data, ground-based surface temperatures and assimilation model outputs. In MIRS, a surface type pre-classification algorithm determines surface type over both land (snow versus non-snow) and ocean (sea ice versus open water). Figure 30 and Figure 31 present performance assessment results computed from routine daily monitoring process for the MIRS retrieved global TPW versus NWP analysis fields and versus radiosonde measurements. Figure 32 also shows global distribution maps of the MIRS retrieved TPW and the TPW retrieved from GDAS.

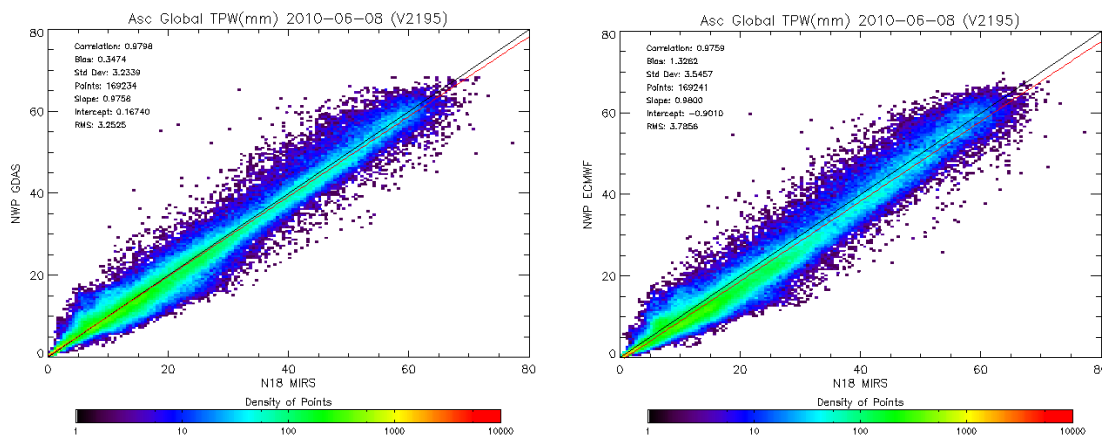


Figure 30. Performance assessment results computed from routine monitoring for MIRS retrieved global TPW with respect to GDAS (left panel) and ECMWF (right panel)

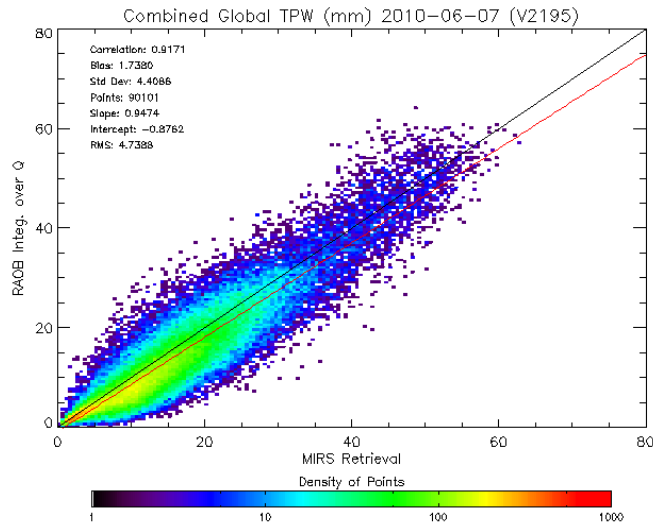
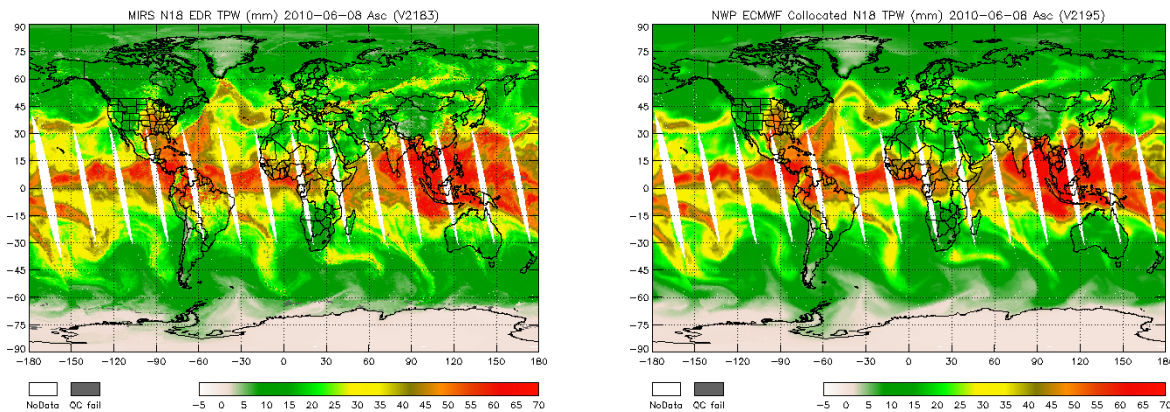


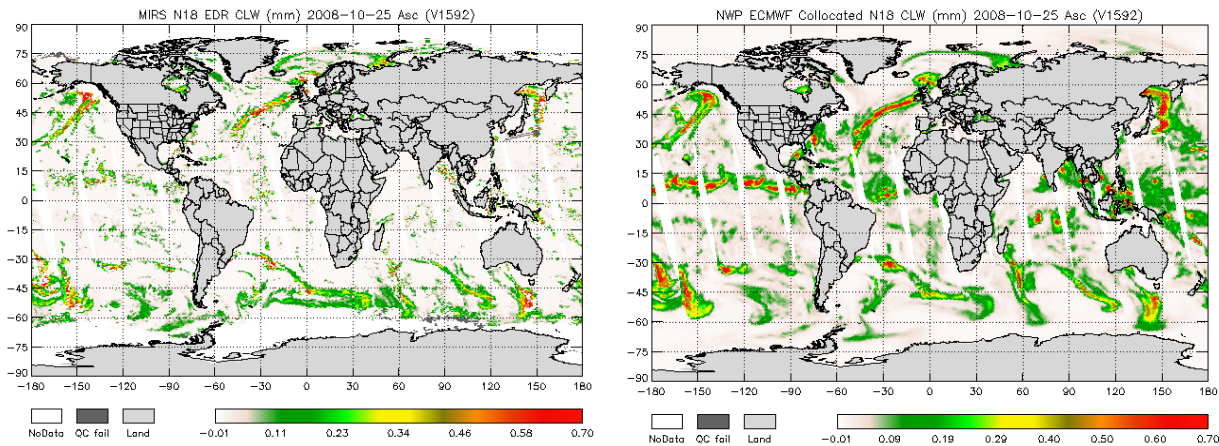
Figure 31. Performance assessment results computed from routine monitoring for MIRS retrieved global TPW with respect to TWP derived from radiosonde measurements



*Figure 32. Example of routine comparison of global distribution of TPW retrieved from MIRS for NOAA-18 AMSU-MHS (left panel) and from collocated ECMWF (right panel).*

### 6.3.2 Non-Precipitating Cloud Liquid Water (CLW)

The non-precipitating cloud liquid water amount is derived from vertical integration of the cloud liquid amount profile (main MIRS product fields). Figure 33 presents the comparison of this product from MIRS to collocated ECMWF analysis fields. The MIRS CLW is valid over ocean only. It is important to note that the ECMWF definition of CLW contains both precipitating and non-precipitating liquid water, whereas MIRS CLW contains non-precipitating liquid water only.



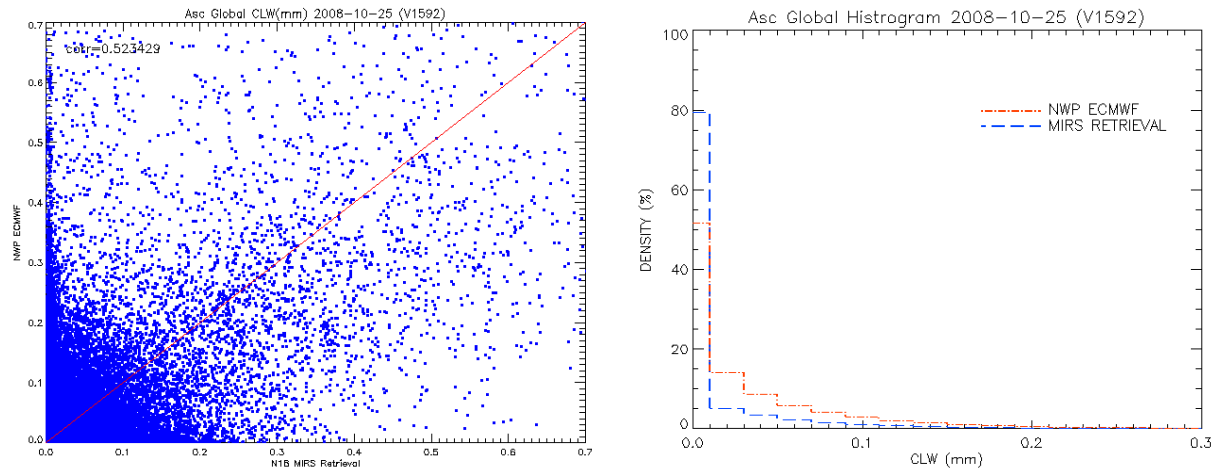


*Figure 33. Integrated Cloud Liquid Water (CLW) retrieved from MIRS (upper left) and from ECMWF analysis (upper right). Included are a scatter and density histogram to show the correlation of MIRS NOAA-18 AMSU-MHS retrieved CLW to ECMWF, as well as the distribution of each.*

Figure 34 shows a scatter plot and histogram of the MIRS NOAA-18 AMSU-MHS retrieved CLW to collocated CloudSat CLW. The collocation set contains approximately 22,000 points over ocean surface, and spans the time period of October 2008 through November 2008. The collocation criteria are strict, and follow a time constraint of 2 minutes, a distance constraint of 25 km, and are only for AMSU-MHS scan angles  $\pm 10^\circ$  of nadir.

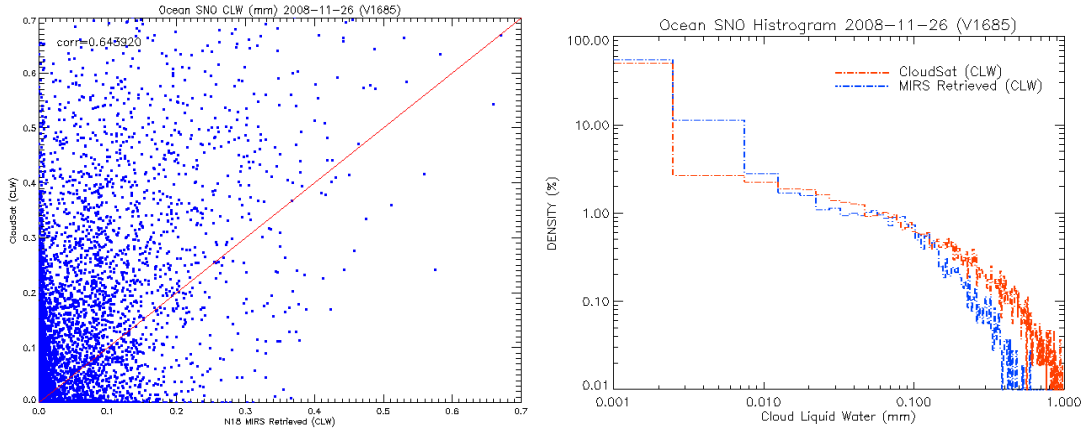


*Figure 34. Performance assessment results of MIRS NOAA-18 AMSU-MHS and CloudSat CLW. Scatter plot (left) and density histogram (right). The correlation between MIRS and CloudSat CLW is 0.64.*

### 6.3.3 Rain Rate

As described in section 3.3.2.3 the MIRS rain rate is a precipitation product solely based on the MIRS hydrometeor products CLW, RWP, and IWP. The algorithm to derive rain rate takes advantage of the physical relationship found between atmospheric hydrometeor amounts and surface rain rate. The MIRS rain rate algorithm uses a multi-linear regression approach that requires integrated CLW, IWP, and RWP (in mm), and a set of regression coefficients

corresponding to each hydrometeor in order to retrieve the instantaneous rain rate in mm/hr over ocean and land. The regression coefficients are static components in the algorithm that have been determined based on an off-line training using collocated sets of rainfall rate and hydrometeor products from both the Penn State University and the National Center for Atmospheric Research Mesoscale Model (MM5) data for the ocean case and from the Operational Microwave Surface and Precipitation System (MSPPS) for the land case. Figure 35 illustrates the comparison of MIRS rain rate (left) to MSPPS rain rate (right) for August 1, 2014.

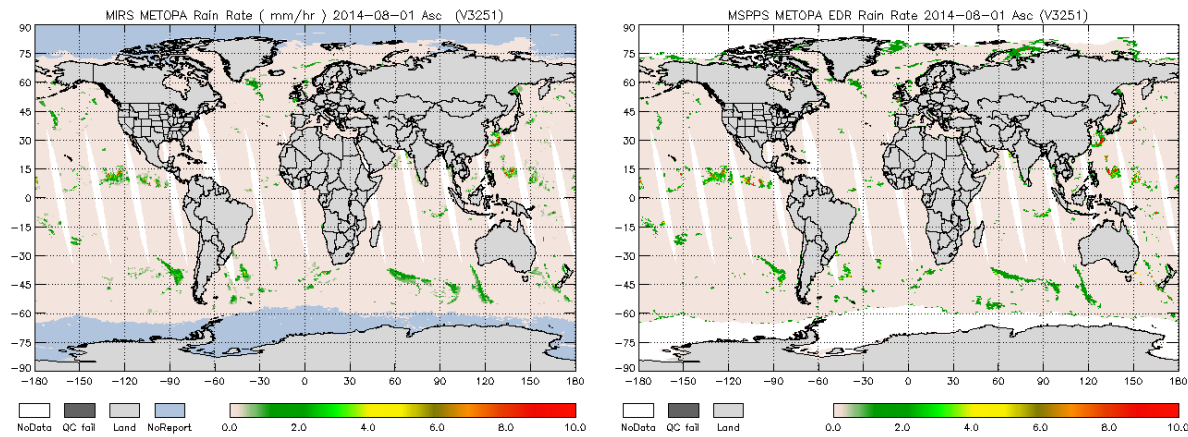


Figure 35. MIRS derived Rain Rate (left) compared to Operational MSPPS Rain Rate (right) for Metop-A on August 1, 2014.

Figure 36 displays a quantitative comparison between the MIRS and MSPPS rain rates. Scatter plots are shown for rain rates over land (left) and ocean (right) surfaces. The correlations are 0.85 and 0.71 respectively.

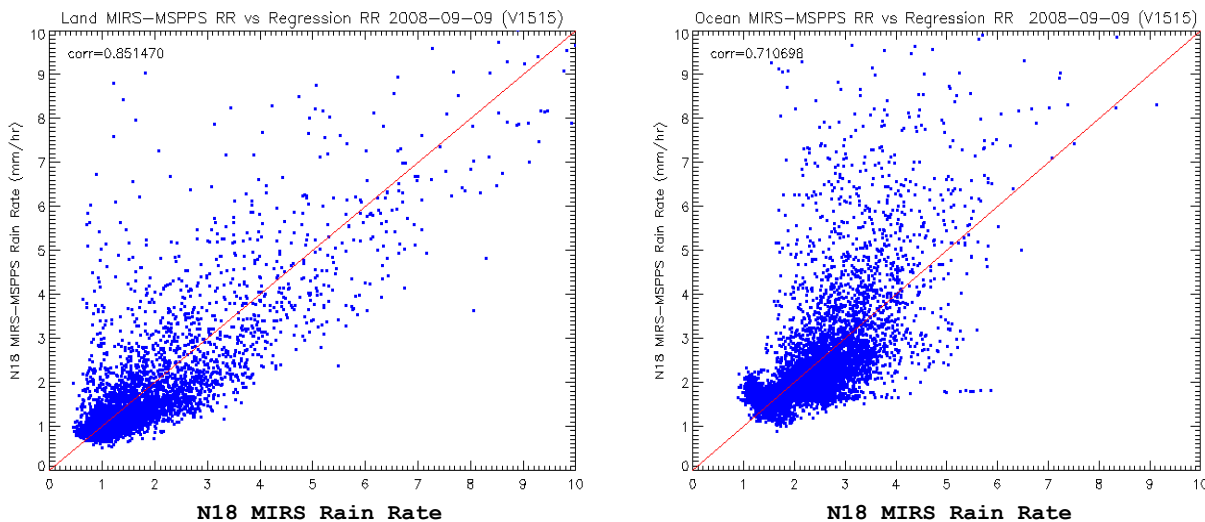


Figure 36. Scatter plots of MIRS rain rates vs. MSPPS for NOAA-18 for September 9, 2008 over land (left) and ocean (right). The correlations are 0.85 and 0.71 respectively.

Comparisons of the MIRS derived rain rate are also made to rain gauge and surface radar at the International Precipitation Working Group (IPWG) project, and internally at STAR to NOAA/NCEP Climate Prediction Center (CPC). The IPWG performs large-scale validation and inter-comparisons of daily rainfall estimates from operational and semi-operational satellite rainfall rate retrievals against rain gauge and ground-based radar. The CPC rain gauge analysis contains information from over 8000 stations across the U.S. and Mexico, gridded at  $0.5^{\circ}$  resolution. From MIRS, rainfall rate retrievals from NOAA-18, Metop-A and F18 are used to compute the daily rainfall rate in mm/day over the U.S., South America, and Australia. Optionally, MIRS rainfall rate from NOAA-19 and F18 may also be included in the composite or replace NOAA-18 and F18, respectively. This precipitation estimate is then compared to the gridded rain gauge, radar, and other rainfall rate retrieval algorithms.

Figure 37 shows the comparison of MIRS rainfall rates compared to rain gauge and radar for 13Z May 20, 2009 to 12Z May 21, 2009, compiled by IPWG. The correlations for the MIRS rain rate are 0.75 and 0.62 between radar and rain gauge, respectively.

Figure 38 shows the time series of statistics (correlation and false alarm ratio) computed at IPWG, and monitored within STAR.

Figure 39 shows the comparison of MIRS rainfall rates with CPC rain gauge analysis, as well as the timeseries for correlation and detection failure ratio. The record of sensor measurements, along with the record of CPC data, are retained for the time period and accumulated on a daily basis in order to assess the daily variability or stability of the MIRS daily rainfall rate. This record also aids in the quick assessment of algorithm changes which may affect the rainfall rate estimation, it retained measurements can be reprocessed.

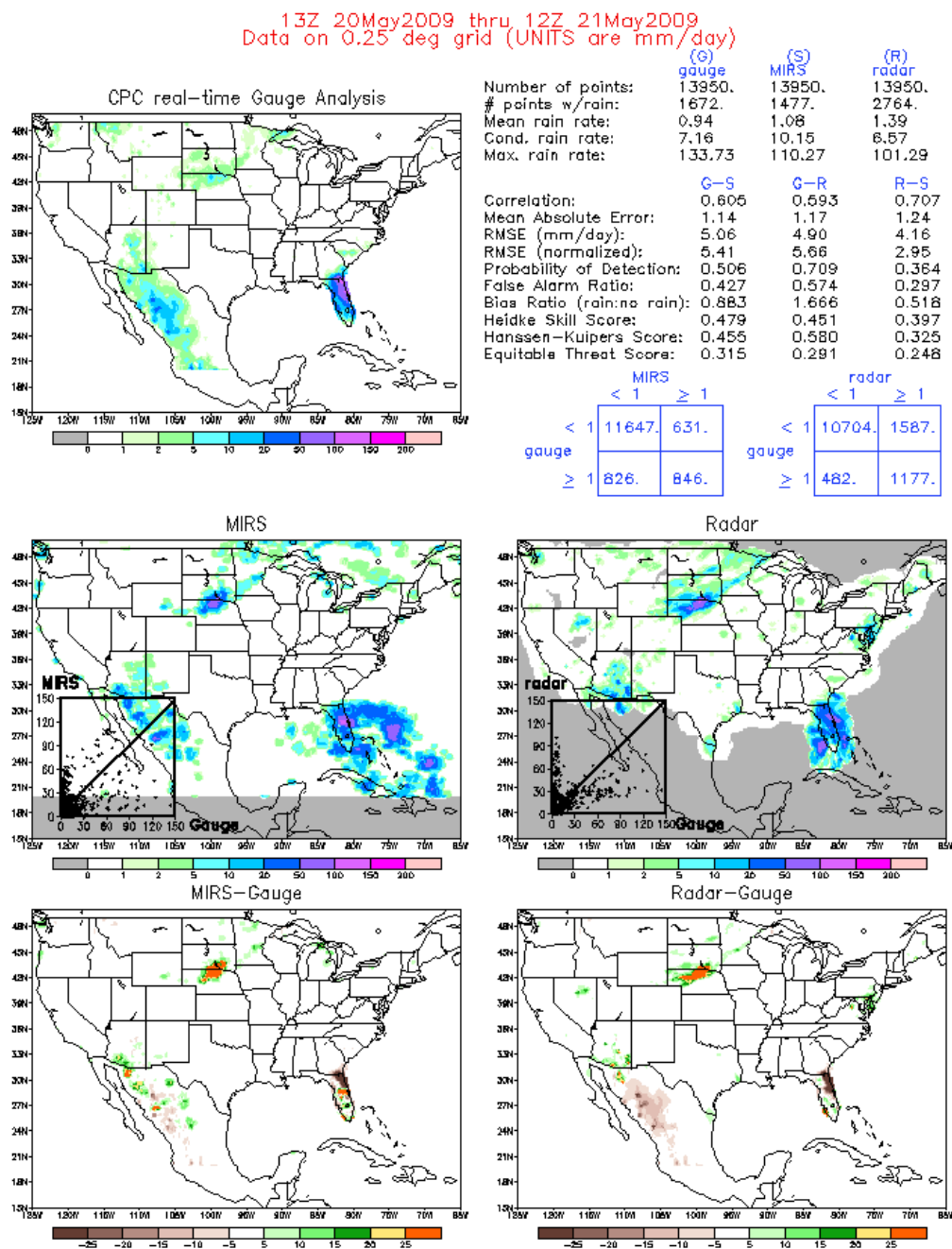
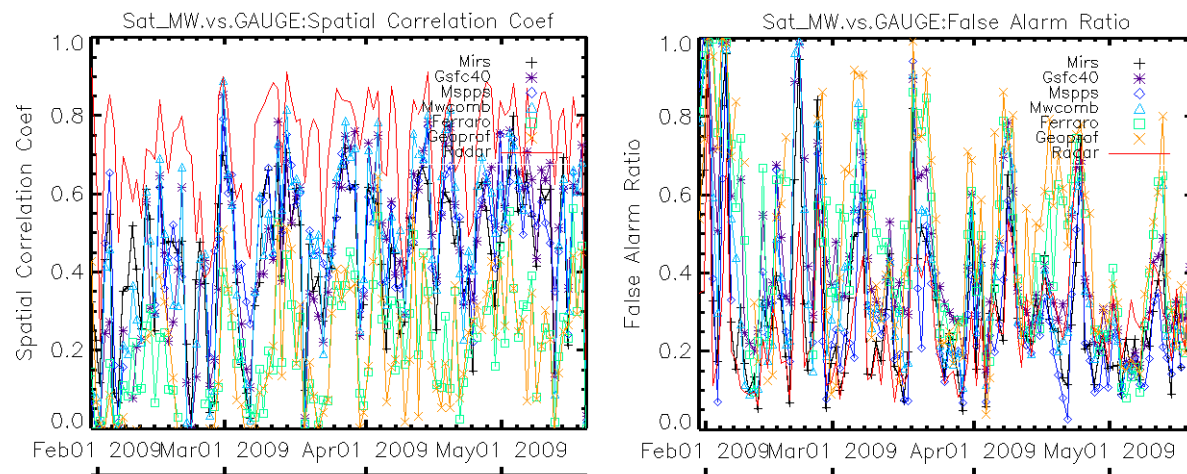


Figure 37. IPWG assessment of MIRS rainfall rate (mm/day) compared to rain gauge and radar observations over the continental U.S. from 13Z May 20, 2009 to 12Z May 21, 2009.



*Figure 38. Timeseries of MIRS rainfall rate (mm/day) correlation (left) and false alarm ratio (right) compared to rain gauge observations over the continental U.S. The black line represents MIRS, while the red line represents radar versus rain gauge.*

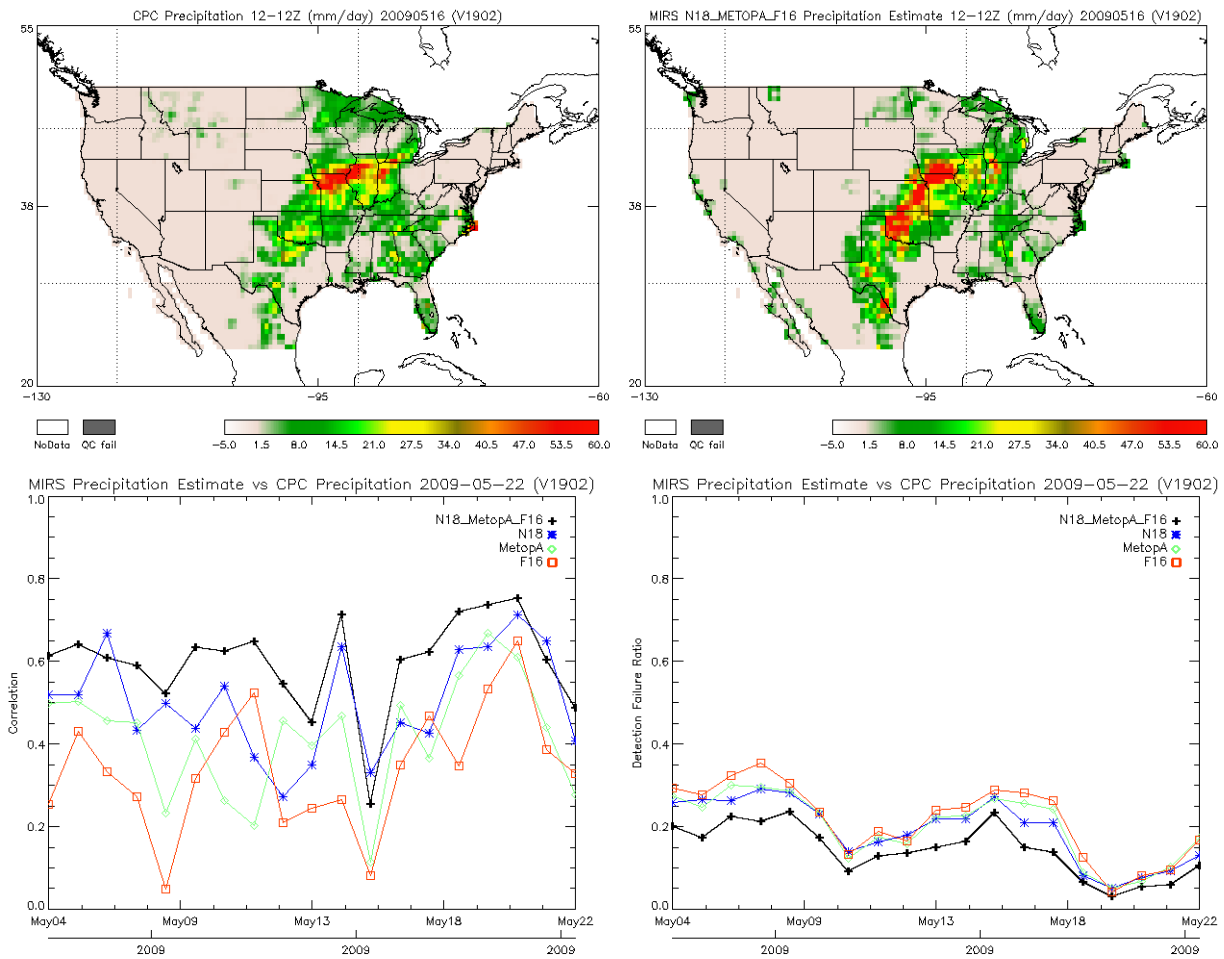


Figure 39. MIRS daily rainfall rate (upper left) and CPC rain gauge analysis (upper right) from May 15, 2009 12Z to May 16, 2009 12Z. Timeseries of MIRS daily rainfall rate correlation (bottom left) and detection failure ratio (bottom right) compared to CPC, stratified by sensor.

### 6.3.4 Rain Water Path

RWP is a post-processed product valid over both ocean and land based on the vertical integration of the retrieved rain water profile. Figure 40 shows an example of the MIRS RWP product for NOAA-18 valid on June 10, 2010. Results from several years' collocation comparisons with the TRMM 2A12 product are shown in Figure 41 and Figure 42. Given the inherently large temporal and spatial variability of RWP, the intrinsic differences between algorithms, and the time and space collocation limitations, the high degree of difference in the comparisons is not surprising.

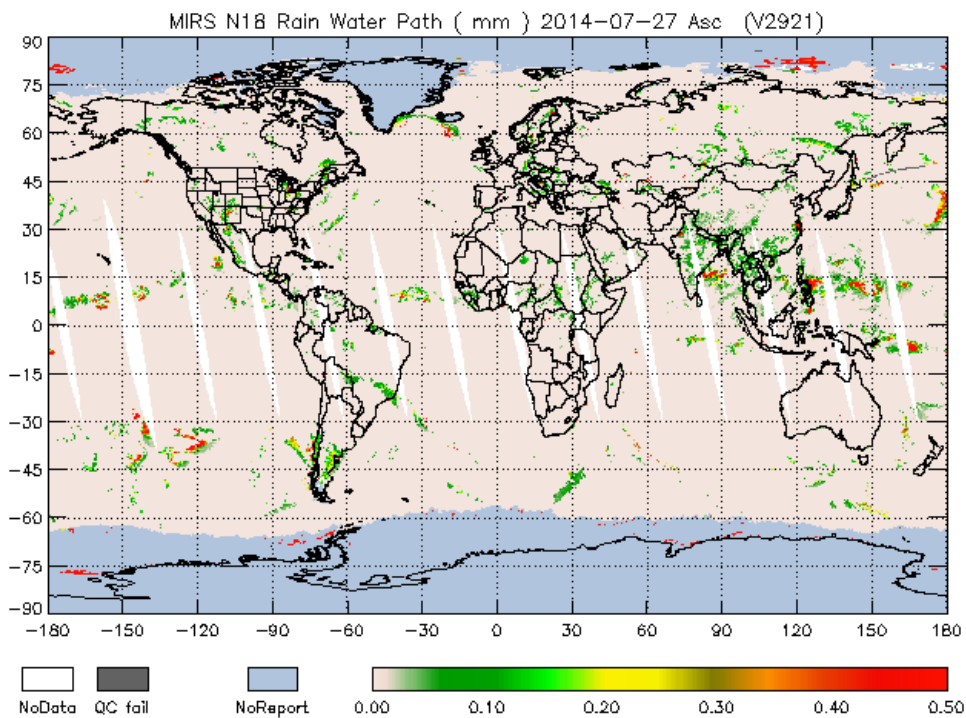


Figure 40. MIRS rain water path retrieval for NOAA-18 valid on July 27, 2014

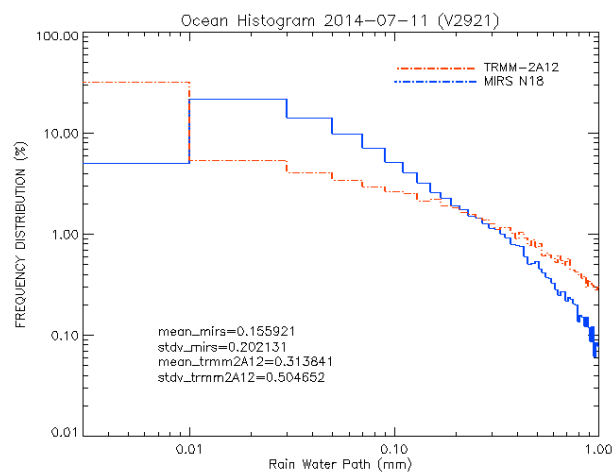
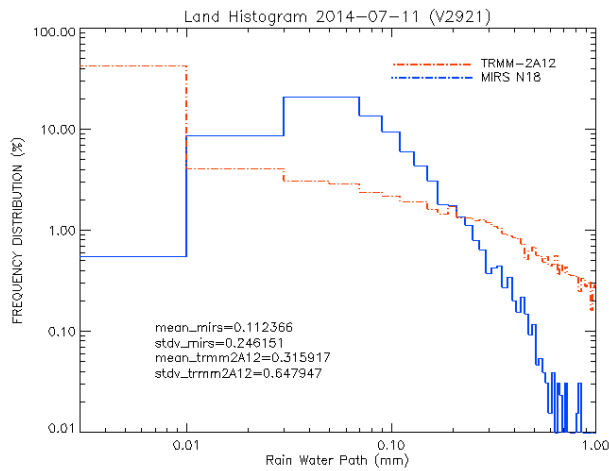


Figure 41. Comparison of MIRS rain water path for NOAA-18 with TRMM 2A12 product over ocean.



*Figure 42. Comparison of MIRS rain water path path for NOAA-18 with TRMM 2A12 product over land.*

### 6.3.5 Ice Water Path

IWP is a post-processed product valid over both ocean and land based on the vertical integration of the retrieved rain water profile. Figure 43 shows an example of the MIRS IWP product for Metop-B valid on July 27, 2014. Results from several years' collocation comparisons with the TRMM 2A12 product are shown in Figure 44 and Figure 45. Given the inherently large temporal and spatial variability of IWP, the intrinsic differences between algorithms, and the time and space collocation limitations, the high degree of difference in the comparisons is not surprising.

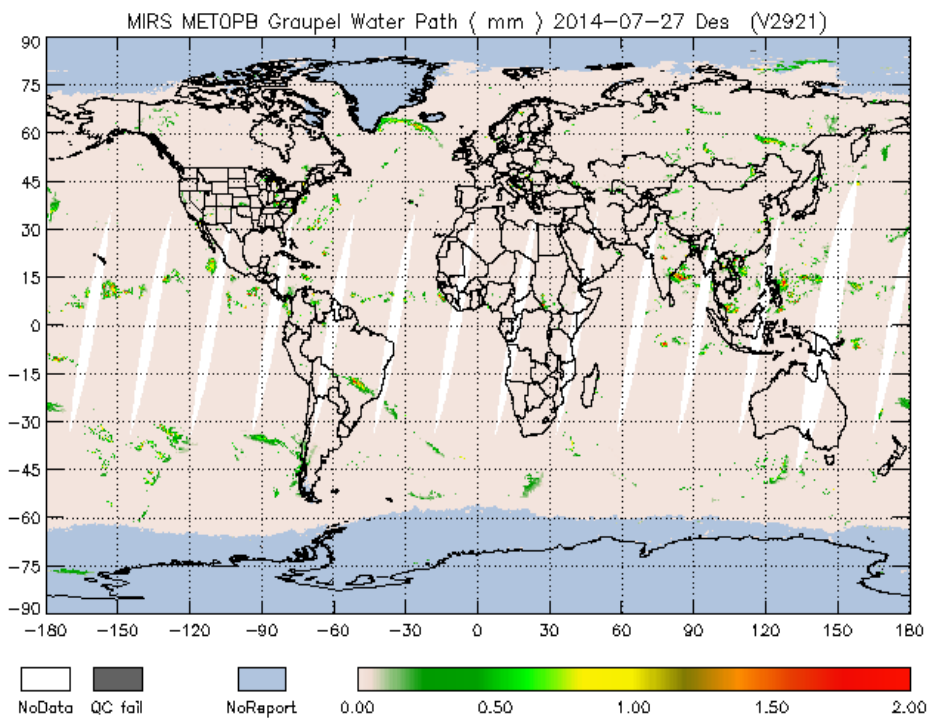


Figure 43. MIRS ice water path retrieval for Metop-B valid on July 27, 2014

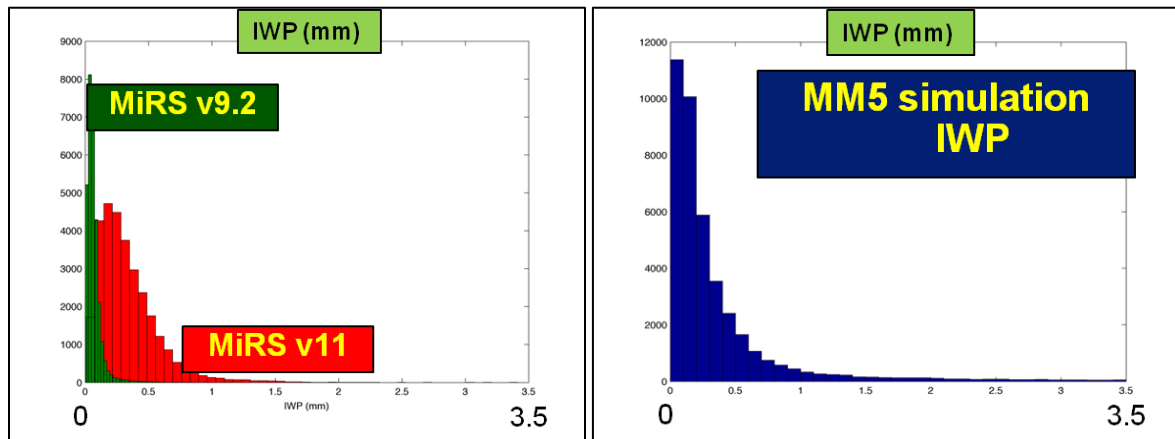


Figure 44. Comparison of MIRS ice water path path retrieval histograms for Metop-B with MM5 simulated histograms. For MiRS, both v9.2 (previous version of MiRS) and the current v11 algorithms are shown indicating improved agreement with MM5 distribution in the current v11 algorithm.

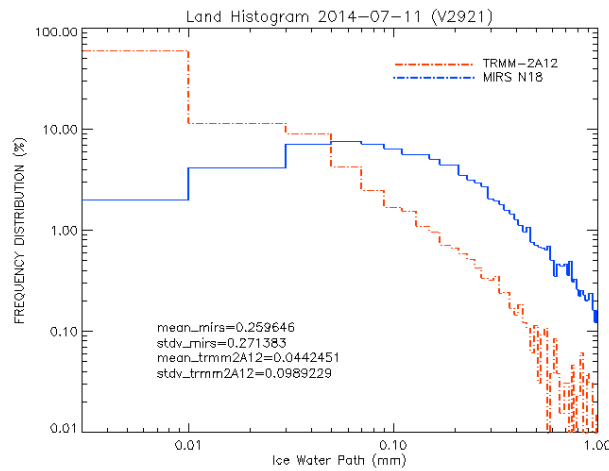


Figure 45. Comparison of MIRS ice water path path for NOAA-18 with TRMM 2A12 product over land.

### 6.3.6 Snow Water Equivalent (SWE)

The SWE product uses the retrieved surface emissivities as inputs and a catalog of surface emissivities and snow pack properties derived off-line from a one-layer Dense Media Radiative Transfer snow emissivity model. The retrieved MIRS emissivity spectra are compared with those from the catalog to find the closest match. Independent evaluation of this physically-based technique was performed against measured SWE data recorded in US and Canadian Prairie regions over a 5-year period between years 2001 and 2005. The SWE measurements were collocated with the AMSU data which were used as input to run MIRS. Figure 46 shows scatter plots and performance statistics of MIRS and MSPPS SWE products. MIRS SWE shows improved performance as compared to MSPPS algorithm, as demonstrated by higher correlation and smaller root mean square error.

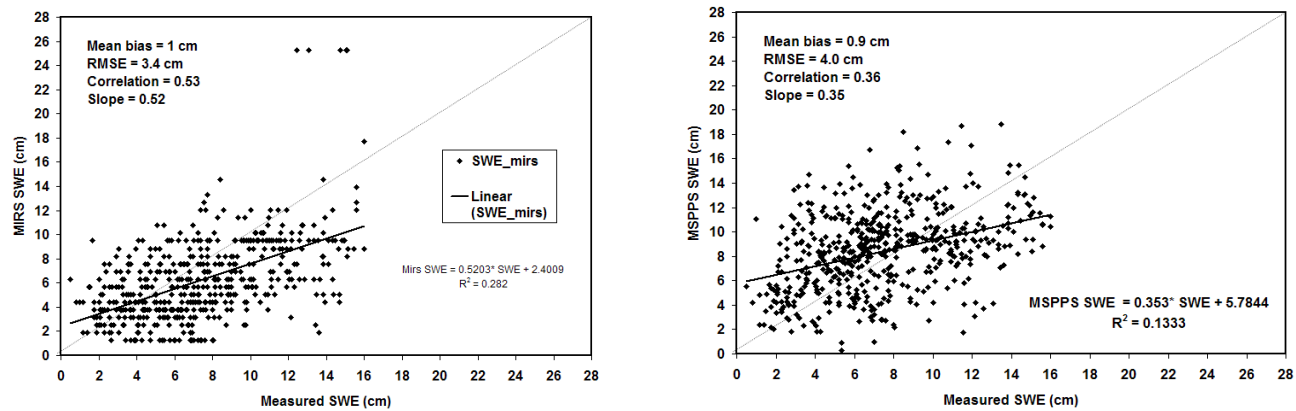


Figure 46. Scatter plots and performance statistics of MIRS (top) and MSPPS (bottom) SWE versus measured SWE.

A comparison of the MIRS SWE product with the JAXA AMSR2 SWE is shown in Figure 47. The retrieved fields agree fairly well in terms of snow cover extent and amount, although some differences can be seen in the actual spatial patterns of snow water.

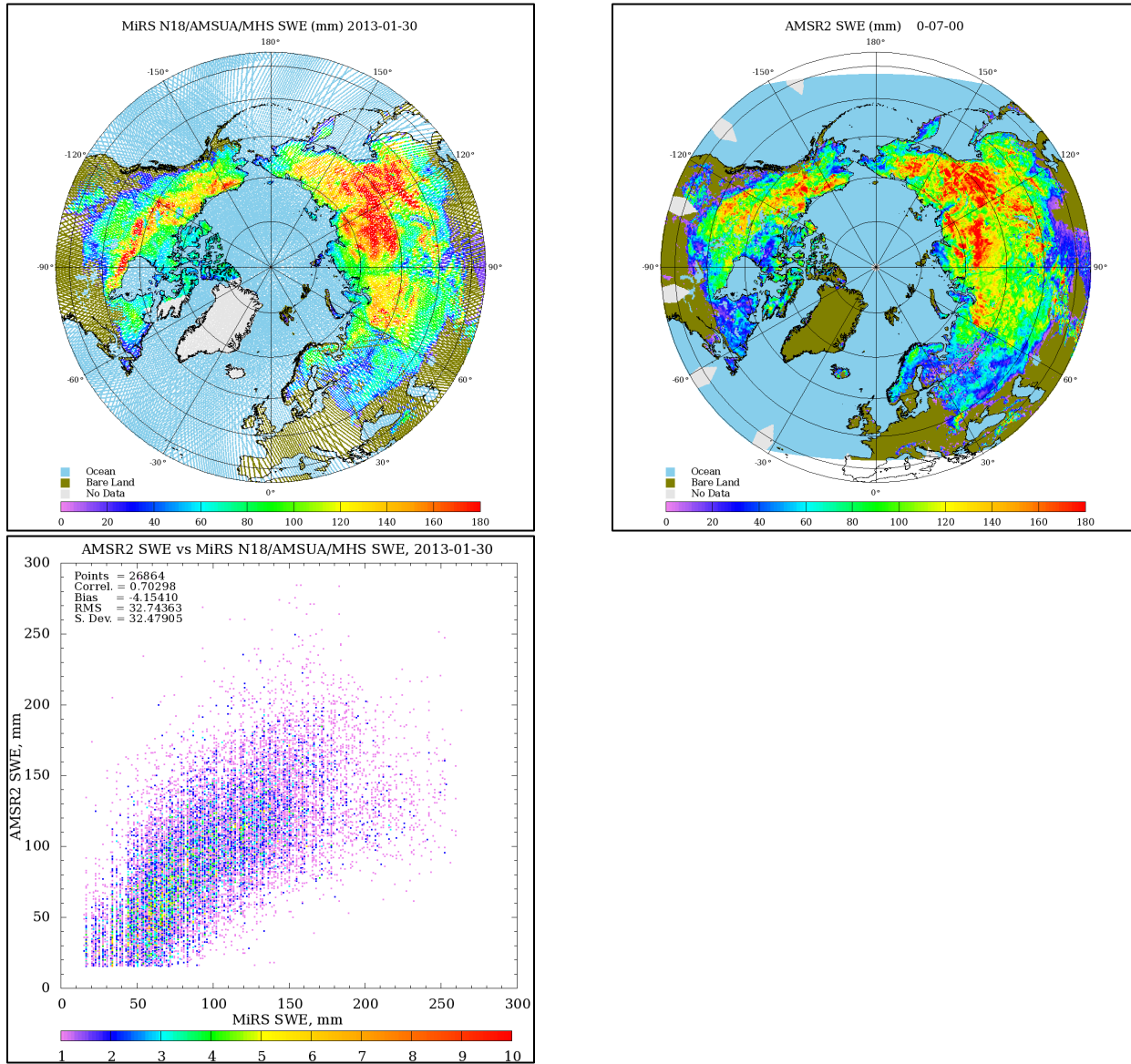


Figure 47. Comparison of MIRS N-18 AMSU/MHS snow water equivalent product (top left) with that from AMSR2 JAXA algorithm (top right) for January 30, 2013, along with corresponding scatterplot (bottom left).

### 6.3.7 Snow Grain Size (SGS)

SGS is retrieved at the same time as the SWE product, since the Dense Media model accounts for the effects of both snowpack characteristics on the microwave emissivity. A comparison of MiRS retrieved SGS from both N18 AMSU/MHS and F18 SSMIS with the GlobSnow analysis over Asia in Figure 48 shows relatively good agreement. SGS is difficult to validate in an absolute sense

since there are few in situ measurements at a scale and density that are commensurate with microwave satellite observations.

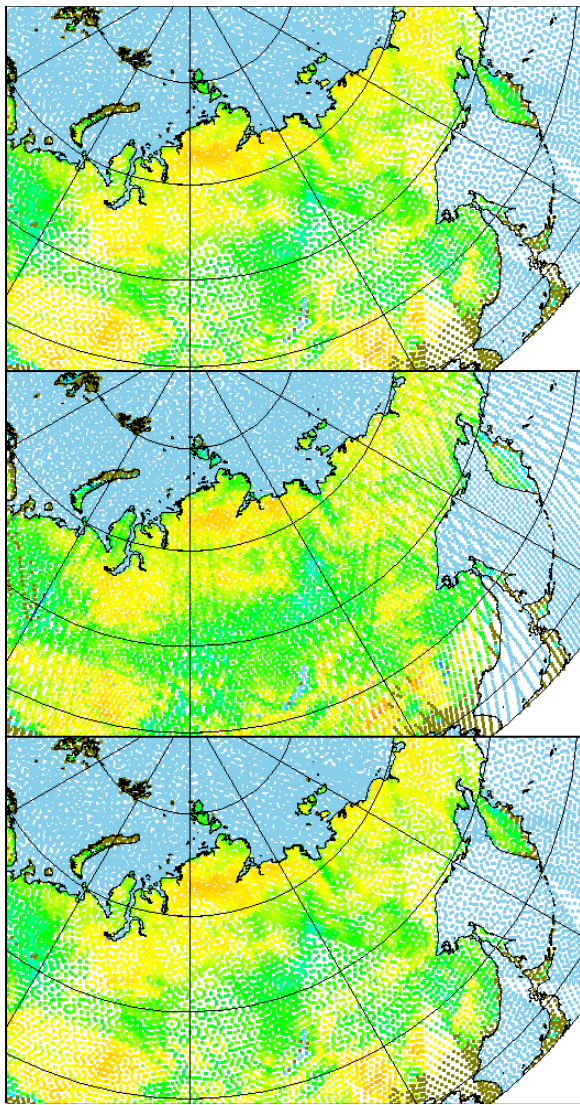
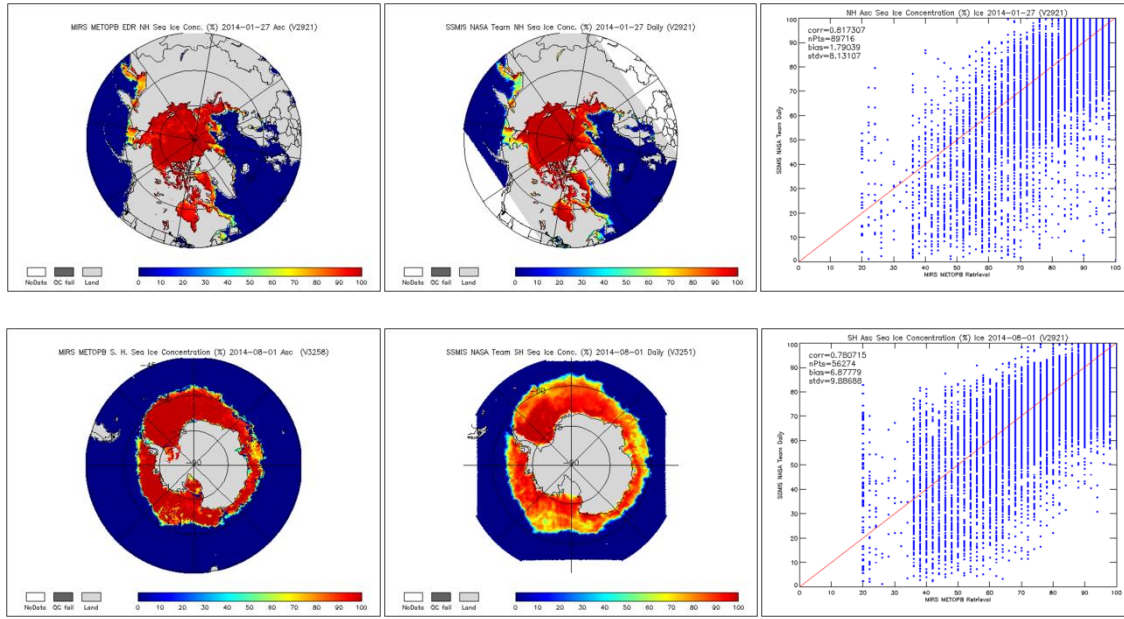


Figure 48: Comparison of N18 (top left), and F18 (top right) SGS retrievals (radius, mm) on January 30, 2013 with the GlobSnow analysis (bottom left). GlobSnow grain size is not an operational product. Courtesy of FMI/ESA.

### 6.3.8 Sea Ice Concentration (SIC)

The SIC product uses MIRS retrieved surface emissivities and skin temperature as inputs and a catalog of surface emissivities and ice fractions derived off-line from emissivity spectra of water and ice surface types. The retrieved MIRS emissivity spectra are compared with those from the catalog to find the closest match and compute SIC. The performance of the MIRS SIC product is routinely monitored by comparisons with MSPPS SIC product, as well as with the SIC from AMSR2 microwave measurements. The comparison with AMSR2 has the advantage of being an independent assessment from a completely different microwave sensor. Non-routine assessments

have been made by comparisons with the 4-km NOAA's Interactive Multi-Sensor Snow and Ice Mapping System (IMS). The IMS sea ice concentration was computed at the microwave sensor resolution by collocation and footprint matching. Figure 49 shows an example of routine retrieval maps and scatter plots of MIRS retrieved SIC and the SIC retrieved from the F17/SSMIS NASA Team algorithm. **Error! Reference source not found.** summarizes performance statistical results of MIRS and MSPPS retrieved SIC versus that computed from collocated IMS data.



*Figure 49. Scatter plots and performance statistics of MIRS Metop-B (left) SIC retrievals when compared with F17/SSMIS NASA Team (center) SIC on January 27, 2014, and August 1, 2014. Scatter plots are shown for Northern Hemisphere (top) and Southern Hemisphere (bottom).*

|              | <b>December</b> |             |              |
|--------------|-----------------|-------------|--------------|
|              | <b>IMS</b>      | <b>MIRS</b> | <b>MSPPS</b> |
| <b>Mean</b>  | <b>98.5</b>     | <b>96.7</b> | <b>92.4</b>  |
| <b>Bias</b>  |                 | <b>-1.8</b> | <b>-6.1</b>  |
| <b>RMSE</b>  |                 | <b>9.2</b>  | <b>11.9</b>  |
|              | <b>April</b>    |             |              |
|              |                 |             |              |
| <b>Means</b> | <b>98.3</b>     | <b>96.2</b> | <b>95.5</b>  |
| <b>Bias</b>  |                 | <b>-2.1</b> | <b>-2.8</b>  |
| <b>RMSE</b>  |                 | <b>8.4</b>  | <b>9.5</b>   |
|              | <b>October</b>  |             |              |
|              |                 |             |              |
| <b>Means</b> | <b>96.3</b>     | <b>88.5</b> | <b>80.9</b>  |
| <b>Bias</b>  |                 | <b>-7.8</b> | <b>-15.4</b> |
| <b>RMSE</b>  |                 | <b>17.3</b> | <b>20.8</b>  |

Table 14. Performance statistics of MIRS and MSPPS SIC versus SIC computed from collocated IMS data over the Northern hemisphere during 2006.

### 6.3.9 Sea Ice Age (SIFY, SIMY)

Both first year and multiyear sea ice concentration (SIFY, SIMY) are retrieved as well as the total SIC. Figure 50 shows a comparison between MiRS F18 SSMIS retrievals of SIFY and SIMY and the operational OSI-SAF dominant ice type analysis. Agreement between the MiRS products and the independent OSI-SAF type is very good.

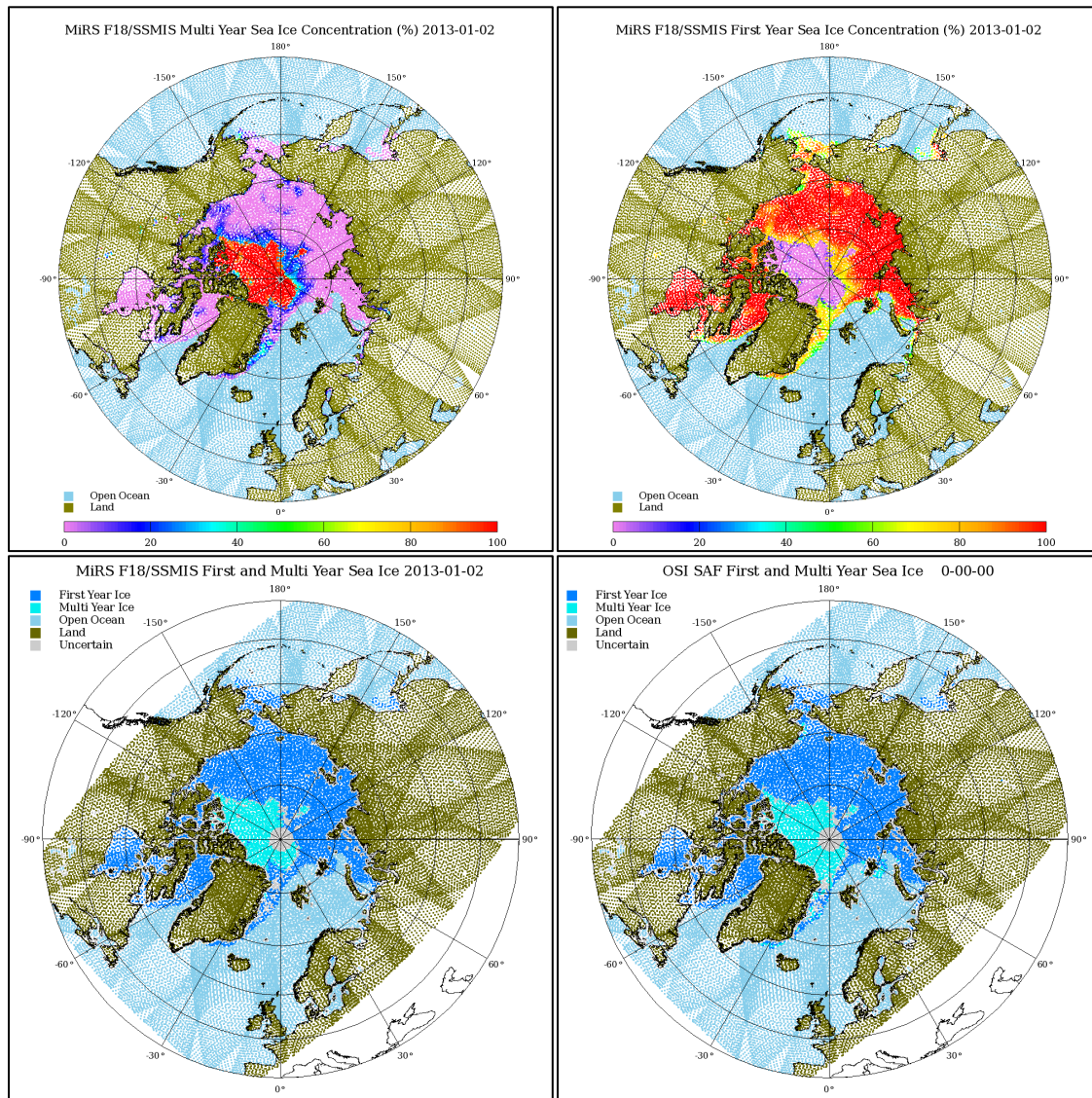


*Figure 50: Comparison of MiRS F18 SSMIS first year sea ice concentration (SIFY) and multiyear concentration (SIMY) with dominant ice type analysis from the OSI-SAF operational system on January 2, 2013. OSI-SAF data available courtesy of NMI/EUMETSAT.*

### 6.3.10 Snowfall Rate (SFR)

The heritage MSPPS algorithm for snowfall rate has been integrated into MiRS. Figure 51 shows a comparison between MiRS MetopB AMSU/MHS retrievals of SFR over the CONUS, compared with the retrieval map of MSPPS SFR from the OSPO official website. Agreement between the MiRS SFR and the MSPPS SFR is high, indicating that the algorithm has been successfully integrated.

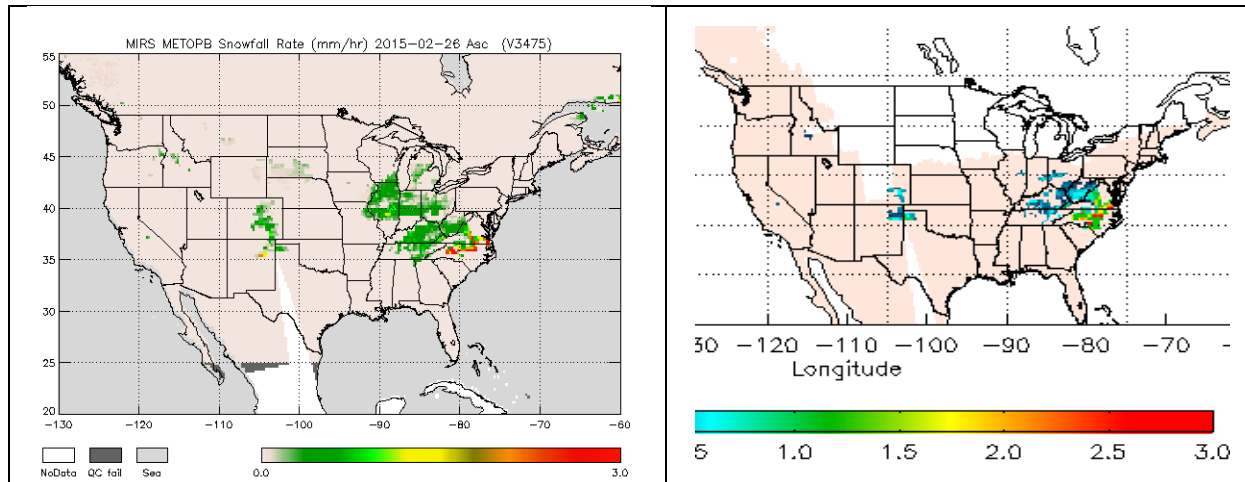


Figure 51: Comparison of MiRS MetopB SFR (left) on February 26, 2015 with MSPPS SFR from OSPO website (right).

## Section 7.0 MIRS Products Dissemination

### 7.1 Retrieved Products Dissemination

The retrieved MIRS products are converted to other level II and III formats. These output files are described in Section 5.0. More detailed descriptions are provided in the ICD. This section describes the dissemination of these files to users.

### 7.2 Product Maps Dissemination

In addition to the dissemination of MIRS output product files, a tool has been designed to allow the monitoring of global and regional retrievals through generation of image maps. This MIRS Online Monitoring Tool (MOMT) is available online and can be accessed via the following URL address: "<http://mirs.nesdis.noaa.gov/>". Figure 52 is a snapshot of the MIRS web site with the menu options.

A snapshot of the MOMT display features is presented in Figure 53. It is important to note that this tool is not tied to any particular sensor and as such it can display products from different microwave sensors.

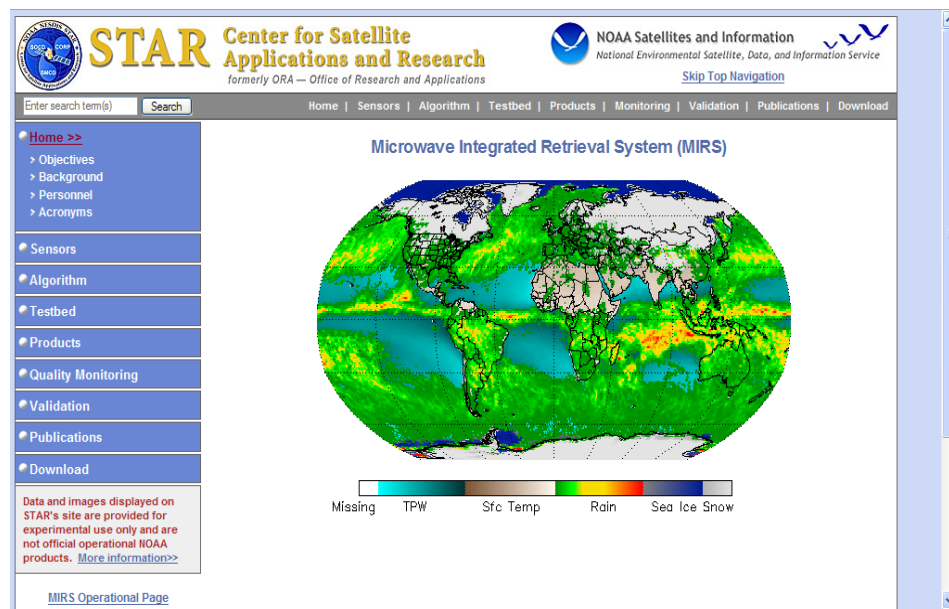


Figure 52. Snapshot of the MIRS Menu Options

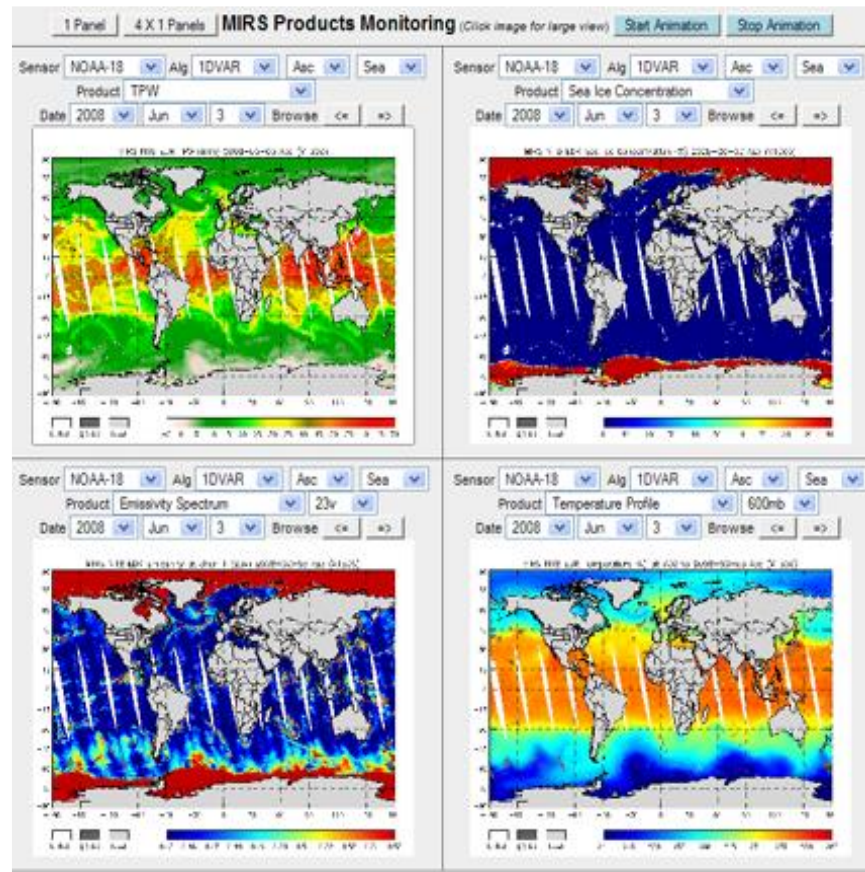


Figure 53. Snapshot of the MIRS Online Monitoring Tool (MOMT)

### 7.3 Quality Assurance Monitoring

The quality parameters of convergence ( $\chi^2$ ) and quality control (QC) are provided as part of the retrieved product fields. These parameters are also displayed through the Online Monitoring Tool (MOMT). Descriptions of these parameters were provided in Section 5.

## Section 8.0 MIRS Software Implementation Procedure

### 8.1 Obtaining the MIRS Software

Before obtaining the MIRS software package the potential user must sign a licensing agreement and sign up to an email list. This email list is expected to be used for a low volume notification procedure to alert users of problems, fixes and updates. All interested users should send an email to the following addresses to request the licensing agreement: *Quanhua.Liu@noaa.gov* (*science lead*), *Sid.Boukabara@noaa.gov* (*MIRS oversight board chair*), *Ralph.Ferraro@noaa.gov* (*oversight board member*) and *Limin.Zhao@noaa.gov* (*oversight board member*).

Once part of the email list, users can access MIRS software package by downloading the Delivery Algorithm Package (DAP):

#### 8.1.1 Accessing the Delivery Algorithm Package (*DAP*)

A tar package has been created following the NPOESS Data Exploitation (NDE) program standard. The DAP can be accessed on-line and downloaded from the MIRS web site:  
[“https://star.nesdis.noaa.gov/mirs”](https://star.nesdis.noaa.gov/mirs).

The download is password protected and users need to contact the MiRS team for password information ([Quanhua.Liu@noaa.gov](mailto:Quanhua.Liu@noaa.gov) or [Christopher.Grassotti@noaa.gov](mailto:Christopher.Grassotti@noaa.gov)).

### 8.2 Description of the MIRS Package

The MIRS package (from the DAP) contains all source codes, scripts, makefiles, data and coefficients needed to run MIRS for NOAA-18, NOAA-19, METOP-A, METOP-B , METOP-C AMSUA/MHS, DMSP F16, F17 and F18 SSMIS, Megha-Tropiques SAPHIR, as well as NPP and NOAA-20 ATMS. Preliminary capability for processing JPSS-2 (NOAA-21) ATMS is also included. Note that the variational retrieval in MIRS is sensor-independent and can therefore be implemented for other microwave systems. The list of MIRS package delivery items includes 1) source codes, 2) scripts, 3) makefiles, 4) coefficients, 5) sample data, 6) documentation, 7) CRTM forward model package, 8) benchmark files for verification, and 9) GUI-based tool to control MIRS execution.

### 8.3 How to Install, Compile and Run

#### 8.3.1 Preliminary Steps

- 1- Get the DAP from the web site as explained above.
- 2- Put the DAP in the directory where you want to install the main *mirs/* directory.
- 3- Unzip and untar it if you have a zipped/tarred copy.
- 4- **NOTE:** It is important to examine the README file that is located in the main *mirs/* top level directory immediately after untarring (if necessary) since it may have additional and/or updated information pertaining to the current DAP.

- 5- Go to the “/setup” top level directory and edit the following files:
  - a. “paths”: This file contains paths and options used by the makefiles. Update the CRTM and library paths as well as the conversion option to big endian (leave it alone if you use Linux, change it to blank if you use it under IBM/AIX). The paths should point to the local version of the MIRS installed. Set the HDF4 and HDF5 paths to locally installed library paths if you are processing FY-3 or NPP ATMS data. Set the JAVA\_HOME path to the locally installed library path if you are using the MIRS Control Panel (MCP) GUI.
  - b. “paths\_idl.pro”: This file contains the paths to the IDL toolboxes that come with the package. Change these paths to point to your locally installed MIRS. Modify only if you plan to use IDL tools that come with MIRS (covariance generation matrix, EOF decomposition tool, radiometric and geophysical visualization, convergence monitoring, performances monitoring, products maps generation tool, etc)
  - c. “xxx\_pcf.bash”: These Paths & Configuration Files (PCFs), one per sensor xxx, are used by the BASH script that runs the testbed. Change the paths to point to your local MIRS only when you plan to use the MIRS testbed. This is also the file to edit if you want to point to other raw data than those provided in the package.
  - d. A number of other options are also available within the PCFs which can control the way the applications will run. A description of these options is provided in the PCF itself

One can also choose to use the GUI-based MCP to perform all the tasks described above. The MCP can be implemented by executing the following commands in the “/gui” top level directory:

*make* – for compiling and,

*make run* – for running the MCP. The MCP panel will pop up.

Moreover, the MCP allows the user to generate scripts tailored to their needs. The use of this alternative (instead of making hand-made changes to the script) is encouraged. One can for instance generate a bare-bone script to perform the basic MIRS daily retrieval operations (without the daily production of monitoring figures) which could later be submitted to the cronjob (or OPUS for the case of the OSPO operational machine) on an orbital basis. One can also create another script that does only the daily image product generation. This latter can also be submitted to the cronjob but on a different schedule (once daily for example).

### **8.3.2 How to Run MIRS**

Modes of running MIRS were described in this document. The following provides instructions for a testbed run via the BASH Sequence Control Script (SCS) and for a direct execution of 1DVAR application.

#### **8.3.2.1 Testbed Run**

- 1- Go to “/scripts” top level directory and edit the sensor-dependent BASH SCS. For NOAA-18, the SCS is named “n18\_scs. bash”. The SCS can be run either without or with an argument, the latter being a date in format of xxxx-xx-xx, e.g. ‘n18\_scs. bash 2014-09-12’. By default, running without an argument automatically processes data for the day of yesterday. You can also run the script in an orbital mode via a switch in the PCF file. In this case, the argument must be the orbit filename without directory path. The directory path where the level 1-b data are located is specified in the PCF file.
- 2- Go to the “/setup” top level directory and update the PCFs with path names and options.
- 3- Execute the sensor specific SCS e.g., *n18\_scs. bash 2014-09-12* for NOAA-18 for daily processing mode on September 12, 2014, or execute for instance “*n18\_scs. bash NSS.AMAX.NN.D14255.S0051.E0246.B4798283.GC*” for orbital processing mode.

### **8.3.2.2 Direct Application Run (1DVAR)**

- 1- Go to “/src/1dvar” and compile 1DVAR source code (if this has not already been done) by typing “make”. This will automatically compile and link the library and the CRTM tool. One can execute ”make clean” to purge all object and executable files.
- 2- Go to ”/data/ControlData” and edit the control configuration file, e.g., “*n18\_CntrlConfig\_1dvar.in*” for NOAA 18 AMSU-MHS. The file contains the switches and file names needed for 1DVAR to run properly.
- 3- Run 1dvar executable by typing: “[full path]/bin/1dvar </[full path]/data/ControlData/ *n18\_CntrlConfig1dvar.in*” If the “MonitorPrint” switch parameter is turned ON in the control file, convergence information will scroll down on the screen.

## **8.4 Directory Tree Structure**

The factors that played a role in the directory structure design were sometimes conflicting with each other. These are (1) operationally streamlined, (2) research cohesiveness, (3) keeping all of MIRS into one package, and (4) having a stand-alone package (*that does not require user to provide its own files/structure*). The adopted directory structure shown in Figure 54 (software diagram) and

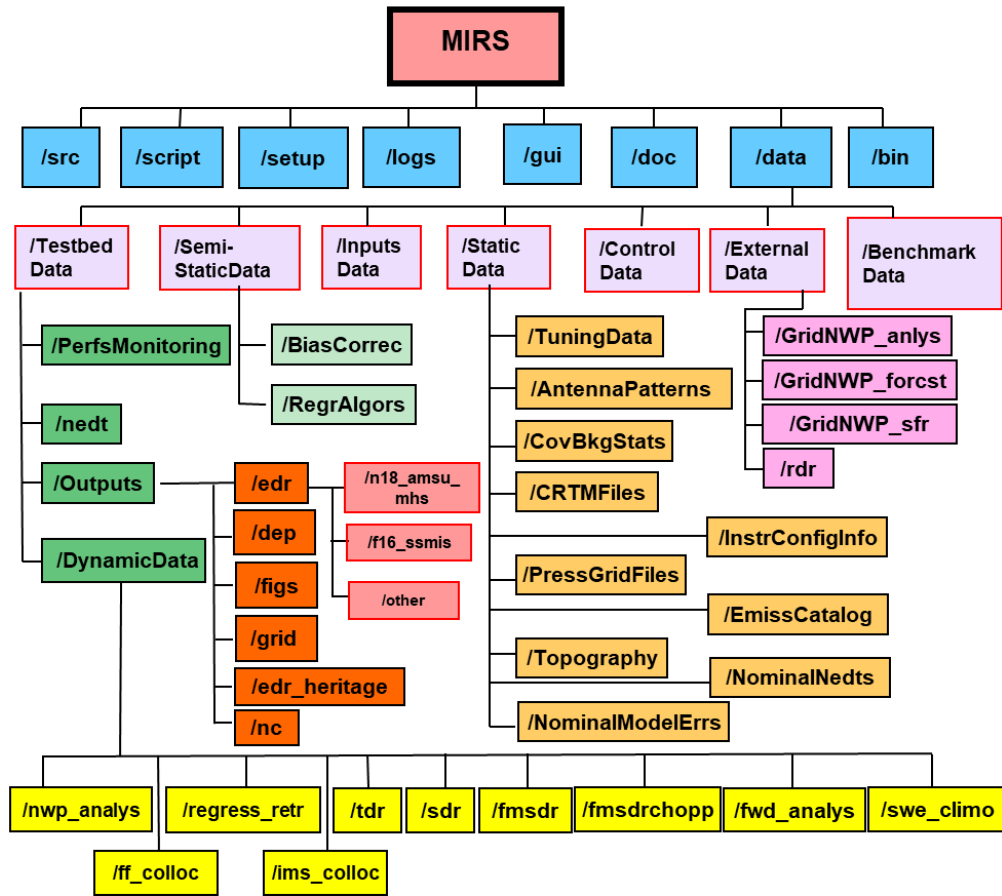


Figure 55 (data diagram), is a compromise between all these factors. The flowcharts present the user with a generic description of how the software package is organized. The data directory structure is defined in the PCF files. The user can modify this structure by defining a new structure in the PCF file. Note that the PCF files and thus the directory structure can also be reconfigured via the MCP tool.

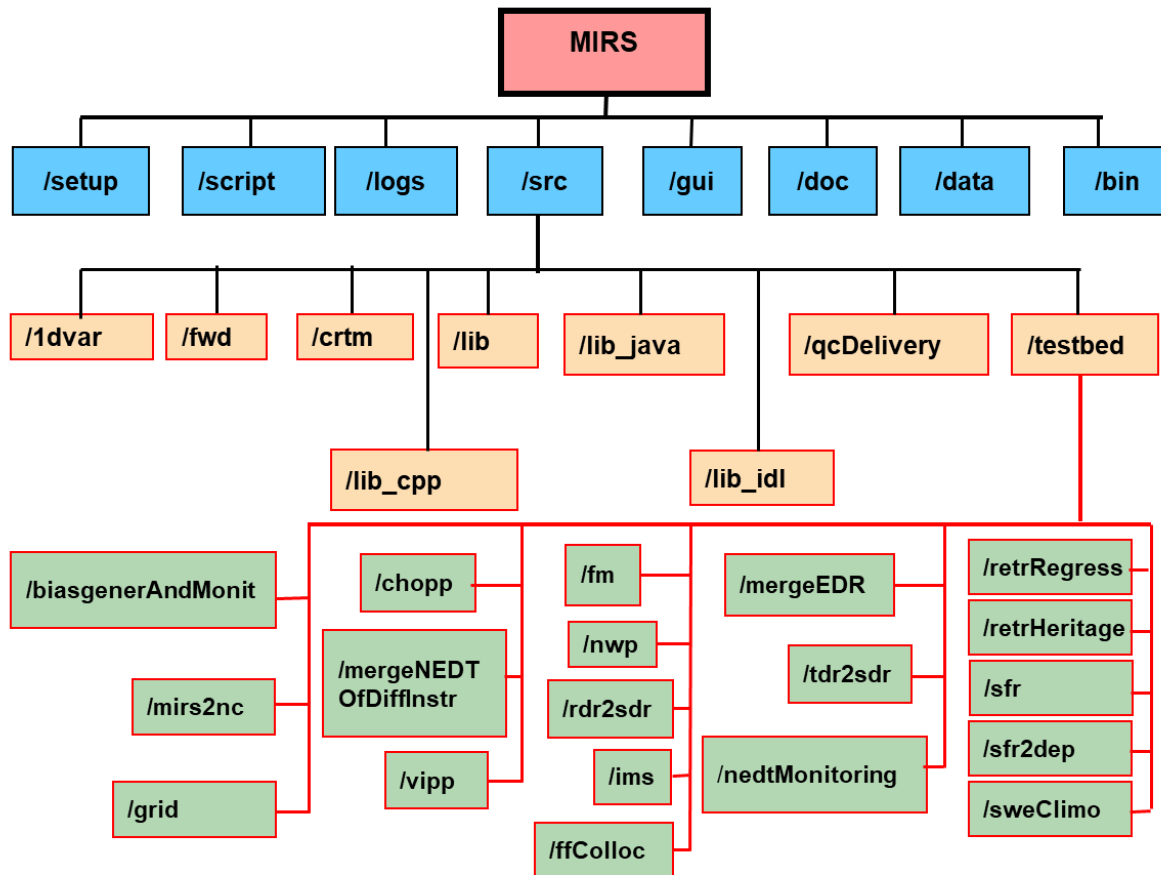


Figure 54. MIRS source code directory structure

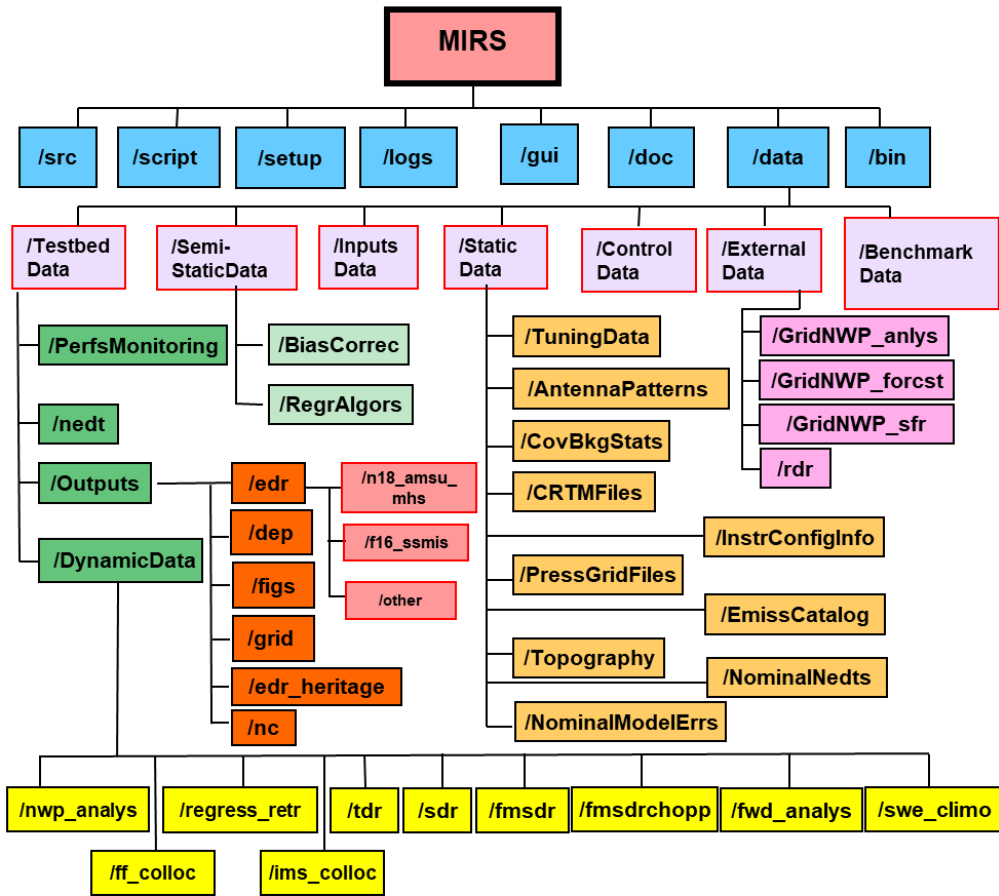


Figure 55. MIRS data directory structure

## 8.5 Benchmark Testing

A number of preprocessed files are delivered as part of the MIRS package to serve as benchmark testing references. These benchmark files are located in the “/data/BenchmarkData” directory and include the following files:

- MIRS retrieved main (EDR) and derived (DEP) product files.

Note that these benchmark files were generated in a Big-Endian mode so that testing could be performed on any machine using Big or Little Endian convention. They have been generated using Fortran-95 code and Linux operating system installed on a 32-bit machine, with a byte-swap option turned on. For consistency, it is suggested that the library I/O subroutines be used to read these files. Minor differences due to numerical accuracies are expected when comparing to outputs generated using a 64-bit machine.

The benchmark files can be compared with those generated from the MIRS package using the IDL code that comes with the delivery package. The IDL code is located in the “/src/qcDelivery” directory.

## 8.6 Licensing

Please send an email to request the licensing agreement. This is a necessary step to be granted permission to run MIRS. Please send requests to:

*[Quanhua.Liu@noaa.gov](mailto:Quanhua.Liu@noaa.gov) (MiRS Science Lead and Task Monitor)*

## 8.7 Referencing MIRS

When a reference to MIRS is needed, it is recommended to refer to the MIRS project by the following:

Boukabara, S., K. Garrett, W. Chen, F. Iturbide-Sanchez, C. Grassotti, C. Kongoli, R. Chen, Q. Liu, B. Yan, F. Weng, R. Ferraro, T. Kleespies, and H. Meng. MiRS: An all-weather satellite data assimilation and retrieval system. *IEEE Trans. Geosc. Rem. Sens.*, 2011.

## Appendix A. Acronyms and Abbreviations

| Acronym | Definition                                            |
|---------|-------------------------------------------------------|
| 1DVAR   | One dimensional variational assimilation              |
| AD      | Adjoint                                               |
| ADA     | Advanced Double-Adding                                |
| AMSU    | Advanced Microwave Sounding Unit                      |
| AOI     | Area-Of-Interest                                      |
| ASCII   | American Standard Code for Information Interchange    |
| ATBD    | Algorithm Theoretical Basis Document                  |
| ATMS    | Advanced Technology Microwave Sounder                 |
| CLW     | Non-Precipitating Liquid Cloud Amount                 |
| CRTM    | Community Radiative Transfer Model                    |
| DoD     | Department of Defense                                 |
| DAP     | Delivery Algorithm Package                            |
| EDR     | Environmental Data Records (Geophysical parameters)   |
| EOF     | Empirically Orthogonal Function                       |
| EOS     | Earth Observing System                                |
| FM      | Footprint-Matched                                     |
| GDAS    | Global data Assimilation System                       |
| GUI     | Graphical User Interface                              |
| HRC     | Hurricane Research Center                             |
| ICD     | Interface Control Document                            |
| IGP     | Ice Groupel Profile                                   |
| IMS     | Interactive Multi-Sensor Ice and Snow Mapping Product |
| IST     | Ice Surface Temperature                               |
| IWP     | Ice Water Path                                        |
| JCSDA   | Joint Center for Satellite Data Assimilation          |
| LST     | Land Surface Temperature                              |
| MCP     | MIRS Control Panel                                    |
| MVS     | Minimum variance solution                             |
| METOP   | Meteorological Operational Polar Satellite            |
| MHS     | Microwave Humidity Sounder                            |
| MIRS    | Microwave Integrated Retrieval System                 |
| MOMT    | MIRS Online Monitoring Tool                           |
| MPS     | Maximum probability solution                          |
| MSPPS   | Microwave Surface & Precipitation Products System     |
| NASA    | National Aeronautics and Space Administration         |
| NCDC    | National Climatic Data Center                         |
| NEDT    | Noise Equivalent Delta Temperature                    |

| <b>Acronym</b> | <b>Definition</b>                                                                               |
|----------------|-------------------------------------------------------------------------------------------------|
| NESDIS         | National Environmental Satellite, Data, and Information Service                                 |
| NOAA           | National Oceanic and Atmospheric Administration                                                 |
| NPCP           | Non Precipitating Cloud Profile                                                                 |
| NPOESS         | National Polar-orbiting Operational Environmental Satellite System                              |
| NPP            | National Polar-orbiting Operational Environmental Satellite System (NPOESS) Preparatory Project |
| OPTRAN         | Optical Path TRANsmittance                                                                      |
| OSDPD          | Office of Satellite Data Processing and Distribution                                            |
| PCF            | Paths & Configuration File                                                                      |
| QC             | Quality Control                                                                                 |
| OM             | MIRS Operations Manual                                                                          |
| QP             | Quality parameters                                                                              |
| RWP            | Rain Water Path                                                                                 |
| RR             | Rain Rate                                                                                       |
| SCS            | Sequence Control Scripts                                                                        |
| SDD            | System Description Document                                                                     |
| SDR            | Sensor Data Record                                                                              |
| SFR            | Snow Fall rate                                                                                  |
| SIC            | Sea Ice Concentration                                                                           |
| SSM/I          | Special Sensor Microwave Imager                                                                 |
| SST            | Sea Surface Temperature                                                                         |
| STAR           | Center for Satellite Applications and Research                                                  |
| SWE            | Snow Water Equivalent                                                                           |
| TDR            | Temperature Data Record                                                                         |
| TL             | Tangent Linear                                                                                  |
| TPW            | Total Precipitable Water                                                                        |
| UM             | User Manual                                                                                     |
| VIPP           | Vertical Integration & Post-Processing                                                          |

---

## Appendix B. Bibliography

Boukabara, S, K. Garrett, C. Grassotti, F. Iturbide-Sanchez, W. Chen, Z. Jiang, S. A. Clough, X. Zhan, P. Liang, Q. Liu, T. Islam, V. Zubko, and A. Mims. A physical approach for a simultaneous retrieval of sounding , surface, hydrometeor, and cryospheric parameters from SNPP/ATMS. *J Geophys. Res. Atmos.*, 118, DOI: 10.1002/2013JD020448.2158438, 2013.

Boukabara, S, K. Garrett, W. Chen, F. Iturbide-Sanchez, C. Grassotti, C. Kongoli, R. Chen, Q. Liu, B. Yan, F. Weng, R. Ferraro, T. Kleespies, and H. Meng. MiRS: An all-weather satellite data assimilation and retrieval system. *IEEE Trans. Geosc. Rem. Sens.*, DOI: 10.1109/TGRS.2011.2158438, 2011.

Iturbide-Sanchez, F., S. Boukabara, R. Chen, K. Garrett, C. Grassotti, W. Chen, and F. Weng. Assessment of a variational inversion system for rainfall rate over land and water surfaces. *IEEE Trans. Geosc. Rem. Sens.*, DOI: 10.1109/TGRS.2011.2119375, 2011.

Kongoli, C., S. Boukabara, B. Yan, F. Weng, R. Ferraro. A new sea-ice concentration algorithm based on microwave suface emissivities – Application to AMSU measurements. *IEEE Trans. Geosc. Rem. Sens.*, DOI: 10.1109/TGRS.2011.2052812, 2011.

T. Mo, “*Calibration of the Advanced Microwave Sounding Unit-A radiometers for NOAA-N and NOAA-N'*”, NOAA technical report; NESDIS 106, 2002.

S. Boukabara, F. Weng and Q. Liu. Passive Microwave Remote Sensing of Extreme Weather Events Using NOAA-18 AMSU and MHS, submitted, *IEEE Trans. Geosc. Rem. Sens.*, DOI: 10.1109/TGRS.2011.2052812, 2007.

S-A. Boukabara , F. Weng , R. Ferraro , L. Zhao , Q. Liu , B. Yan , A. Li , W. Chen , N. Sun , H. Meng , T. Kleespies , C. Kongoli , Y. Han , P. Van Delst , J. Zhao and C. Dean . "Introducing NOAA's Microwave Integrated Retrieval System (MIRS)". Presentation at the ITSC-15 conference in Maratea, Italy, October 2006.

Sid-Ahmed Boukabara, Fuzhong Weng and Quanhua Liu, "Microwave Variational Retrieval of Surface and Atmospheric Parameters: Application to AMSU/MHS and SSMI/S sensors." Poster at the American Meterological Society Annual Meeting. Georgia, Atlanta, 2006.

S. Boukabara and F. Weng. "Microwave Emissivity Retrieval Over Ocean in All-Weather Conditions. Validation Using satellite sensors and airborne GPS-Dropsondes". Presentation at the 1st Workshop on Modeling and Remote Sensing of Surface Properties, Paris, France, June 2006.

S. Boukabara and F. Weng . "Passive Microwave Remote Sensing of Extreme Weather Events Using NOAA-18 AMSU and MHS". Presentation at the 9th Specialist meeting on Microwave Radiometry and Applications, San Juan, Puerto-Rico, February 2006.

S. Boukabara and F. Weng. "SSMIS Ocean EDR Algorithms". Presentation at the NRL/JCSDA mini-workshop on preparation for SSMIS radiance assimilation, Monterey, CA, October 2005

Q. Liu and F. Weng, "*One-Dimensional Variational Retrieval Algorithm of Temperature, Water Vapor and Cloud Water Profiles From Advanced Microwave Sounding Unit (AMSU)*", IEEE Trans. on Geosc. and Remote Sensing, vol. 43, No 5, 2005